Call: H2020-ICT-2020-2
Project reference: 101015956

Project Name:
A flagship for B5G/6G vision and intelligent fabric of technology enablers connecting human, physical, and digital worlds
Hexa-X

Deliverable D3.2

Initial models and measurements for localisation and sensing

Date of delivery:	01/10/2022	Version:	1.0
Start date of project:	01/01/2021	Duration:	30 months

Document properties:

Document Number:	D3.2
Document Title:	Initial models and measurements for localisation and sensing
Editor(s):	Ehsan Moeen Taghavi (OUL), Henk Wymeersch (CHA)
Authors:	Ehsan Moeen Taghavi (OUL), Henk Wymeersch (CHA), Ali Behravan (EAB), Kim Schindhelm (SAG), Andreas Wolfgang (QRT), Vijaya Yajnanarayana (EAB), Simon Lindberg (QRT), Musa Furkan Keskin (CHA), Hui Chen (CHA), Tommy Svensson (CHA), Hao Guo (CHA), Mohammad Ali Nazari (CHA), Yu Ge (CHA), Alejandro Ramirez (SAG), Rafaela Schroeder (OUL), Traian E. Abrudan (NOF), Mohammad Hossein Moghaddam (QRT)
Contractual Date of Delivery:	01/10/2022
Dissemination level:	PU[1]/
Status:	Final
Version:	1.0
File Name:	Hexa-X D3.2_v1.0

Revision History

Revision	Date	Issued by	Description
0.1	14.06.2022	Hexa-X WP3	First inputs from all partners
0.2	30.06.2022	Hexa-X WP3	Updated before internal WP3 review
0.3	01.08.2022	Hexa-X WP3	Version for cross-task reviews
0.46	08.08.2022	Hexa-X WP3	WP3 internal review complete
0.5	26.08.2022	Hexa-X WP3	Version for external review
0.6	16.09.2022	Hexa-X WP3	Update after external review
0.7	16.09.2022	Hexa-X WP3	Version for PMT review
1.0	30.09.2022	Hexa-X WP3	Final version for submission to EC

[1] CO = Confidential, only members of the consortium (including the Commission Services)
PU = Public

Abstract

This report provides the results of the initial findings towards models, methods, signals, measurements, and the protocols for radio-based localisation and mapping from the Hexa-X work package 3: “6G High-Resolution Localisation and Sensing,” as well as providing the vision of how the accurate location and sensing information can enable and enrich applications as well as supporting communications and security. The report also defines research lines for future work in Hexa-X.

Keywords

6G localisation and sensing, models, methods, measurements, and enhanced services.

This project has received funding from the European Union’s Horizon 2020 research and innovation programme under grant agreement No 101015956.

Executive Summary

This report is the second deliverable of the Hexa-X project work package 3: "6D High-Resolution Localisation and Sensing". This deliverable focuses on the initial findings towards models, methods, signals, measurements, and the protocols for localisation and mapping, as well as providing the vision of how accurate location and sensing information can enable and enrich applications.

In this document, firstly, the main concepts in radio localisation and sensing are detailed in a tutorial-like manner, describing the appropriate methods, as well as fundamental performance limitations. Secondly, the main potential technology enablers for localisation and sensing toward 6G are highlighted, as well as important challenges related to the wireless propagation channel and radio hardware impairments.

Initial findings on methods, signals, and protocols for accurate localisation and sensing are reported, considering spatial signal optimisation, detection and channel parameter estimation, 6D (3D position and 3D orientation) localisation as well as simultaneous localisation and mapping under the impact of hardware impairments, integrated sensing and communication, and approaches for interference mitigation. It is revealed that in the 100 GHz – 300 GHz range, higher resolution in range and angle provides superior localisation compared to 5G, although the reduction of transmission power and the increased path loss may impact the potential applications. Also, for the experimental activities, a platform is developed for integrated communications, localisation, and sensing to make a proof of concept, to verify simulation results, and to demonstrate different use cases.

Finally, a crucial aspect of 6G, according to Hexa-X, is that localisation and sensing will not be a by-product of communications development but will instead be integrated into the system from the start, and thus is a main design target of 6G. Toward this, a vision for how location and sensing information can be used to support, enable, and enrich novel applications will be sketched. In addition, potential benefits of location and sensing information for improving communications and security are investigated as use cases.

Table of Contents

List of Figures

List of Tables

List of Acronyms and Abbreviations

2D	Two-dimensional
3D	Three-dimensional
5G	Fifth generation
6D	Six-dimensional
6G	Sixth generation
AE	Auto-encoder
AGV	Automated guided vehicles
AoA	Angle-of-arrival
AoD	Angle-of-departure
BCE	Binary cross-entropy
BF	Beamforming
BS	Base station
CCE	Categorical cross-entropy
CE	Channel estimation
CFO	Carrier frequency offset
CKM	Channel knowledge map
CPI	Coherent processing interval
CRB	Cramér-Rao bound
CS	Compressed sensing
CSI	Channel state information
CSIT	Channel state information at the transmitter
DA	Data-aided
DBSCAN	Density-based spatial clustering of applications with noise
DFT	Discrete Fourier transform
DFTS-OFDM	Discrete Fourier transform-spread orthogonal frequency-division multiplexing
DL	Downlink
DMRS	Demodulation reference signal
DT	Data transmission
EC	European Commission
EE	Energy efficiency
ESPRIT	Estimation of signal parameters via rotational invariant techniques
FFT	Fast Fourier transform
FIM	Fisher information matrix
FR1	Frequency range 1
FR2	Frequency range 2
GHz	Gigahertz
GIS	Geographic information system
GLRT	Generalised likelihood ratio test

GNSS	Global navigation satellite systems
GOSPA	Generalised optimal subpattern assignment
GPS	Global positioning system
H2020	Horizon 2020
HAD	Human activity detection
HWI	Hardware impairment
ICI	Inter-carrier interference
IMU	Inertial measurement unit
IoV	Internet-of-vehicle
IP	Incidence point
IQ	In-phase and quadrature
IRC2LS	Integrated radar communication, computation, localisation, and sensing
ISAC	Integrated sensing and communication
KPI	Key performance indicator
LBAC	Location-based access control
lidar	Light detection and ranging
LoS	Line-of-sight
LS	Least squares
LSCPA	Large-scale cooperative predictor antenna
MAE	Mean average error
MAPRT	Maximum a-posteriori ratio test
MC	Mutual coupling
MCRB	Misspecified Cramér-Rao bound
MEB	Mapping error bound
MHz	Megahertz
MIMO	Multiple input, multiple output
ML	Maximum likelihood
MLE	Maximum likelihood estimation
MMLE	Mismatched maximum likelihood estimation
mmW	Millimetre-wave
MR	Moving relay
MSE	Mean squared error
MUSIC	MUltiple SIgnal Classification
N/A	Not applicable
NDA	Non-data-aided
NLL	Negative log-likelihood
NLoS	Non-line-of-sight
NR	New radio
OEB	Orientation error bound
OFDM	Orthogonal frequency-division multiplexing
OMP	Orthogonal matching pursuit

P2P	Point-to-point
PA	Predictor antenna
PAN	Power amplifier nonlinearity
PDSCH	Physical downlink shared channel
PEB	Position error bound
PMBM	Poisson multi-Bernoulli mixture
PN	Phase noise
PRS	Positioning reference signal
QoS	Quality-of-service
RA	Receive antenna
radar	Radio detection and ranging
RAT	Radio access technology
RF	Radio frequency
RFC	Radio frequency chain
RIS	Reconfigurable intelligent surface
RMSE	Root-mean-square error
RSRP	Reference signal received power
RSS	Received signal strength
RTT	Round-trip-time
RX	Receiver
SAR	Synthetic aperture radar
SE	Spectral efficiency
SEB	Synchronisation error bound
SER	Symbol error rate
SINR	Signal-to-interference-plus-noise ratio
SLAM	Simultaneous localisation and mapping
SLAT	Simultaneous localisation and tracking
SNR	Signal-to-noise ratio
SRS	Sounding reference signal
SVM	Support vector machine
TDoA	Time-difference-of-arrival
ToA	Time-of-arrival
TX	Transmitter
UE	User equipment
UL	Uplink
ULA	Uniform linear array
UPA	Uniform planar array
UWB	Ultra-wide band

1 Introduction

Hexa-X is one of the 5G-PPP projects under the European Union (EU) Horizon 2020 framework. It is a flagship project that develops a Beyond 5G (B5G)/6G vision and an intelligent fabric of technology enablers connecting human, physical and digital worlds. This document is the second deliverable of Work Package 3 (WP3), "6G High-Resolution Localisation and Sensing". The work in WP3 focuses on two main folds: (i) to explore the potential of technological advances in communication systems (including from within the project) for the purpose of localisation and sensing, leveraging the geometric nature of the propagation channel at millimetre wave (mmW) frequencies (including 100-300 GHz), while accounting for severe hardware limitations; (ii) to harness high-resolution location and map information for existing (communication, security) and novel applications. The research, as three main tasks (T3.1, T3.2, and T3.3), focuses on the following key aspects related to high-resolution localisation and sensing:

- T3.1: Definition of use cases and requirements, complemented with a gap analysis.
- T3.2: Development of methods, signals, and protocols for localisation and mapping.
- T3.3: Establishment of location and mapping-enhanced service operation.

The relation of WP3 within Hexa-X, its tasks, and main interfaces are shown in Figure 1-1.

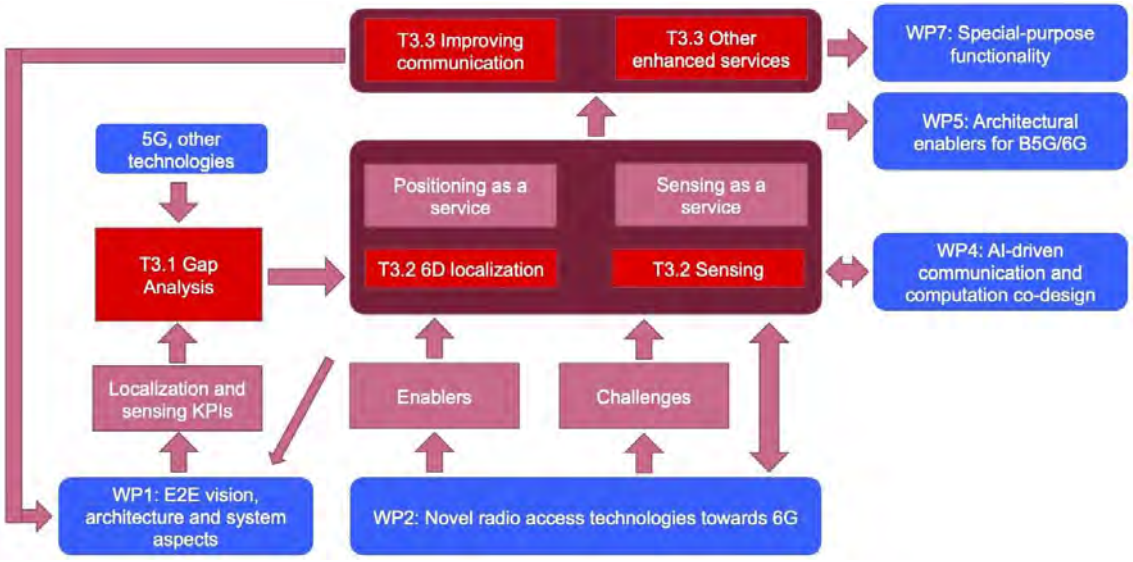

Figure 1-1. WP3 and its tasks in relation to Hexa-X.

1.1 Objective of the document

In the deliverable D3.1 [HEX21-D31], the gap analysis between the current performance of localisation and sensing in 5G 3GPP with the target key performance indicators (KPIs) deduced from the Hexa-X use case families was investigated. The main target of the present document is to deepen the insights on models and measurements for localisation, sensing, and the enhanced services provided from location and mapping. To support this, initial findings and plans related to the models, methods, signals, measurements, and protocols for radio-based localisation and mapping are provided as well as the vision of how the accurate location and sensing information can enable and enrich applications.

1.2 Structure of the document

The remainder of this deliverable is structured as follows. Section 2 provides an overview of localisation and sensing, describing the fundamentals, main potentials, and associated challenges in 6G localisation and sensing. Section 03 presents the initial methods, measurements, and results of localisation and sensing in 6G, quantifying the main benefits over 5G and the experimental setups developed within Hexa-X for localisation and sensing. As a complement to previous sections, which describe how location and sensing information are obtained, Section 4 describes how this information can be used for enabling and enriching applications as well as to support communications and enhanced security. Finally, the conclusions are drawn in section 5.

2 Overview of mobile radio-based localisation and sensing

This section briefly introduces the main concepts in radio localisation and sensing, summarising the corresponding material from [HEX21-D31]. Also, the main potentials and the associated challenges in 6G localisation and sensing are presented.

2.1 Radio localisation and sensing: overview

Below the fundamentals of localisation and sensing are described, addressing various aspects such as terminology, methods, and limitations.

2.1.1 Localisation

Radio localisation is the process of estimating the location of a device from (radio-based) sensor measurements. Examples include the global positioning system (GPS), ultra-wideband (UWB) positioning, and 5G positioning. The location can be in 2D (horizontal plane), 3D (including altitude), and 6D pose (including position or orientation). Base stations (BSs) commonly serve as location and time references, while the user equipment (UEs) have unknown and time-varying locations, which should be estimated through the exchange of signals (in uplink (UL) or downlink (DL), or a combination of both) with the BSs. The most common measurements include received signal strength (RSS), time-of-arrival (ToA), angle-of-arrival (AoA), angle-of-departure (AoD), and Doppler frequency shift. From ToA, measurements such as time-difference-of-arrival (TDoA), and round-trip-time (RTT) are derived. The location estimation accuracy depends on (i) the accuracy of the underlying measurements; (ii) the relative position of the BSs with respect to the UE. Hence, localisation performance can be improved by improving the measurements and the geometric placement of the positioning infrastructure.

2.1.2 Sensing

Sensing is the operation of the sensor, which is any device, module, machine, or subsystem that detects events or changes in its environment. In the context of this deliverable, sensing can be categorised as:

- Radar-type sensing, for localising and tracking passive objects or targets (including unconnected users).
- Non-radar-type sensing, such as extracting features from objects (e.g., material sensing), and classifying states of the environments (e.g., indoor and outdoor).

In most radar-like sensing applications, targets or objects are tracked over time, a method known as multi-target tracking or multi-object tracking. When the UE acts as a radar, this becomes a *simultaneous localisation and mapping* (SLAM) or a *simultaneous localisation and tracking* (SLAT) problem, where SLAM considers static objects while SLAT also considers moving targets. SLAM and SLAT can be performed in a relative or absolute frame of reference.

2.1.3 Localisation and sensing methods

Localisation and sensing involve the iterative application of several processes:

- **Signal design:** the design of signals in time, frequency, and space to support positioning and sensing. When a priori information about the UEs or environment

is available, signals can be designed to optimise the localisation or sensing performance of a specific UE or a group of UEs [KWS+21].

- **Signal transmission and reception:** The designed signal is transmitted over the radio channel and acquired at the receiver. The signal is subjected to analogue and digital impairments. The receiver obtains in-phase and quadrature (IQ) samples of the received signals for further processing. This process involves synchronisation, phase noise tracking, and filtering.
- **Channel parameter estimation:** The sampled signal is applied to a parametric channel estimation routine, which returns estimations of the ToA, AoD, AoA, and Doppler of the line-of-sight (LoS) path and possibly multipath components.
- **Localisation, sensing:** The channel parameters are provided to the localisation, mapping, or tracking routine. This routine aims to solve the inverse problem of inferring the state of the UE (i.e., location and orientation) or the environment from the estimated channel parameters [ZB11].

2.1.4 Performance limitations

Several factors limit the performance of localisation and sensing:

- **Resolution:** To estimate the parameters of a signal path during the channel estimation, the path should be resolvable (separable) in at least one domain among delay, AoD, AoA, or Doppler.
- **Accuracy:** Even under sufficient resolution, paths may be weak, thus limiting the accuracy of the estimated parameters.
- **Environment:** The propagation environment plays a vital role in the localisation and sensing performance (e.g., via blocking, scattering, or molecular absorption).
- **Mobility:** Objects and users are mobile, which limits the coherent processing duration of the waveforms used for sensing and localisation.
- **Range:** The maximum distance depends on the signal-to-noise ratio (SNR) at the receiver, which in turn, depends on the coherent processing interval (CPI), transmit power, and pathloss.
- **Model mismatch:** In general, unmodeled effects due to radio hardware impairments or propagation effects will lead to reduced localisation and sensing performance.

2.2 Potential for localisation and sensing in 6G

This section highlights the main potentials for localisation and sensing in 6G, namely *extreme performance* and *integrated radar, communication, computation, localisation, and sensing* (IRC2LS). Then, the main enablers are described from a radio perspective, followed by the main challenges, which will drive the work in WP3, depicted in Figure 2-1.

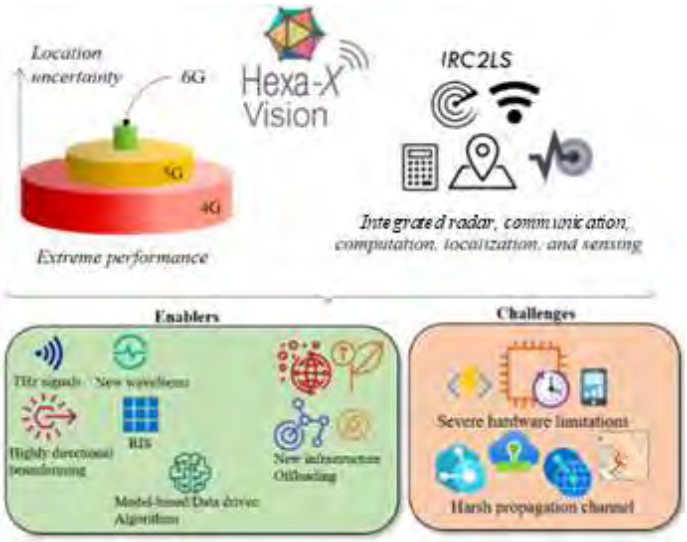

Figure 2-1. The Hexa-X vision for localisation and sensing, including the main enablers and challenges [WSM+21].

2.2.1 Extreme performance

As pointed out in [HEX21-D21], the 6G radio access technology (RAT) will operate at various frequency ranges encompassing not only present-day 3GPP NR FR1 (410 MHz – 7125 MHz) and FR2 (24250 MHz – 52600 MHz) but upper mmW ranges as well. Furthermore, by operating at the high carrier frequency and providing large bandwidths, the 6G radio access interface permits a small form factor, highly dense antenna arrays which enable pencil-like beamforming, as well as very fine delay resolution, which, in turn, permits resolving and then harnessing multipath components on the spatial and temporal domains. As a result, use cases detailed in [HEX21-D31], which require or benefit from highly accurate localisation and sensing, will also become possible.

2.2.2 Integrated radar, communication, computation, localisation, and sensing

Future 6G networks are expected to involve highly dimensional wireless channels in terms of increased number and density of connected devices, greater antenna array size, and wider bandwidth usage compared to present-day cellular systems. Although this characteristic imposes formidable computational challenges to estimate and track channel parameters in very high dimensions, it also imposes high overhead if real-time channel state information (CSI) needs to be acquired, relying solely on typical pilot-based channel training and feedback techniques. As an alternative, detailed environment mapping of the channel parameter features together with main aspects affecting the wireless channels (such as blockages, reflectors, and scatterers) can support communication procedures, such as beam alignment, system capabilities adaptation, channel features, and location of communicating transceivers prediction, with reduced overheads. However, while such ideas were already present in 5G, they are mainly optional [TMR+14]. In 6G, in contrast, harnessing location and sensing information will be critical to support efficient communication**.**

Channel (parameter) estimation is one of the key steps for communication, localisation, and sensing methods. This is based on comparing the received signal with the transmitted signal. Different levels of knowledge may be available about the transmitted signal.

2.2.2.1 Data signals for channel parameter estimation

In an integrated sensing and communication system, there is usually ongoing data transmission that can be utilised for sensing at no additional cost. Compared to sensing with pilots, it is expected that using data should perform slightly worse since data lacks certain characteristics of the reference signals such as close to ideal auto-correlation properties as well as peak to average properties of modulated data as compared to that of pilots. There are two scenarios for sensing using data, namely

- *Data-aided (DA) sensing:* data is known at the receiver. In a monostatic setup, the transmitter and receiver use the same hardware; the receiving part knows the transmitted signal and can thus treat it as a pilot.
- *Non-data-aided (NDA) Sensing:* Here, two scenarios can be envisioned
  - Data is decoded first, and then sensing is done based on this decoded data (decision-feedback NDA).
  - Sensing is done based on knowledge of other structures in the signals, for instance that the signals are transmitted with a certain QAM-constellation, etc.

Figure 2-2 shows two examples of DA sensing and NDA sensing where in (a) transmitter and receiver are connected to the same sensing processing unit, which means that the data is known at the receiver, and the receiver simply needs to perform a matched filtering with the known transmitted sequence to estimate the channel. In contrast, Figure 2-2(b) shows the example where the transmitted data should first be decoded, and then the channel is estimated based on decoded data. The second scenario is more generic and common in network implementation; however, it obviously implies a lower performance due to the data decoding error, as compared to case (a) in the figure.

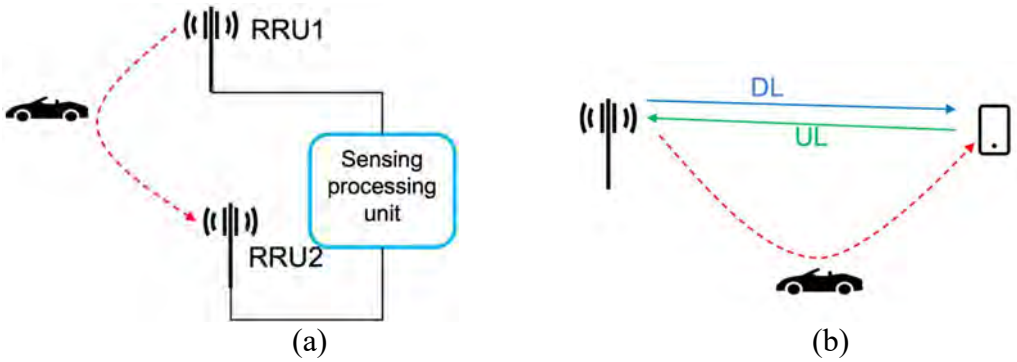

Figure 2-2. Two scenarios of sensing: a) with known data; b) with unknown data.

It should be noted that using data for sensing poses additional difficulties, e.g., ensuring a specific contiguous space-time-frequency transmission (sensing usually requires large BW and frequent transmissions). Also, non-data-aided sensing requires re-encoding, re-modulating those decoded bits because the connection between the "raw bits" and resulting waveform at the PHY layer is not straight-forward.

2.2.2.2 Pilot signals for channel parameter estimation

In bistatic or multistatic setups, the aforementioned sensing processing unit may not be available, in which case, channel parameter estimation is based on designed pilot signals. Communication systems also depend on channel estimation based on pilots, which is one of the main reasons for the existence of pilots. These can also be reused for channel estimation for localisation and sensing methods. However, for communication applications, there is an optimal number of pilots, after which the improvement in channel

parameter estimation is offset by a reduction in effective rate. In contrast, the optimal number of pilots for localisation and sensing applications is infinite, so one would instead want as many pilots as possible. These different needs for communication, localisation, and sensing applications must be considered when developing a system to support both of them. There are different possible solutions to this problem; one option could be to simply increase the number of available pilots in the communication signals (at a cost in effective rate), or to make it possible to schedule entire symbols for localisation and sensing applications where all resources could be used for pilots.

2.2.2.3 Bistatic sensing

The basic principle of bistatic sensing is the same as any other type of sensing. A signal is transmitted, and by comparing the received signal with the transmitted, one can localise objects in the surroundings. What is specific for bistatic sensing though, is that the transmitter and receiver are located at different locations using different hardware. As accurate time synchronisation is crucial for sensing applications, using different hardware for transmitter and receiver inherently introduces some errors in sensing. In addition to sensitivity to synchronisation error, inaccuracies in position and orientation of the transmitter and receiver can cause errors in sensing measurements. On the other hand, the advantage of bistatic sensing is the possibility of using many different units to cooperate and together even being able to generate a detailed map of the surroundings.

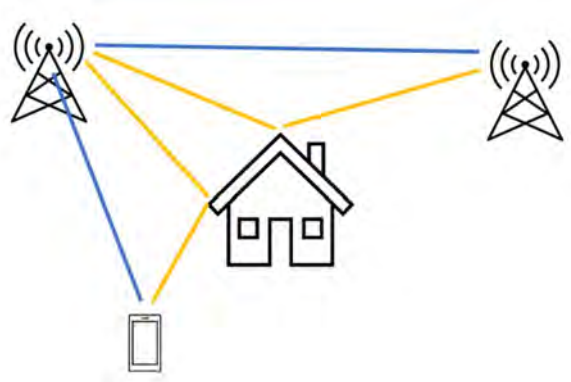

Figure 2-3. A simple example of how bistatic sensing can be performed both with a base station and a user device, but also between two base stations. The blue lines indicate line-of-sight paths, and the yellow are reflected paths.

Bistatic sensing can be used in several different areas, both for user-centric applications but also as a network service. One use case could be within autonomous driving, where vehicles in cooperation with other connected devices nearby can detect possible obstacles and dangers. Another application could be for better cooperation between base stations. By letting the base stations together analyse the area around themselves using bistatic sensing, obstacles which might interfere with the connection to other devices can be identified. This can help in coordinating communication with user devices when they move towards areas where the connection is expected to be bad.

2.2.3 Radio enablers

Various technical developments enable the potential of extreme performance and IRC2LS, studied and advanced in Hexa-X, as a collaboration between WP2 (Novel radio access technologies towards 6G) and WP3. Examples of these enablers are listed below (see [HEX21-D21, HEX21-D31] for more details):

- **Sensing with large bandwidths and large antenna arrays:** significant resolution enhancements are expected compared to 5G in terms of delay and angles.
- **Reconfigurable intelligent surfaces (RIS):** new types of infrastructure can boost localisation and sensing performance, especially when existing infrastructure is insufficient. A RIS can be used to allow a signal to reach its destination when no LoS can be achieved. Whenever the position of the RIS is known in advance, reception of the signal through a RIS will provide additional information relevant to localisation.
- **Joint hardware and waveform:** a single device is envisioned to support the triad of communication, sensing, and localisation.
- **Algorithmic developments:** advances in both model-based and machine learning methods will lead to increased performance.

2.2.4 Challenges

To fully harness the radio enablers for extreme performance and IRC2LS, two fundamental challenges have been identified:

1. **Hardware impairments**, which affect localisation and sensing more severely than communication; and
2. **Insufficient knowledge of channel models,** which also affects localisation and sensing more severely than communication, as WP3 activities rely explicitly on the geometric properties of the channel and thus require a deep and detailed understanding of the propagation phenomena.

2.2.5 Context-aware services and applications

In this project, context-aware services are defined as services that incorporate information about the environment. Environmental information can be manifold and play a significant role in the internet of things vision where all things are connected and monitor their surroundings. From the internet of things, perspective information can be generated by the mobile communication network itself or come from other sources that monitor the environment (such as surveillance cameras or condition monitoring sensors such as temperature sensors, etc.). The focus for Hexa-X is clearly on sensing capabilities that can be generated from the network itself, e.g., highly accurate localisation and newly designed radar-like sensing to optimise the core service of communication. But it is important to include other information providers, consumers, and prosumers (both producers and consumers) because only then is it possible to draw the big picture of what might be possible in the future with emerging (context-aware) services and applications and which role next-generation mobile networks will play in this ecosystem.

3 Methods, signals, and protocols for localisation and mapping

In this section, methods, signals, and protocols for localisation and mapping in communication systems are presented (see also Section 2.1.3). The following subsections focus on the topics of signal design, detection and channel parameter estimation, and localisation methods.

3.1 Spatial signal design for localisation

This section describes how spatial signals at the BS (i.e., the precoders used by the BS to create a desired transmit beampattern) can be optimised to improve localisation performance and elaborates on the differences between communication-optimal and localisation-optimal beams. In this context, spatial signal design refers to both the design of individual beams transmitted in different time windows and the power allocation between those tailor-made beams. This section also illustrates the conditions (in terms of the level of BS-UE synchronisation) under which the BS should illuminate the NLoS paths with more power than the LoS path.
In mmW systems, both time-based (ToA and TDoA) and angle-based (AoA and AoD) measurements provide geometrical information and contribute to localisation. Under multipath conditions, performing joint localisation and synchronisation of a UE is possible by using downlink signals transmitted by a single BS through delay and angle-based measurements and multipath exploitation [MMB+19]. Enhanced pilots for positioning in the time-frequency domain, i.e., downlink positioning reference signals (PRS), have already been introduced in 5G NR specifications [38.211, Sec. 7.4.1.7], aiming to cover the available bandwidth with a staggered pattern of orthogonal frequency-division multiplexing (OFDM) pilots to improve delay resolution and accuracy. To further improve positioning performance, signal design can also be performed in the spatial domain to boost the accuracy of angle-based measurements [KJM+22]. Here, spatial signals refer specifically to precoding vectors employed by a BS to steer downlink signals towards the desired direction. In a UE tracking scenario, downlink precoders can be optimised to maximise the localisation accuracy of UE under a-priori information on the locations of UE and incidence points. Such localisation-optimal precoders might differ from the commonly used SNR-maximising directional beams in communication-only scenarios (as in the Discrete Fourier transform (DFT) codebook). In a nutshell, the problem of spatial signal design involves finding the optimal BS precoders for multipath-assisted localisation of a UE under imperfect BS-UE synchronisation and certain prior knowledge of UE location and multipath environment.

Methodology
A downlink mmW multiple-input multiple-output (MIMO) OFDM communications scenario with a single BS and a UE is considered, as shown in Figure 3-1. The BS transmits sequential OFDM pilot frames where each frame contains a certain number of symbols and subcarriers. Each frame is precoded by a distinct precoding vector to allow the UE to estimate AoD from the BS. In compliance with the sparse nature of mmW MIMO channels [HGR+16], the channel between the BS and the UE is assumed to consist of a small number of paths, each characterised by a complex channel gain, delay, AoA at the UE, and AoD at the BS. Due to imperfect synchronisation, the path delays include the effect of unknown clock bias, which is assumed to have a zero-mean Gaussian

distribution with a certain variance (referred to as clock bias uncertainty). In this setup, the problem of interest for spatial signal design is to determine the optimal precoding matrix (consisting of individual precoding vectors used for each frame) that maximises the localisation performance of the UE.

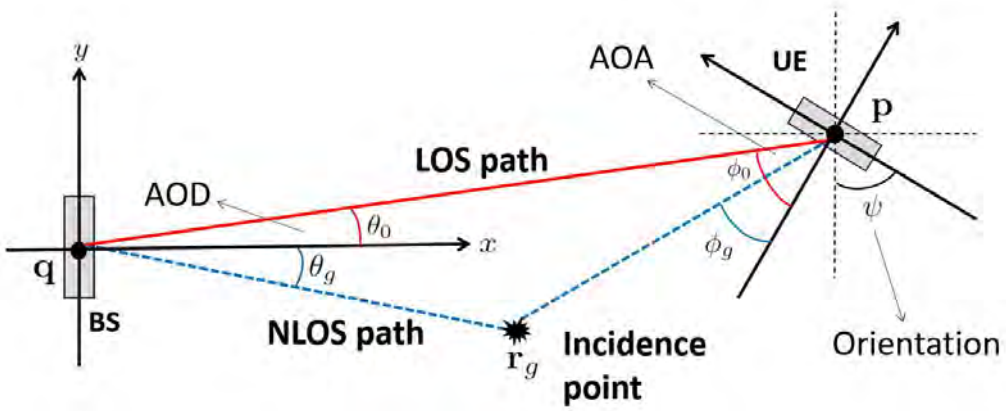

Figure 3-1. Localisation geometry for mmW MIMO setup with known BS position, unknown UE position, orientation and clock bias, and unknown incidence point location.

The methodology to solve this signal design problem is as follows:

- To quantify the localisation accuracy, a suitable performance metric needs to be derived. To this end, Cramér-Rao bound (CRB) on position estimation, i.e., position error bound (PEB), is adopted as the optimisation metric and derived as a function of the precoding matrix.
- The signal design problem is formulated under perfect knowledge of UE and multipath parameters, and the structure of the optimal beams is derived based on theoretical investigation of the optimal solutions to the resulting problem, which reveals directional and derivative beams [KJM+22] (similar to the difference beams employed in monopulse radars [Nic06]), as seen from Figure 3-2. The derivative beam refers to the derivative of the directional beam with respect to the AoD (this can be noticed from the beampatterns in Figure 3-2.). A weighted combination (in the form of power allocation) of directional and derivative beams provides the optimal solution to the spatial signal design problem at the BS under perfect knowledge of the UE location. The intuition behind this theoretical result is that the directional beam maximises the SNR towards the UE location while the derivative beam enables the UE to accurately estimate small angular deviations from the boresight through its sharp curvature (i.e., small changes in angle lead to large changes in amplitude).
- The robust design problem is formulated under imperfect knowledge of UE location and incidence points by adopting the worst-case PEB minimisation approach, which minimises the maximum PEB over the uncertainty region defined by the a-priori knowledge of UE and incidence point locations. This is called unconstrained design (i.e., not restricted to a certain type of codebook).
- As a low-complexity alternative to unconstrained design, a codebook-based low-complexity design is proposed using directional and derivative beams, pointing towards the AoDs of the multiple paths
- Convex optimisation-based strategy is developed to find the optimal time sharing/power allocation among the beams in the proposed codebook.

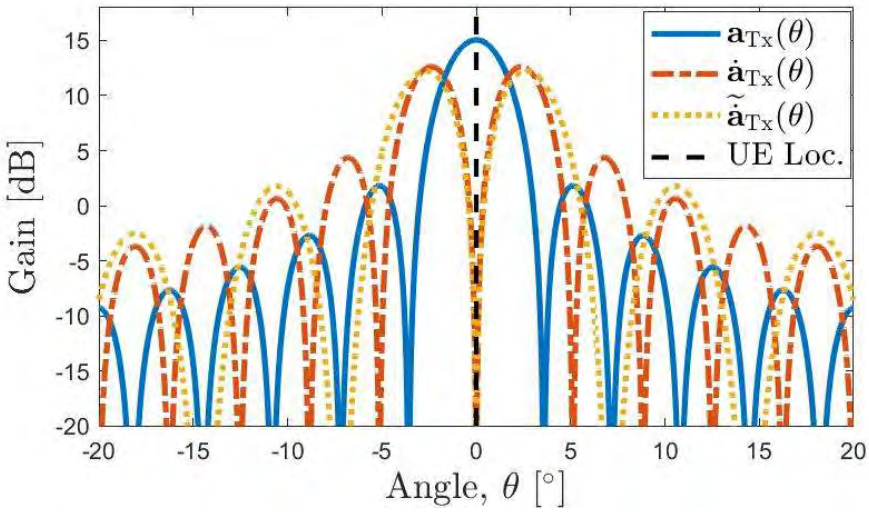

Figure 3-2. Uniform linear array (ULA) beampatterns at the BS transmitter belonging to the directional beam (blue solid line), digital derivative beam (red dashed line), and analogue derivative beam (yellow dot line).

Results

A two-path scenario with a LoS and a non-line-of-sight (NLoS) path is considered for performance evaluations, mimicking an outdoor open space scenario with a LoS and a ground reflection. To illustrate different PEB regimes of operation, the worst-case PEB (i.e., maximum PEB over the given uncertainty region) is plotted with respect to clock bias uncertainty, as shown in Figure 3-3. It is observed that under almost perfect synchronisation (i.e., low uncertainty on clock bias), the main limiting factor for the PEB is the accuracy of the LoS parameters since the LoS path alone is sufficient to localise the UE in this LoS-limited regime (due to clock synchronism). On the other hand, for the NLoS-limited regime, where clock bias uncertainty is high, increasing the reflection coefficient of the NLoS path improves the localisation accuracy since the NLoS path is needed to localise the UE under large synchronisation errors. Therefore, under low (high) clock bias uncertainty, the beams illuminating the LoS path should be allocated more (less) power than those illuminating the NLoS path.

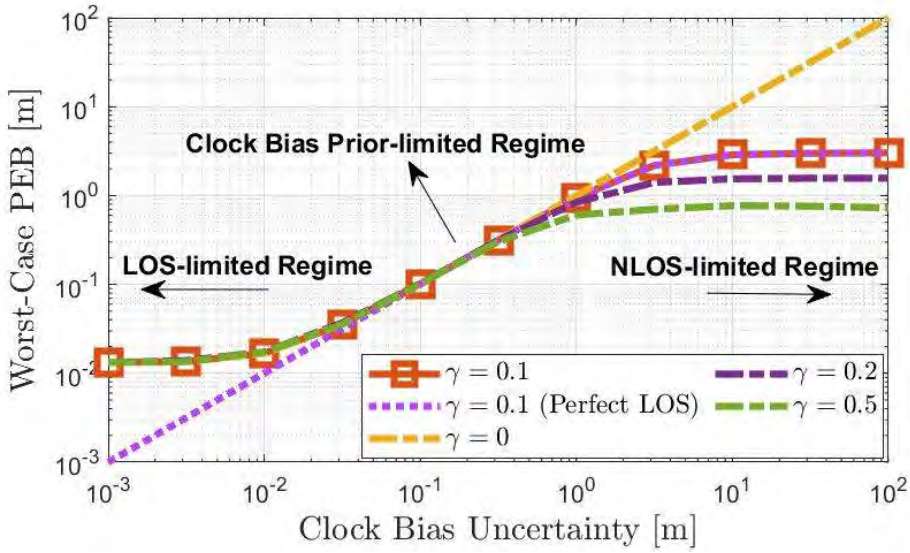

Figure 3-3. PEB regimes with respect to clock bias uncertainty, where γ is the reflection coefficient of the NLoS path. Here, "perfect LoS" refers to the hypothetical case where the LoS parameters are perfectly estimated at the receiver without any estimation error.

Figure 3-4 shows the PEB performances of

- the proposed codebook-based design (both digital and analogue versions), which contains both directional and derivative beams,
- the optimal unconstrained design (found by the worst-case PEB optimisation approach without any codebook constraints), and
- the benchmark (sum) codebook, which contains only directional beams.

The proposed design with both analogue and digital architectures can achieve the same performance as the optimal unconstrained design and significantly outperforms the benchmark codebook, which employs only directional beams. This indicates that incorporating derivative beams into the standard sum codebook improves the localisation accuracy.

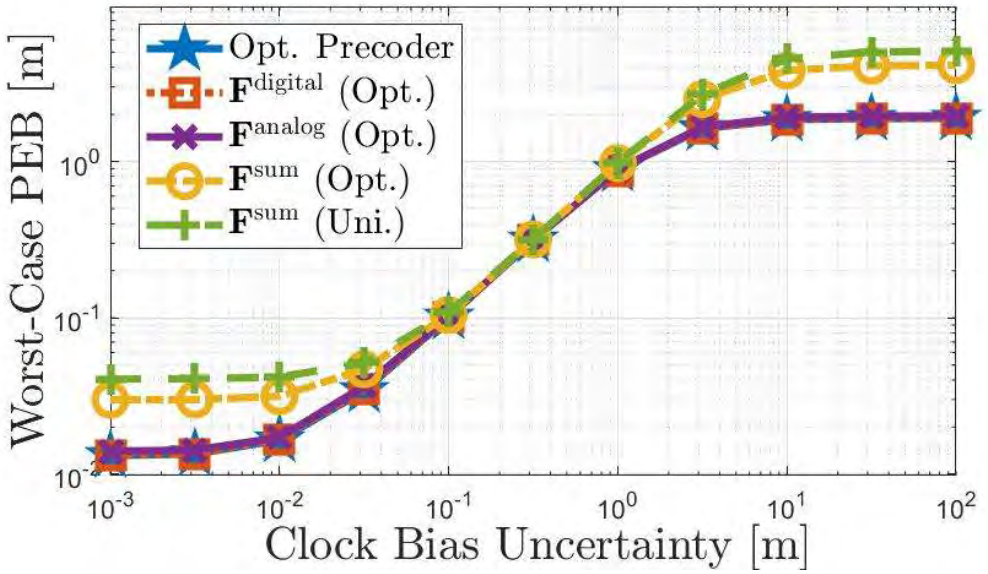

Figure 3-4. Worst-case PEB with respect to clock bias uncertainty, obtained by different precoding schemes. "Optimal precoder" refers to the optimal unconstrained design, "digital" and "analogue" correspond to the proposed codebook-based designs with directional and derivative beams, and "sum" denotes the codebook with only directional beams. "Opt." means power-optimised codebook, while "Uni." means codebook with uniform power allocation among its beams.

To provide insights into the differences between localisation-optimal and SNR-maximising beams, the aggregated beampatterns of the proposed and benchmark schemes are illustrated in Figure 3-5 for low clock bias uncertainty. As seen from the figure, although the sum beams (i.e., directional beams) maximise the SNR towards the UE location, they are not optimal in terms of positioning performance (as seen from Figure 3-4) since the derivative beams in Figure 3-2. are needed to help the UE to identify small deviations from the boresight direction, leading to better AoD and localisation accuracy.

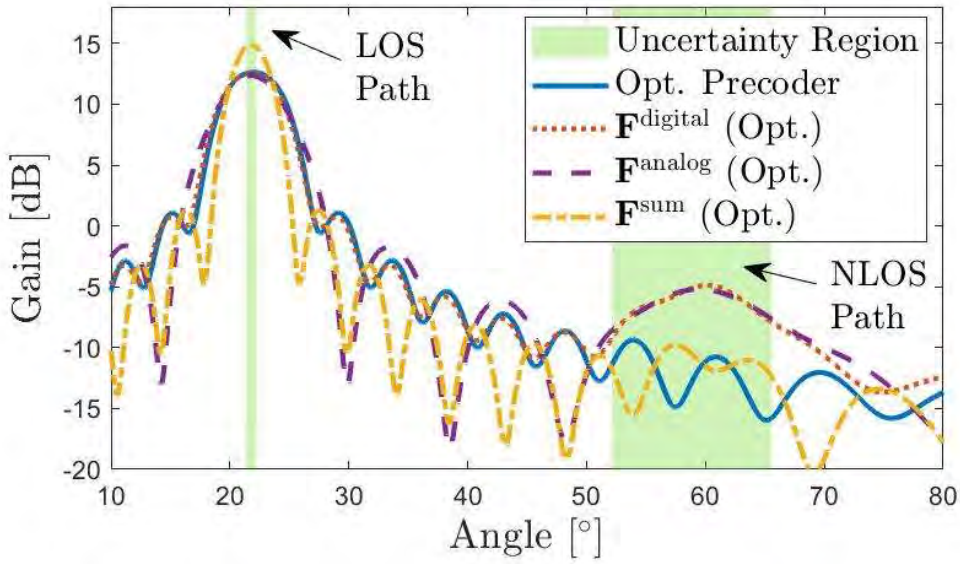

Figure 3-5. Beampatterns of the considered precoding schemes for low clock bias uncertainty (1 mm). The shaded regions describe the a priori knowledge (e.g., obtained via tracking routines) regarding the LoS direction (around 22 degrees) and the NLoS direction (around 60 degrees). The legends are defined in Figure 3-4.

Conclusions and outlook

The spatial signal design problem is studied for a mmW MIMO downlink localisation setup and it is observed that the localisation-optimal codebook employed by the BS should contain a balanced combination of directional and derivative beams. Different regimes of operation (LoS- and NLoS-limited regimes) are identified with respect to varying levels of synchronisation between the BS and the UE. In addition, the accuracy gains provided through derivative beams are illustrated and the resulting beampatterns are depicted to highlight the key differences between standard SNR-maximising directional beams and the newly introduced codebook containing both directional and derivative beams. Future studies will focus on extensions to multi-user scenarios.

3.2 Detection and channel parameter estimation

Before performing localisation and sensing algorithms, signal detection and channel parameter estimation are needed, which are described in this subsection.

3.2.1 Structured and unstructured channel estimation

RISs have been proposed as a solution to improve the coverage and mitigate the frequent blockages in mmW MIMO communications. To utilise the gains of RIS deployment to the communication systems, accurate channel state information (CSI) is required. However, CSI acquisition for RIS-based systems is very challenging due to the large number of passive elements at RIS, which are not connected to any baseband processing units. Therefore, introducing a few active elements at RIS has been proposed as a remedy to simplify the CSI acquisition at the sacrifice of additional power consumption. With this assumption, estimating the entire BS-RIS-UE channel can be divided into two point-to-point (P2P) MIMO channel estimation (CE) subproblems.

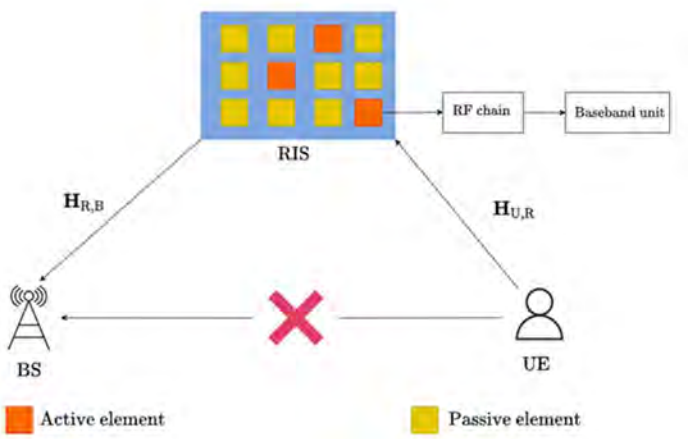

Figure 3-6. Hybrid RIS-assisted MIMO systems.

System model

Consider that *M* elements are active at the RIS. For CE, the one-way training detailed in [SHB+22] was followed. Figure 3-6 shows the hybrid RIS architecture with both passive and active elements. By adopting the assumption of a block fading channel, the coherence time is divided into two blocks, the first for CE and the second for data transmission (DT). To achieve better performance, the CE block is further divided into K sub-blocks. In each sub-block, the UE sends the training sequence to both the BS and the RIS. The training sequence is received by the active elements at RIS, while the passive elements reflect it to the BS. After the reflection, the signal is combined at the BS. Note that the CE is divided into two stages.

1. The first stage aims to recover the channel matrix UE-RIS based on the received signals at the RIS.
2. At the second stage, the target is the recovery of the channel matrix in RIS-BS from the received signals at the BS.

The estimation of the individual channels, UE-RIS and RIS-BS, can be addressed by deep learning [TAA21], structured [SHB+22], or unstructured methods [JC20]. The comparison between structured and unstructured CE will be the main focus.

Methodology

Unstructured methods, such as least squares (LS) [JC20], do not take advantage of any prior information on the propagation environment. Typically, unstructured CE algorithms have low computational complexity. However, a large training overhead is needed to achieve effective performance. In addition, those algorithms are more suitable for scenarios with rich scattering environments, such as sub-6GHz systems [SZL+22]. In the hybrid RIS CE, the LS algorithm can be applied to recover the UE-RIS channel matrix (or equivalent channel vector) from the received signals at RIS.

Structured CE methods have been proposed as one promising solution to reduce the training overhead. In particular, those methods are more suitable for mmW bands, where the channel sparsity can be leveraged in developing the CE algorithm. Thereby, the CE can be addressed via compressed sensing (CS) techniques, such as off-the-grid atomic norm minimisation (ANM) [CD20] or on-the-grid orthogonal matching pursuit (OMP) [LGL16]. ANM is a super-resolution algorithm capable of avoiding the basis mismatch, a common issue for on-the-grid CS methods, such as OMP. Thanks to its superior performance, the hybrid RIS CE problem is formulated following the ANM technique.

In order to provide insights on the CE for hybrid RIS, the trade-off between the structured and unstructured CE will be shown below.

Numerical results

One disadvantage of the hybrid RIS architecture is the higher power consumption due to the active elements. This motivates the study on energy efficiency (EE) of such a hybrid RIS-aided system, incorporating the channel estimation process. The simulation results for the energy efficiency (EE) versus transmitting power are shown in Figure 3-7.

Note that the structured CE for both passive and hybrid RIS architectures is implemented via ANM. Specifically, the passive RIS architecture follows the two-stage CE procedure detailed in [HWJ21]. The unstructured CE for hybrid RIS is addressed using the LS algorithm. Table 3-1 summarises the parameters setup for the simulations. First, the numerical results for the hybrid RIS versus passive RIS architecture with structured CE are discussed. Despite the higher power consumption due to the active RIS elements, the hybrid RIS via structured CE can outperform the passive RIS when the transmit power is low, such as *5 dBm*. However, the EE for both cases decreases for a high transmit power, such as *15 dBm*. The formulation of the EE can explain those results. In particular, the EE depends on the average effective spectral efficiency (SE) and the total power consumption. Note that the total power consumption depends on the required power for the CE and data transmission (DT) phase. Therefore, due to the saturation of the average effective SE and the increased total power consumption, the EE of the system decreases. In addition, Figure 3-7 shows that the structured CE achieves better performance compared to its counterpart, i.e., unstructured CE. These results are expected due to focus on the mmW frequency bands, where the structured methods can well exploit the sparsity of the channels. Moreover, the results are aligned with the theoretical analyses of the structured and unstructured CE in the literature [SZL+22].

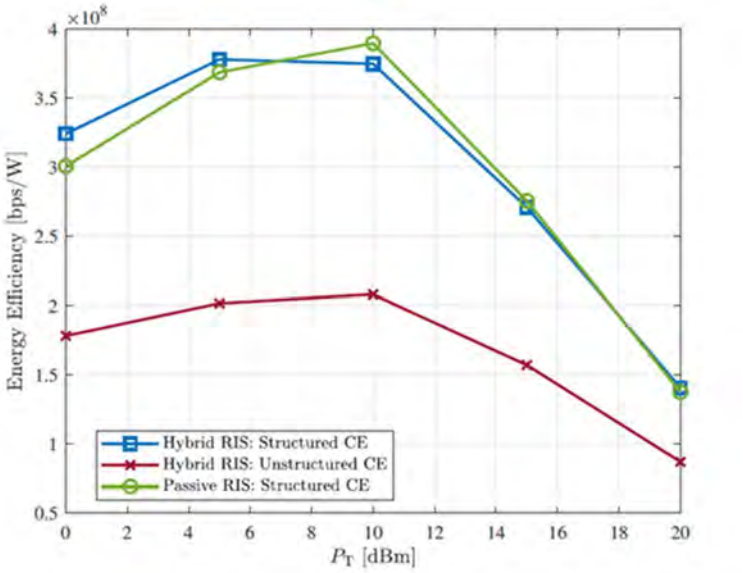

Figure 3-7. Energy efficiency of the RIS assisted MIMO systems versus transmit power.

Table 3-1. Parameters setup for the hybrid RIS.

Parameter	Value
Number of antennas/elements at BS, RIS, UE	16, 32, 16
Number of paths	2
Monte Carlo simulations	1000
Training Overhead (number of time slots)	40
Number of active elements	2
Number of RF chains at RIS	2
Number of RF chains at BS and UE	8
Path loss exponent	3
Carrier frequency	28 [GHz]
Bandwidth	100 [MHz]
Noise power density	−173 [dBm/Hz]
Transmit power	0 : 5 : 20 [dBm]
Number of time slots in a coherence time interval	500
Reference distance	1 [m]
Distance between BS and UE	30 [m]
Horizontal distance between UE and RIS	10 [m]
Vertical distance between UE and RIS	2 [m]
Power amplifier efficiencies	0.5
Static power	10 [mW]
Power consumption for one passive element	1.5 [mW]
Power consumption for each active element	10 [mW]
Power consumption for one RF chain	31.6 [mW]
Power dissipation at the receiver	10 [mW]

Conclusions and outlook

The trade-off between structured and unstructured CE has been studied. Numerical results show that the hybrid RIS via structured CE can achieve better performance than the unstructured CE. For future work, deploying the hybrid RIS for channel tracking in MIMO systems is considered.

3.2.2 Radar sensing under inter-carrier-interference

Inter-carrier interference (ICI) poses a severe challenge for OFDM integrated radar-communications systems in high-mobility scenarios due to the loss of orthogonality of subcarriers at the receiver, caused by Doppler shifts of mobile objects, [KWK21]. Figure 3-8 shows the range profiles of an OFDM radar in the presence of three objects in the environment. When the objects are stationary (i.e., moving at the same velocity as the radar; for example, cars moving in the same direction), the corresponding peaks in the range profile can be identified. However, when the objects are moving at a high velocity with respect to the radar (e.g., oncoming cars from the opposite direction), they lead to the ICI effect, which increases the side-lobe levels and reduces the dynamic range. As seen in Figure 3-8, this causes the masking of weak targets.

This section focuses on ICI mitigation and exploitation algorithms in OFDM radar sensing [KWK21].

- From the perspective of mitigation, the goal is to detect targets in the environment and estimate their delay-Doppler-angle parameters by cancelling the effect of ICI on radar observations so that the resulting performances are similar to those achieved in the absence of ICI.
- The aim of ICI exploitation is to utilise the Doppler information embedded in ICI to resolve Doppler ambiguity.

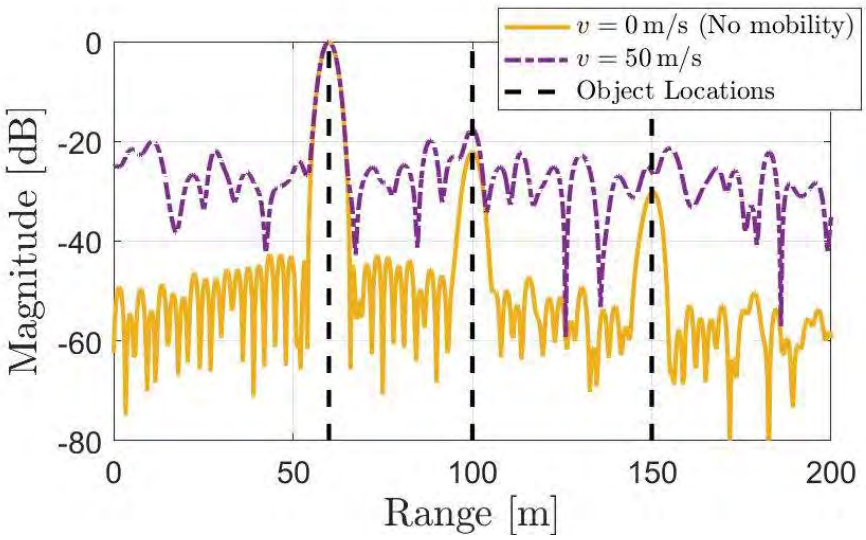

Figure 3-8. Range profiles of OFDM radar with and without relative mobility, showing the impact of ICI on the detection performance.

Methodology

The OFDM radar sensing problem under ICI is formulated as a joint carrier frequency offset (CFO)/channel estimation problem, drawing parallelism to OFDM communications [KWK21]. Given the OFDM radar observations in the form of a space/slow-time/fast-time data tensor collected over antenna elements, symbols, and subcarriers, a three-step algorithm is proposed to detect multiple targets under the impact of ICI and estimate their delay-Doppler-angle parameters, as shown in Figure 3-9:

- First, angle estimation is performed using the Multiple Signal Classification (MUSIC) algorithm [Sch86] for preliminary target detection in the angular domain. Since the spatial covariance matrix of the observations is independent of target delays and Dopplers, this step does not require the knowledge of delay-Doppler detections.
- In the second step, for each detected angle, the problem of joint beamforming, channel, and CFO estimation is formulated and solved, leading to unstructured channel estimation and CFO estimation. To account for multiple targets at each angle, GLRT and OMP-based iterative interference cancellation is applied.
- In the final step, delay-Doppler estimation is performed using the estimated unstructured channels, and the CFO estimation is utilised to resolve Doppler ambiguity since the CFO values represent the true target Doppler.

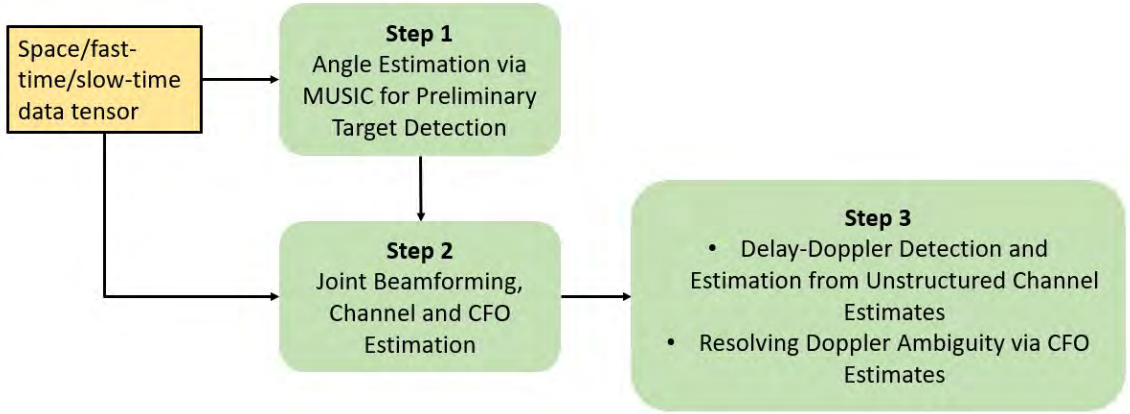

Figure 3-9. Three-step ICI-aware multi-target detector and delay-Doppler-angle estimator.

Results

Using the simulation parameters in Table 3-2 and the scenario with the five targets in Figure 3-10, the detection and estimation performance of the proposed ICI-aware sensing algorithm is evaluated.

Table 3-2. OFDM simulation parameters for radar sensing under ICI.

Parameter	Value
Carrier Frequency	60 GHz
Total Bandwidth	50 MHz
Number of Subcarriers	2048
Subcarrier Spacing	24.41 kHz
Symbol Duration	40.96 μs
Cyclic Prefix Duration	10.24 μs
Range Resolution	3 m
Unambiguous Range	6144 m
Number of Symbols	64
Total Symbol Duration	51.2 μs
Block Duration	3.28 ms
Velocity Resolution	0.76 m/s
Unambiguous Velocity (Standard)	$\pm$24.41 m/s
Unambiguous Velocity (ICI Exploitation)	$\pm$62500 m/s
Number of TX Antennas	8
Number of RX Antennas	8

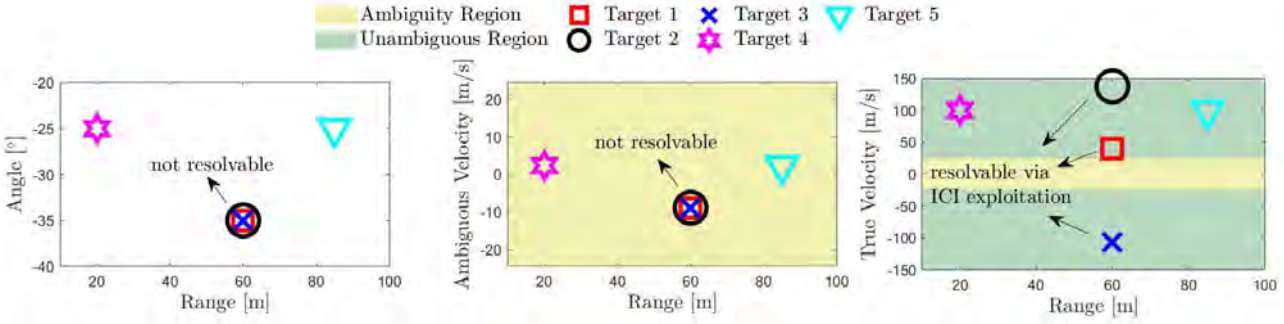

Figure 3-10. Scenario with five targets in range-angle-velocity domains, where SNRs are 20, 15, 10, 10, -10 dB, respectively.

The results of Step 1 (angle estimation via MUSIC) are presented in Figure 3-11, along with those of ordinary beamforming (BF). While MUSIC can correctly identify target angles, ordinary BF fails to resolve two angles due to the small number of RX antennas.

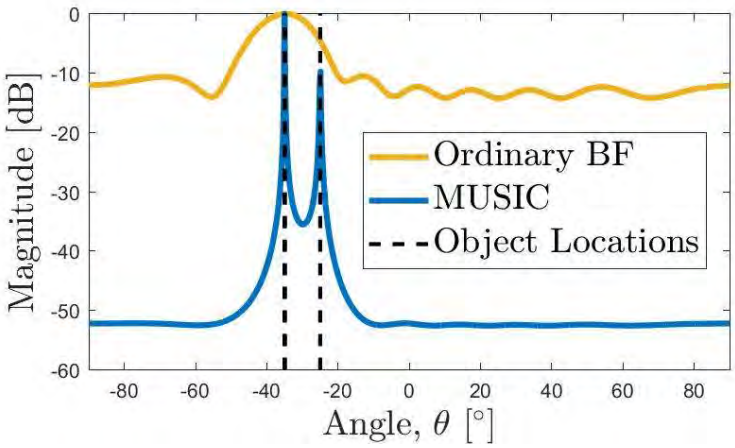

Figure 3-11. Angle estimation via MUSIC and standard beamforming in OFDM radar. The MUSIC spectrum shows the two different angles of the five objects in Figure 3.10.

The results of Step 2 (CFO estimation and iterative interference cancellation) are presented in Figure 3-12. As the algorithm proceeds through iterations, weaker targets (i.e., those with lower SNR) start to stand out in the CFO spectrum, indicating the impact of interference cancellation. Initially at iteration 0, the target with velocity around 40 m/s can be detected as the strongest one. After cancelling the contribution of this target, the target with velocity around 140 m/s stands out in the CFO spectrum at iteration 1. Next, the target with velocity around –110 m/s has the highest peak at iteration 2 after cancellation of the echoes of the strongest two targets. At the final iteration (iteration 3), all target echoes are cancelled out and the detection threshold is not crossed, which terminates the iterations.

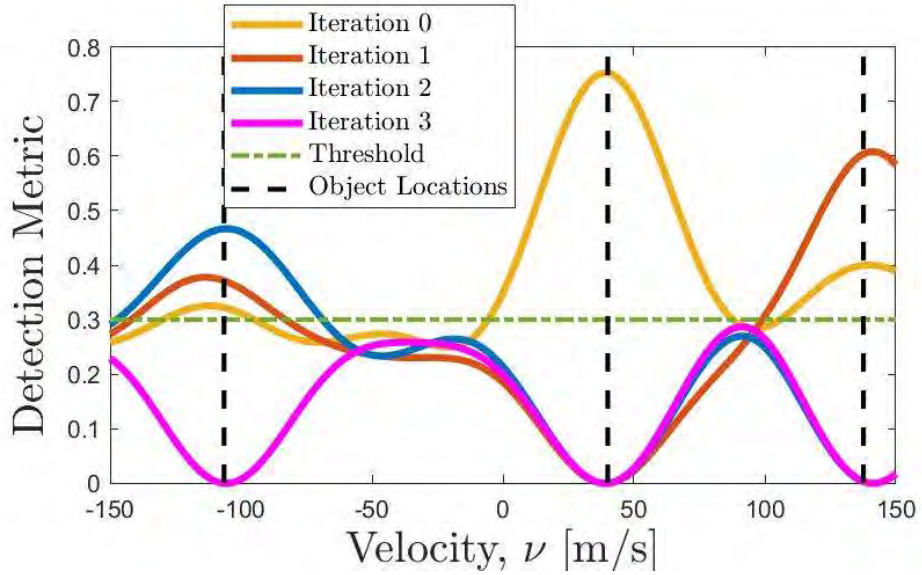

Figure 3-12. Evolution of CFO spectrum obtained through consecutive iterations of the OMP-based iterative interference cancellation procedure. The detection metric takes values between 0 and 1, and a high value means a high probability of target presence. The detection threshold is set to a heuristic value (0.3). The CFO spectrums correspond to the beamformed observations at angle –35 degree, thus showing the three targets at angle –35 degree in Figure 3-10.

Figure 3-13 illustrates the range profiles obtained by the proposed algorithm and the FFT benchmarks in Step 3. The proposed algorithm can recover back the weak target immersed in ICI-induced high side-lobe levels and achieve a range profile that is very similar to the ICI-free case. In Step 3, after estimating Doppler from unstructured channels, CFO estimates are used to resolve Doppler ambiguity (i.e., the so-called ICI exploitation approach). This provides two benefits, as illustrated in Figure 3-10: (i) increasing the maximum unambiguous Doppler and (ii) resolving targets located at the same delay-Doppler-angle cell.

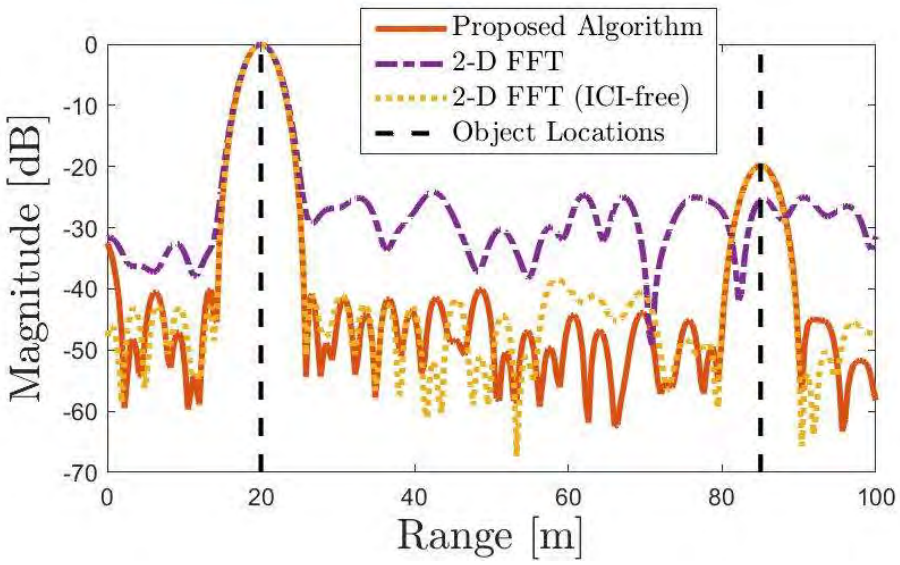

Figure 3-13. Range profiles obtained by the proposed ICI-aware detector and the FFT benchmarks with and without the ICI effect. The proposed algorithm can successfully suppress the ICI-induced side-lobes and recover back the range profile achieved in the ideal case without ICI, which enables detection of the weaker target around 85 m. The range profiles correspond to the beamformed observations at angle –25 degree in Figure 3-10.

Finally, the detection performance of the proposed algorithm is evaluated with respect to SNR for the reference target in a two-target scenario described in Table 3-3. Figure 3-14 shows the probability of detection curves for two different velocities. The proposed algorithm can achieve the same performance as the ideal ICI-free case, while the standard FFT benchmark experiences a substantial loss in detection performance due to ICI.

Table 3-3. Two-target scenario for detection performance evaluation.

	Range	Velocity	Angle	SNR
Target 1	40 m	ν m/s	$-35°$	25 dB
Target 2 (Reference)	80 m	ν m/s	$-25°$	SNR dB

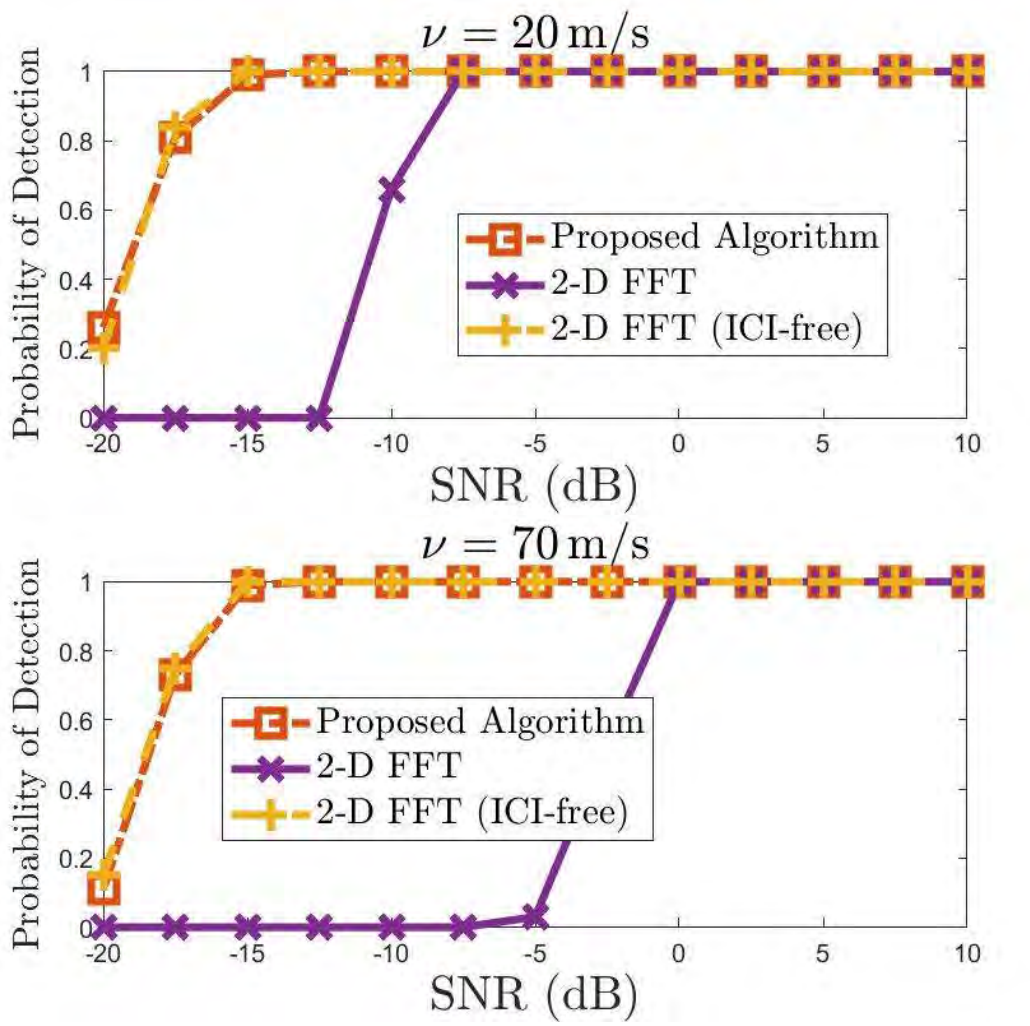

Figure 3-14. Probability of detection with respect to SNR for two different target velocities under the impact of ICI.

Conclusions and outlook

The problem of multi-target detection and delay-Doppler-angle estimation under ICI is studied for an OFDM monostatic sensing setup. Simulation results suggest that ICI can be mitigated almost perfectly using the proposed algorithm, allowing the radar to recover the performance achievable in the absence of ICI. In addition, the ICI effect can be turned from foe to friend by exploiting the corresponding CFO estimates for Doppler ambiguity resolution.

3.3 Methods for localisation, sensing, and SLAM

Localisation algorithms can roughly be categorised into model-based and AI-based methods. In this section, model-based methods such as single snapshot 6D localisation and sensing, simultaneous localisation, and mapping (SLAM), analysis of the impact of hardware impairments, and bistatic sensing are described. In addition, AI-based integrated sensing and communication is also presented.

3.3.1 Model-based localisation and sensing methods

Model-based methods are widely used due to the convenience of performance analysis (e.g., CRB) and available practical algorithms. However, the model mismatch between

the assumed simplified model and the true model affects the localisation and sensing performance. In the following, we will present 6D localisation and sensing, SLAM, analysis of the impact of hardware impairments, and bistatic sensing.

3.3.1.1 Single snapshot-based 6D localisation and sensing

6D localisation and synchronisation refer to the estimation of 3D position and 3D orientation, as well as the clock offset of an unsynchronised multi-antenna user. Mapping (or sensing) can also be considered by estimating the 3D positions of incidence points (IPs), i.e., the reflections surfaces and/or scatterers [NSJ+22]. The goal of 6D localisation is to estimate unknowns using snapshot observation obtained from downlink MIMO-OFDM signals. In snapshot-based localisation, signals are considered during a short time interval to avoid modelling time evolution of parameters.
The 6D localisation information is of great importance for communication and many practical applications. One way to obtain this information is through technologies such as the combination of global navigation satellite systems (GNSSs) (for 3D position) and inertial measurement units (IMUs) (for 3D orientation). Such solutions can be inefficient in cost, complexity, or coverage (for example, GNSS might fail in indoor environments). The alternative is to exploit the mmW communication infrastructure for 6D localisation.

Methodology
The system model is a downlink mmW MIMO scenario consisting of a single arbitrary-array multi-antenna BS. The user also has an arbitrary multi-antenna array. The orientation of BS and UE show how their antenna arrays with respect to a reference orientation in the global coordinate frame are arranged. The rotation matrices in the spatial orthogonal group (SO)(3) are considered to represent orientation.
The position and orientation are known for the BS, but not for the UE. There are M+1 paths between BS and UE, including the LoS and M≥1 NLoS paths, each corresponding to a single-bounce reflecting point at an unknown position (multi-bounce reflections are weaker and ignored in this study), which is to be estimated (see Figure 3-15). In case the LoS path is not available, the method must be modified.

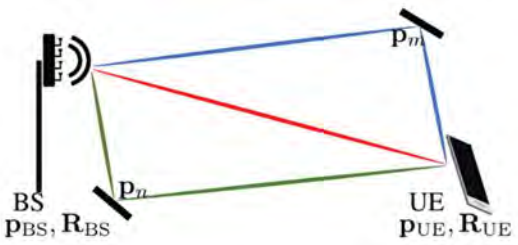

Figure 3-15. Schematic of the system model for 6D localisation with a single BS.

Using a two-stage localisation process, the marginal posterior densities of AoAs, AoDs, and ToAs are first determined based on the received OFDM signals. Then, a maximum likelihood estimation (MLE) scheme is run to determine the localisation unknowns (i.e., position, orientation and clock offset). The former could be done through various channel parameter estimators, including estimation of signal parameters via rotational invariant techniques (ESPRIT), generalised approximate message passing (GAMP), orthogonal matching pursuit, etc.
The latter consists of non-convex optimisation over the products of rotation matrices manifold, i.e., SO(3), and Euclidean space. To solve the optimisation problem, iterative algorithms are implemented, exploiting projection/retraction operations to/from the

tangent (i.e., Euclidean) spaces from/to the SO(3). The iterative algorithms are initialised by an ad-hoc estimation of unknowns obtained from the geometrical analysis. If the initial values are not given properly, the iterative algorithms might reach local optima.
In the ad-hoc estimation process, the UE rotation matrix is estimated first, based on an axis-angle analysis, considering the AoAs and AoDs, without any knowledge of positions. Then given the estimate of UE orientation, all the positions are obtained from TDoA measurements. Finally, the clock offset is estimated. The process includes a 1D search, i.e., uniform griding, over the finite interval $[0,2\pi)$, and a convex optimisation problem (with a closed-form solution in many cases) for each value in the 1D search. The complexity is much less than searching for all unknowns.

Results

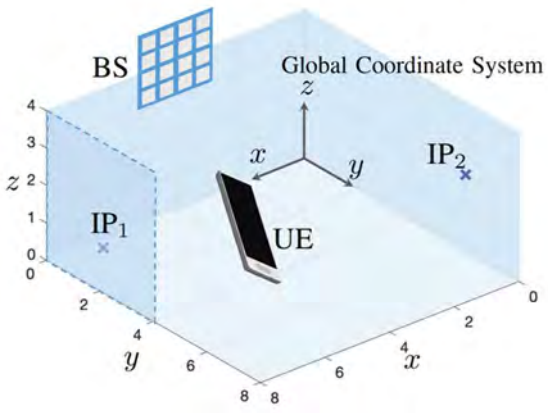

Figure 3-16. The indoor scenario considered in simulations with default parameters.

Table 3-4. Default simulation parameters. Parameters that vary are marked with ∗.

Parameter	Symbol	Value
Propagation Speed	c	3×10^8 m/s
Carrier Frequency	f_c	28 GHz
Subcarrier Spacing	Δ_f	120 kHz
# Subcarriers*	N_f	3333
# OFDM Symbols	K	10
Transmit Power*	P_{TX}	10 dBm
Noise PSD	N_0	-174 dBm/Hz
UE Noise Figure	n_0	13 dB
BS # Antennas*	N_{BS}	64 (8×8)
UE # Antennas*	N_{UE}	4 (2×2)
BS Position	$\mathbf{p}_{\mathrm{BS}}$	$[4, 0, 4]^{\mathsf{T}}$
BS Orientation	$\mathbf{R}_{\mathrm{BS}}$	$\mathbf{R}_x(-\pi/2)$
UE Position*	$\mathbf{p}_{\mathrm{UE}}$	$[5, 4, 1]^{\mathsf{T}}$
UE Orientation*	$\mathbf{R}_{\mathrm{UE}}$	varying
IP Positions*	$\mathbf{p}_m$	varying
Reflection Coefficient*	Γ_{ref}	$[0.2, 0.8]$, 0.7
Clock Offset	b	100 ns
# Monte Carlo Simulations	N_s	1000

Using the simulation scenario depicted in Figure 3-16 and the parameters given in Table 3-4, the performance of the proposed localisation scheme is evaluated and compared with the lower bounds obtained from the Fisher information matrix (FIM) analysis. It is observed from Figure 3-17 and Figure 3-18 that the performance of both MLE and ad-hoc estimators is improved by increasing the transmit power, closely following the corresponding bounds. The gap between the performance of ad-hoc estimation and CRB is negligible for a large range of transmit powers, and that can even be tightened using MLE. The deviation of performance of the proposed estimator from the bound in low SNR regimes is reduced in the case of 2 incidence points. The tightness of MLE to the CRB, and the negligible gap between the ad-hoc estimator's performance and the lower bounds for a practical range, show the efficiency of the proposed estimation algorithms.

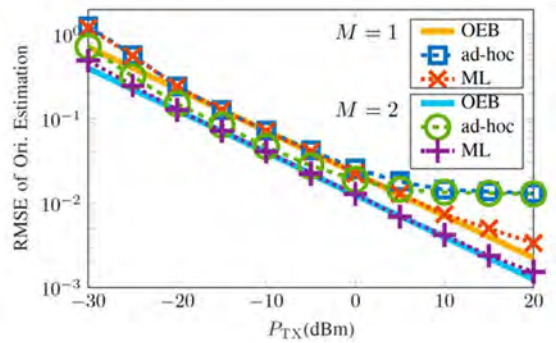

Figure 3-17. RMSE of orientation estimation.

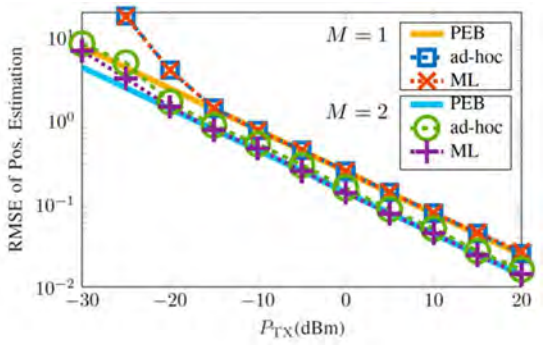

Figure 3-18. RMSE of position estimation.

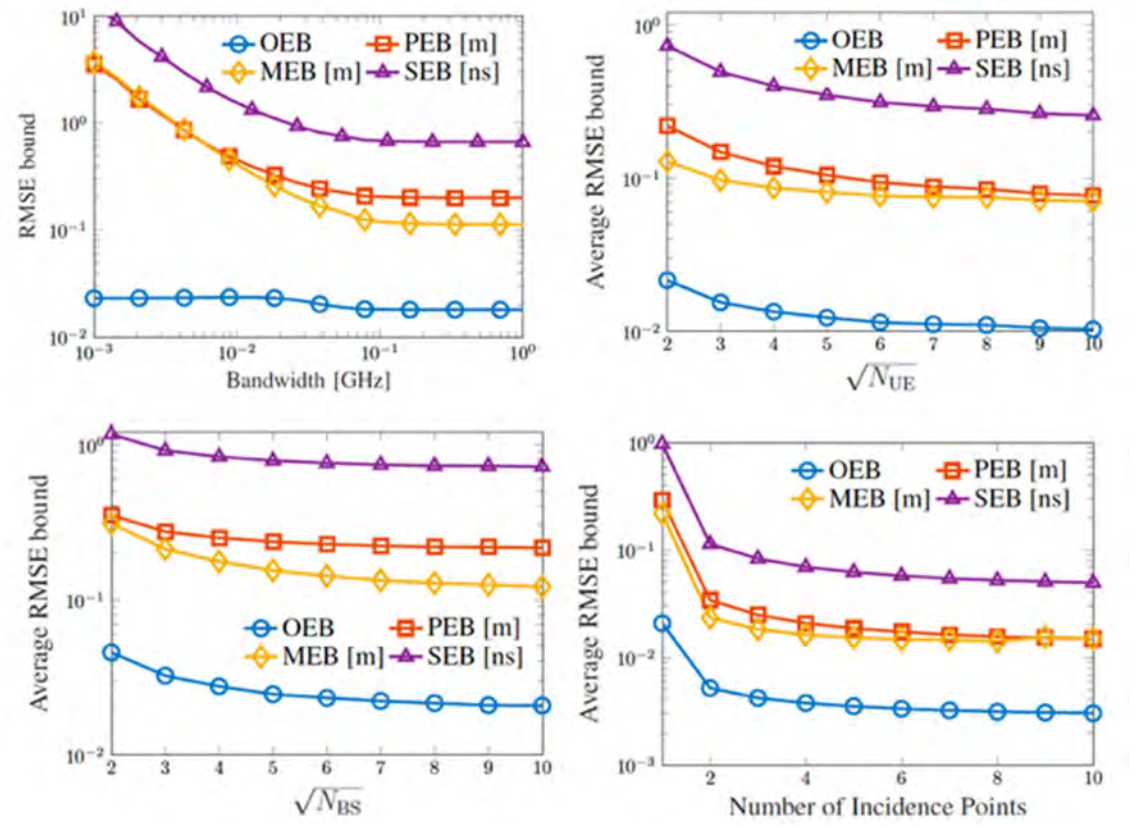

Figure 3-19. Impact of bandwidth (top left), number of UE antennas (top right), number of BS antennas (bottom left), and number of IPs (bottom right) on (average) performance error bounds, i.e., orientation error bound (OEB), position error bound (PEB), mapping error bound (MEB), and synchronisation error bound (SEB).

To evaluate the impact of system parameters, one can plot the root mean square error (RMSE) bounds vs. bandwidth, the number of antennas, and the number of incidence points. As observed in Figure 3-19, increasing bandwidth, which leads to higher ToA accuracy and improved delay resolution, decreases the error bounds. The improvements are, however, limited by the accuracy of angle measurements, even if the bandwidth increases. Similarly, an increasing number of antennas provides finer angle resolution, leading to a decrease in the bounds. However, this is also limited by the bandwidth, especially because analogue combining is used with a fixed number of precoders and combiners there is no array gain.

Finally, the greater number of incidence points, the better quality of the estimation on average. This is mostly because more paths provide more information and improve the

estimation, unless the incidence points are at unfavourable positions leading to poor channel parameter estimation for their corresponding paths.

Conclusions and outlook
Evaluation of a 6D localisation scenario with a single BS transmitting a mmW OFDM signal and a multi-antenna UE showed the feasibility of localisation under the presence of the LoS path and at least one resolvable NLoS path. Given the estimated channel parameters, the localisation routine includes an MLE (a high-dimensional non-convex optimisation problem over a product of manifolds) and an ad-hoc routine obtained from the geometrical analysis. The ad-hoc estimates serve as initialisation to the recursive algorithms for solving the MLE problem. Studying the impact of different parameters, such as bandwidth, number of antennas, number of NLoS paths, etc., through evaluation of CRB, also showed that if 2 NLoS paths are provided, the problem is identifiable for most geometric configurations. However, there are still several scenarios to be explored for future research, e.g., where the LoS is blocked, or under the presence of multi-bounce NLoS paths.

3.3.1.2 Simultaneous localisation and mapping (SLAM)

In the SLAM problem, the goal is to estimate the UE location and orientation, synchronise it with the BS, and provide a radar-like map of the environment by using mmW signals, even if the LOS is blocked [GWK+20].

Methodology
Using the raw waveforms directly in SLAM is challenging due to the high dimensionality of the measurement, the complex nonlinear relation to the UE and landmark states (e.g., position and velocity), and the fact that not all paths may be resolvable due to a limited number of transmitter and receiver antennas and bandwidth. While such direct localisation has performance benefits, we instead consider a layered approach, visualised in Figure 3-20, comprising the following steps after downlink transmission [GWK+20]. First of all, channel parameter estimation is performed to recover the channel parameters (angles, delays, gains). Due to the finite resolution at the receiver side, not all paths are resolvable. Hence, the number of estimated paths will be much smaller than the number of propagation paths. Multiple channel estimators, such as MLE, CS, MUSIC, ESPRIT, and others, can be used. After channel estimation, we group the unordered elements in the measurement set in clusters, where each cluster should correspond to one landmark. This removes the need to consider all possible partitions of the measurements in the SLAM method, drastically reducing overall complexity. As measurements are in a high dimension, we firstly project measurements into 3D points and then apply clustering algorithms like density-based spatial clustering of applications with noise (DBSCAN) on those points. The clustering block only clusters measurements from the same source together, but sources of clusters have not been associated. Finally, after clustering, the SLAM filters, such as the Poisson multi-Bernoulli mixture (PMBM)-based SLAM filters, can be implemented to get the estimates of the UE state (i.e., position, heading, and clock bias) and the map of the environment, which can inherently solve the data association problem.

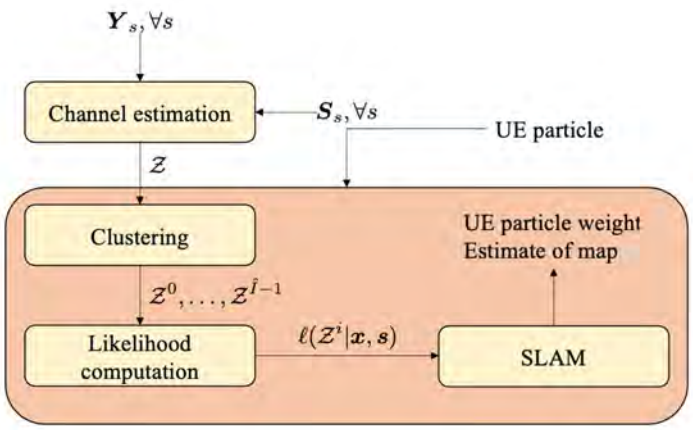

Figure 3-20. The 5G SLAM framework from the observations Y_s.

Results

Consider a scenario with a single BS, a vehicle, and 4 reflecting surfaces, as shown in Figure 3-21. Firstly, we study the performance of the proposed SLAM scheme in mapping. We use the real vehicle states and compare the mapping results of two cases: (1) SLAM filter using all paths in every signal cluster; (2) SLAM filter using the single (specular) path in every cluster. From Figure 3-22, we can find the proposed SLAM scheme can map the environment indicated by the average generalised optimal subpattern assignment (GOSPA) distance. Overall, using all paths is better than using only the specular path, as the solid line is lower in Figure 3-22. The main reason is that using all paths in every cluster provides more information than a single path. Next, we study the performance of the proposed SLAM scheme in UE state estimation. From Figure 3-23, we can see that the proposed scheme is able to estimate UE (e.g., vehicle) positions (in metre), headings (in degree), and clock bias (in metre), and the case using all paths has better performance in positioning, as mean average errors (MAEs) are lower.

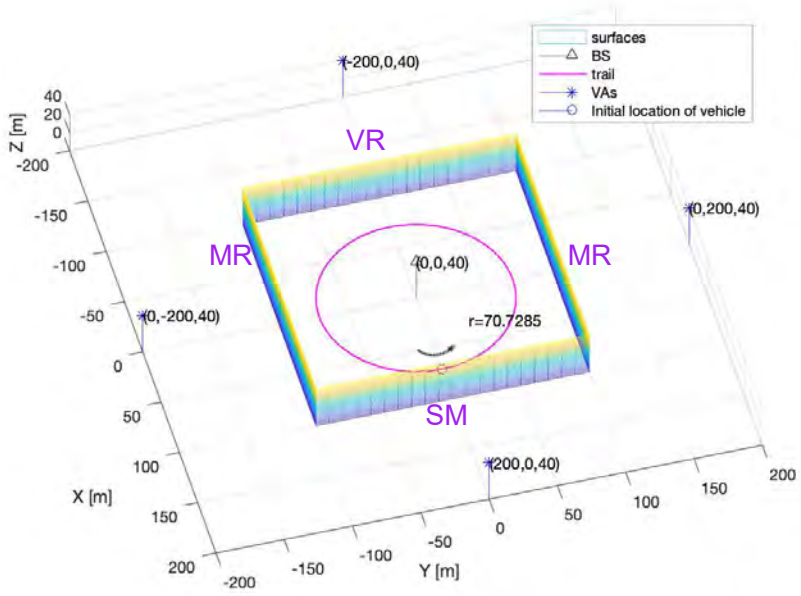

Figure 3-21. The simulation environment with a BS and 4 surfaces. A vehicle moves counter-clockwise along the trail.

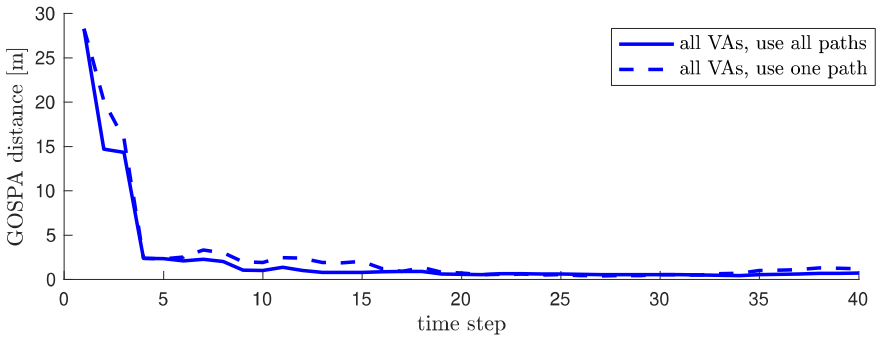

Figure 3-22. The comparison of overall mapping results between two cases.

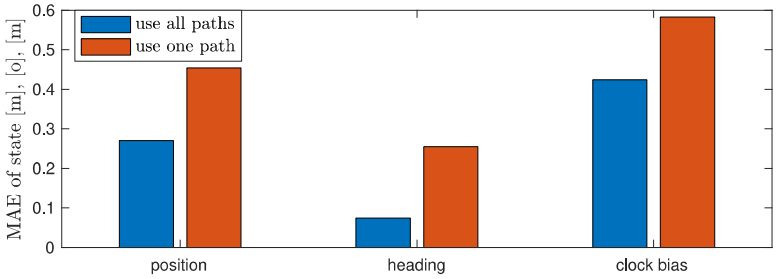

Figure 3-23. The comparison of vehicle state estimation results between two cases.

Conclusions and outlook

The proposed scheme can accurately estimate the UE position and map the environment simultaneously, and it outperforms the scheme using a single path in each signal cluster. The plan includes designing a lower complex channel estimator, using ray tracing data to validate the performance under more realistic operating conditions, and including optimised signal design (precoding and combining) to boost the localisation accuracy.

3.3.1.3 Impact of hardware impairments

Localisation of a user equipment (UE) requires delay and/or angle estimation with uplink or downlink pilot signals. However, hardware impairments (HWIs) distort the signals at both the transmitter and receiver sides and thus affect the localisation performance [CAK+22]. While this impact can be ignored at lower frequencies since the localisation performance is limited, modelling and analysis efforts are needed for 6G to evaluate the localisation degradation due to HWIs. In this subsection, we model various types of impairments and conduct a misspecified Cramér-Rao bound (MCRB) [RH15, FGG+17] analysis to evaluate the HWI-induced performance loss.

Methodology

We consider a simplified uplink scenario with a LoS channel. A BS equipped with an N-antenna ULA is synchronised with a single-antenna UE, both with a single radio-frequency chain (RFC). The assumptions of single-antenna UE, perfect synchronisation, and pure LoS may not be realistic in practice, but are an initial step to analyse and understand HWIs. We set the centre of the BS array as the origin of the global coordinate system. The relation between the AoA θ, the delay τ, and the UE position p can be expressed as $p = \tau c\,[\cos(\theta), \sin(\theta)]$, where c is the speed of light. We select residual phase noise (PN), residual carrier frequency offset (CFO), residual mutual coupling (MC), and power amplifier nonlinearity (PAN). The block diagram of the considered HWIs is shown in Figure 3-24.

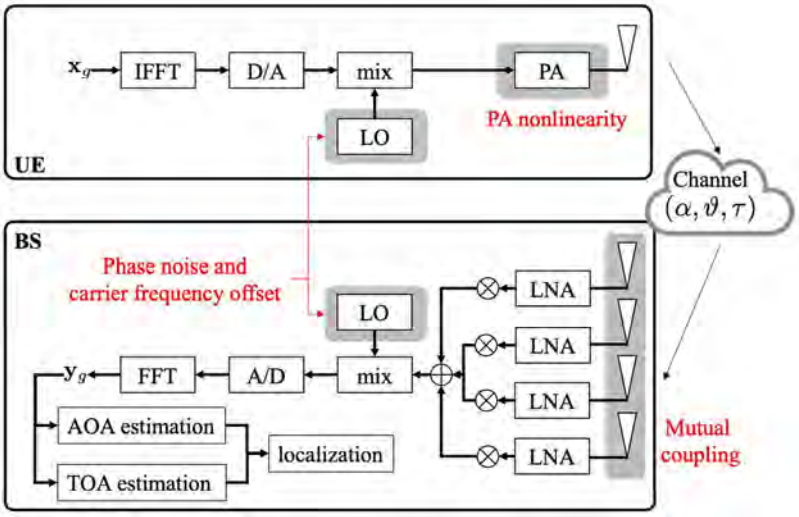

Figure 3-24. Block diagram of considered hardware impairments (marked in gray) at transmitter and receiver. When the localisation algorithm does not have perfect knowledge of the generative model, it operates under model mismatch.

To evaluate the effect of HWIs on localisation, two types of signal models, M1 and M2, are considered. M1 is the true model that considers knowledge of the various HWIs (i.e., PN, CFO, MC, and PAN). M2 is the mismatched model with the practical assumption that not all the HWIs information is available (i.e., the model does not know the PAN and the residual noise of PN, CFO, and MC).

We consider two types of estimators, namely, a MLE and a mismatched maximum likelihood estimation (MMLE). The MLE is employed when the observed signal vector is generated from the same model used by the algorithm (e.g., data from M1 and the estimator uses M1), and we use the CRB to predict the performance in angle, delay, and position estimation under the different models. The MMLE is used when the observed signal vector is generated from a different model than what is used by the algorithm (e.g., data from M2 and the estimator uses M2). For the MMLE, we employ the MCRB [RH15, FGG+17] to quantify the estimation performance loss due to model mismatch.

Results

We first evaluate the position estimation performance of the two estimators (MLE and MMLE). As shown in Figure 3-25, due to the HWIs, the performance using a MMLE coincides with the analytical lower bound (LB) and saturates when the transmission power exceeds *30 dBm*. However, with the knowledge of the impairments, the bound (red curve with square markers) could be lower than the LB (blue curve with circle markers).

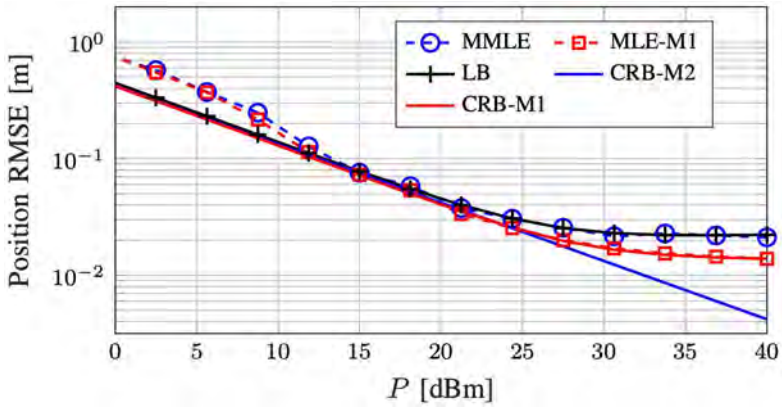

Figure 3-25. Comparison between estimator results and different lower bounds.

To gain a deeper understanding, we study the impact of HWIs on angle and delay estimation, considering different HWIs separately, as shown in Figure 3-26. As a result, we can see those different types of the HWIs affect angle and delay estimation differently.

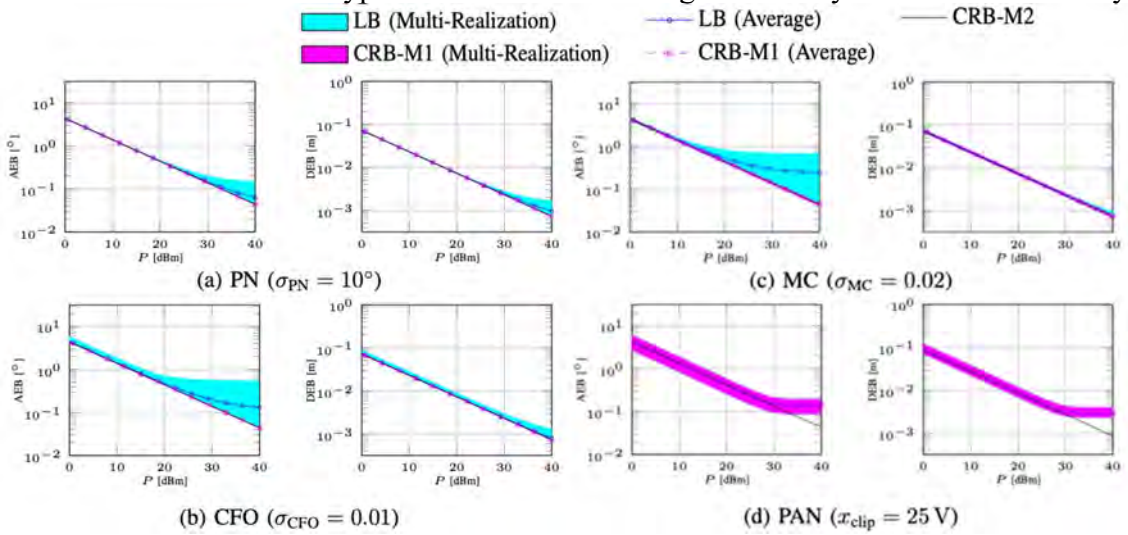

Figure 3-26. Angle error bound and delay error bound for multiple realisations: a) Phase noise; b) Carrier frequency offset; c) Mutual coupling; d) Power amplifier nonlinearity.

We further evaluate the localisation performance as a function of the standard deviation of PN (similar patterns can be seen for CFO and MC) for various values of average transmission power using 100 realisations of PN, as shown in Figure 3-27. The impairments produce a larger perturbation in the high SNR scenario. For low SNR, the noise level is high enough and the effect of the impairments on the PEB is negligible.

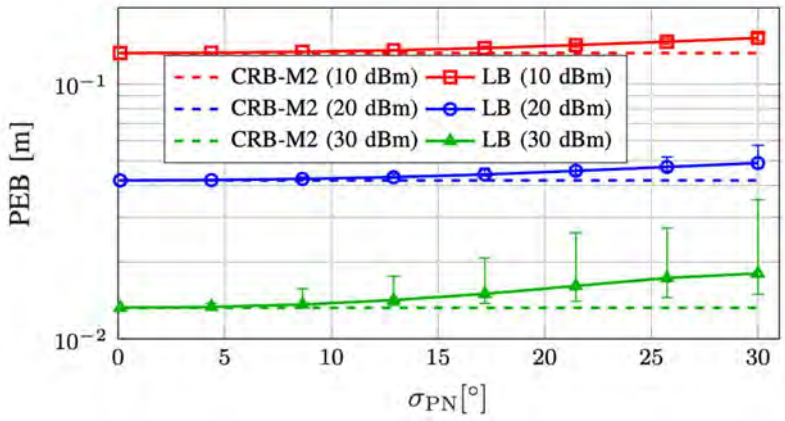

Figure 3-27. PEB vs. phase noise with different transmission power.

Conclusions and outlook

HWIs present a crucial roadblock to achieving high performance in radio-based localisation. We modeled different types of HWIs and utilised the MCRB to evaluate the error caused by the model mismatch. In addition, the effects of residual PN, residual CFO, residual MC, and PAN on angle/delay estimation are evaluated. We found that PN and PAN affect both angle and delay estimation, whereas CFO and MC have a more significant effect on angle estimation. We also observed that with perfect knowledge of the HWIs, the bound is close to the bound of the mismatched model, but will saturate at a certain level in the high SNR regime due to the PAN. In conclusion, dedicated pilot

signal design, HWIs estimation, and mitigation algorithms are needed for accurate localisation in 6G systems.

3.3.2 AI-based localisation and sensing methods

In the previous subsection, we discussed model-based localisation methods. In challenging environments where geometric models cannot be formulated (e.g., many non-resolvable NLoS paths, or under hardware impairment), or when geometry-based localisation cannot handle the processing speed requirements of the system, learning-based methods can be used [CSB+22]. In this subsection, we discuss AI-based methods for integrated sensing and communication under hardware impairments.

3.3.2.1 Integrated sensing and communication

As argued earlier in this deliverable, in monostatic sensing, the communication data can be reused for sensing purposes, as it is known to the radar transceiver. Nevertheless, the signal can be optimised in the spatial domain to favour either communication or sensing performance. However, the optimisation performance of the ISAC systems is sensitive to model mismatch (e.g., optimising using a wrong model that is different from the true model may not provide satisfactory results). The goal of this study is to understand the capability of AI-based data-driven methods for this purpose.

Methodology

A MIMO monostatic sensing scenario and a MISO communication case are considered. The transmitter is divided into an encoder that maps an information message into a complex symbol and a beamformer that steers the antenna energy in a particular direction. The outputs from both networks are energy-constrained as described in [OH17].

The radar channel depends on the presence of a target. If a target is present, the received signal contains the noisy reflection from the target, affected by random pathloss. Otherwise, only the noise is received. The radar receiver chain is divided into a target detector, which estimates the probability of a target in the environment; an angle estimator, which predicts the target AoA; and a variance estimator, whose output is the standard deviation associated with the angle estimation. We apply a threshold to the estimated probability of the target detector during testing to obtain a probability of detection and a false alarm probability.

The communication channel is independent of the target in the environment, and the received signal depends on the AoD from the transmitter, based on the communication receiver location. The communication channel also considers a random pathloss and Gaussian noise at the receiver. The goal of the communication receiver is to recover the transmitted message and minimise the symbol error rate (SER).

Each transmitter and receiver component consists of a feed-forward neural network that is iteratively optimised, represented by blue boxes in Figure 3-28. The input of the beamformer is composed of the beginning and ending angles from the a priori knowledge of the target and communication locations.

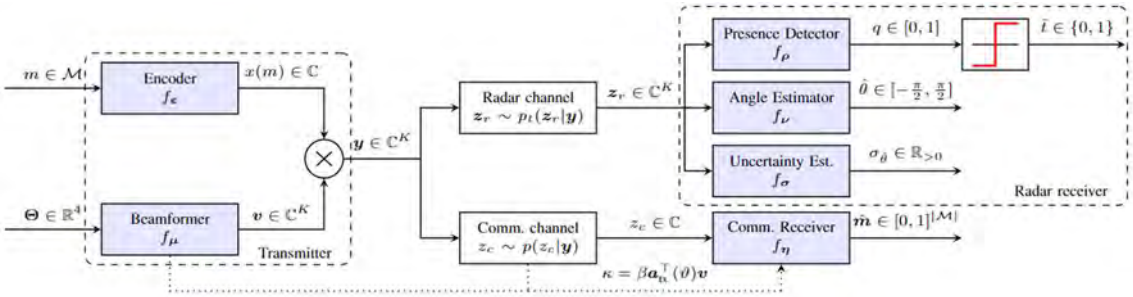

Figure 3-28. Block diagram of the ISAC system model. The highlighted blocks are implemented as trainable neural networks as part of the proposed auto-encoder (AE).

We applied end-to-end learning to train both transmitter and receivers at the same time. It was found that training all four receiver networks simultaneously yielded worse results. Instead, we optimised a radar component together with the communication receiver.
As loss functions, we chose the standard binary cross-entropy (BCE) loss for target detection, the mean squared error (MSE) for angle regression, and the categorical cross-entropy (CCE) loss for communication. In terms of variance estimation, we modelled the angle estimation as a normal unbiased estimator and chose the negative log-likelihood (NLL) loss for this network. Finally, to assess the trade-off between radar and communication, we considered the total loss as a weighted sum of the radar and communication individual losses.

Results

We assumed a uniform linear array (ULA) of 16 antennas at the transmitter, 4 possible information messages and non-overlapping angular sectors for the target and the communication locations, a signal-to-noise ratio (SNR) for the radar channel of *0 dB,* and an SNR of *20 dB* for the communication channel. We also fixed a false alarm probability to 1%. All the layers of the AE are fully connected, and the output layers are designed to meet the constraints of each component's output.
As a transmitter benchmark, we used a quadrature phase shift keying constellation for communication. The beamforming precoder is calculated using fast unit-modulus least squares from [AEL+14, TSF+17]. In the receiver, we apply a ML detector using CSI for communication, and a maximum a-posteriori ratio test (MAPRT) detector [GCH20] for sensing, which generalises the generalised likelihood ratio test (GLRT) detector [CDR01] to the case with random parameters.
We show the ISAC trade-off results in Figure 3-29 (SER vs. detection probability and SER vs. target angle estimation RMSE). Both figures indicate that the trade-off between radar and communication performance for the end-to-end learning approach is close to the baseline. This confirms that ML approaches can perform as good as standard baselines for our scenario.

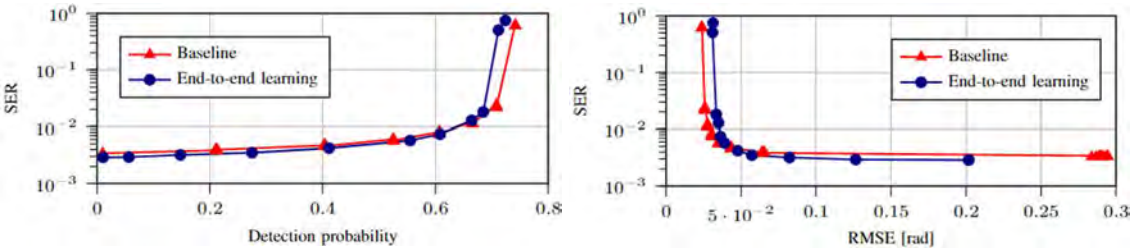

Figure 3-29. ISAC trade-off results without hardware impairments.

Under hardware impairments, we perturb the inter-antenna spacing at the ULA transmitter, assuming a normal distribution centred around half the wavelength. For a

standard deviation of the wavelength over 30, the same ISAC results are depicted in Figure 3-30. We observe that end-to-end learning can adapt to these hardware impairments, whereas standard model-based approach without a perfect model incurs significant performance penalties.

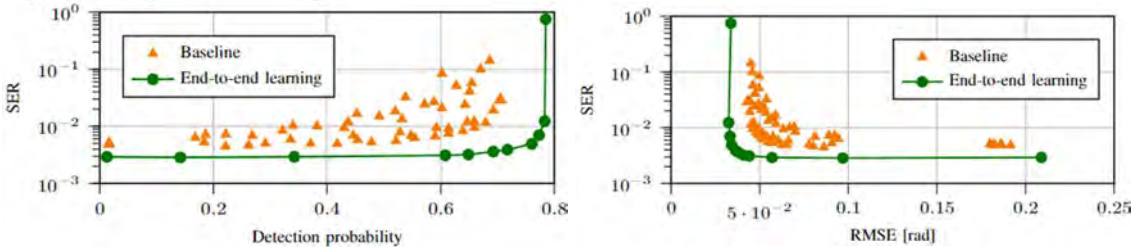

Figure 3-30. ISAC trade-off results with hardware impairments.

Conclusions and outlook

In this work, we have proposed a novel end-to-end AE approach for ISAC, and we have compared the AE performance with standard benchmarks for sensing and communications. Our results demonstrate that the trained AE performs close to the baseline. Moreover, we have shown the robustness of the proposed end-to-end learning approach to account for hardware impairments in the transmitter's antenna array. Some natural extensions to this study include: (i) estimating range through an OFDM system, (ii) using a MIMO communication receiver, (iii) learning across multiple angular ranges, and (iv) making the channel more realistic towards 6G.

3.4 Experimental activities

Several experimental setups are developed within Hexa-X focused on different aspects within the 6G technology. The main purposes of the setups are to make proof of concepts, verify simulation results and demonstrate different use cases. In this work package, a platform has been developed for integrated communication, localisation, and sensing. At first, the concept proof of integrated communication and bistatic sensing has been performed and is presented in this section. Further development of this setup is ongoing and will be extended to a multistatic setup supporting either 2 transmitters and 1 receiver, or 1 transmitter and 2 receivers.

3.4.1 Interference mitigation and coordination

It is acknowledged that interference between sensing nodes will become a severe problem as the number of sensing nodes using time/frequency resources *uncoordinated* increases. Interference can be addressed in three different manners: robust waveforms, reduced likelihood of interference through inter-node communication (non-centralised coordination between nodes), and central resource allocation. These three methods apply equally to both monostatic and bi-static sensing.

The likelihood that two signals interfere with each other can be reduced by using communication and sensing. In this particular case, the focus is on transmitting information embedded in the sensing signal. It is assumed that the underlying system operates at mmW and communication and sensing share the same hardware. Since we are operating at mmW frequencies, where full-duplex is challenging to implement, a bistatic sensing setup is assumed. In the envisioned system, nodes do not communicate directly with each other using a duplex protocol to negotiate the resources (time, frequency) used for sensing. Neither is a central coordination of resources assumed. A practical use-case for such a scenario is where nodes want to perform sensing operations based on bi-static

configurations but have no access to the core network to coordinate the use of time-frequency resources.
Figure 3-31 illustrates the problem to be addressed using three example nodes. Node 1 uses a bi-static (both Tx and RX are located on the same device, but Rx does not have access to the TX signal) setup for sensing the environment. Both Tx and Rx are connected to a common control unit indicated by the dashed line. Node 2 illustrates a node with the same configuration as Node 1, with the difference, that it is only present to provide a sensing signal for nodes in its vicinity. RX2 only has the functionality to listen to the channel and decode other nodes' information. Node 3 is a passive sensing node relying on the Tx signal from Node 1 and 2 to sense the environment. The challenge in such a setup is to avoid interference between the different TX signals. If information on the transmit pattern of a node is included in its transmit signal, other nodes can adopt it to avoid interference. For the lowest overhead, this concept works best if only periodic sensing signals are used, that are mapped into a fixed grid. For example: CPIs of 1ms, 2ms, and 5ms with an update rate of 10Hz, 5Hz, or 2Hz. In this way, each node can create and maintain its channel occupancy grid.

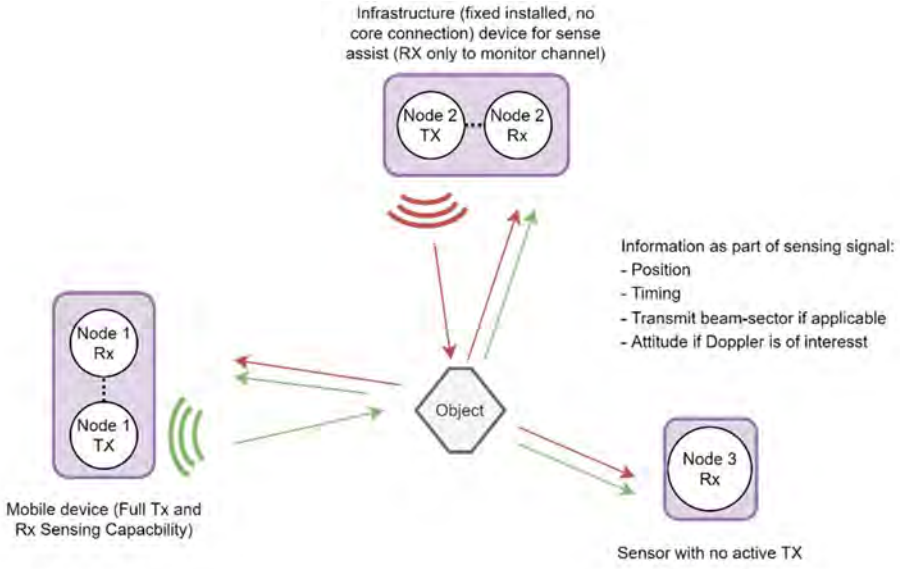

Figure 3-31. Problem formulation and node definition. Green arrows indicate the desired path, while the red arrows represent the interfering path. Note that the direct interference path between nodes is not illustrated explicitly.

Numerical results

In Figure 3-32. , we have illustrated the number of used channels in a system using communication-assisted sensing. The system considered consists of 20 nodes of Type 1, respectively 2 of
Figure 3-31. The different curves illustrate the number of used channels as a function of link miss probability. The different curves represent different interferences distances (dIF). dIF=0m means that the nodes do not interference (low output power), while a dIF=120m implies that a node interferes with all nodes within 120m radius. The link miss probability is the probability that an existing radio link is not detected and will therefore not be considered in the resource selection. The curves show three distinct points:

A. Represents a system operating point where all links are detected, and all nodes can see each other. For the 20 nodes, this means that each node will get an individual timeslot allocated. This would be similar to a resource allocation performed by a centralised unit.

B. No interfering links are detected, and all nodes use the same channel. This corresponds to the Random Access (RA) case.
C. Corresponds to the narrow-beam case and would be represented by a LIDAR system. No other nodes are detected, but no links are missed. All nodes can operate on the same resource.

Note that only a system, that operates in the vicinity of point (A) is suitable for bi-/multi-static sensing. The translation of link miss probability to interfering links is illustrated in Figure 3-33.

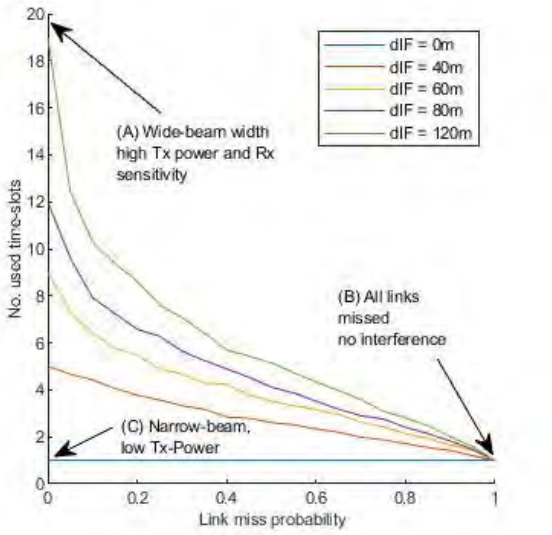

Figure 3-32. Number of used channels vs link miss probability for a system consisting of 20 nodes.

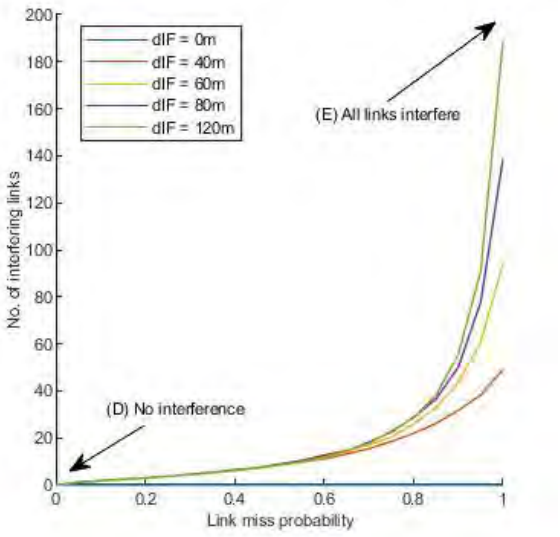

Figure 3-33. Maximum number of simulated interfering links (Interfering Power > SINR threshold for detection) versus link miss probability.

Comparing Random Access (RA) and communication-aided channel access, both methods perform similarly for low channel usage (very narrow beams or the low number of nodes), while communication-aided performs better for higher channel usage. The performance of communication-aided sensing/channel access is mainly limited by:

- Decoding performance (SNR required for decoding sensing information of other nodes)
- Hidden node problem (transmit signal of other nodes is not received but own transmit signal can cause interference)

Note that other access methods like Carrier Sense Multiple Access (CSMA) are not considered since they are not considered in the discussion. These would have to be designed with random pulse repetition interval to be efficient.

3.4.2 Performance evaluation

The first demonstration of integrated sensing and communication has been performed using a bi-static setup with a carrier frequency of 69 GHz. The tests were performed with a distance of 8 m between the transmitter and receiver and with one wall for signal reflections. The setup is shown in Figure 3-34, where the transmitter can be seen in the top left of the picture, the receiver in the bottom right, and the glass wall to the right is used for reflections.

Figure 3-34. The demo setup area with the transmitter in the top left of the figure and the receiver in the bottom right.

The transmitted signal is based on the 5G NR standard, but with an increased subcarrier spacing of 960 kHz and a bandwidth of 400 MHz. A single SSB block is used for synchronisation, while the rest of the signal consists of Physical Downlink Shared Channel (PDSCH) and PDSCH Demodulation Reference Signal (DMRS) data. In both the communication and sensing part, no noticeable difference in performance can be observed between the OFDM and Discrete Fourier transform-spread orthogonal frequency-division multiplexing (DFTS-OFDM) waveforms. In Figure 3-35, the 16-QAM constellation diagram is shown for the OFDM waveform.

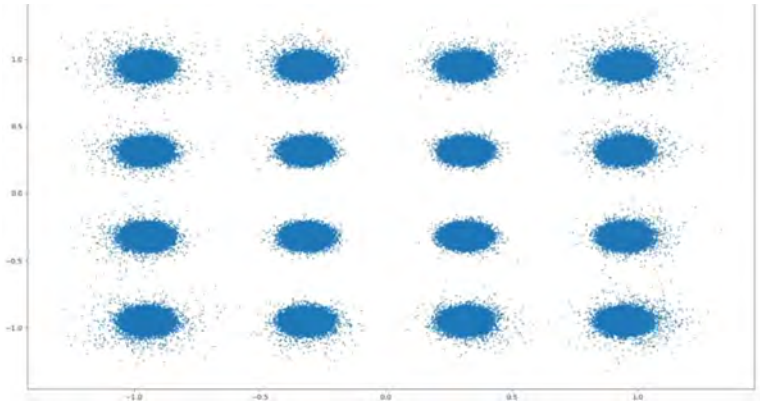

Figure 3-35. To illustrate the communication capability of the setup, we use the constellation plot of a 16-QAM OFDM signal with 960 kHz subcarrier spacing and 400 MHz bandwidth.

For the sensing demonstration, the same waveforms were used, but the beam sweeping capability of both Tx and Rx were utilised. After the initial synchronisation, the beams were changed in a synchronised pattern using 50 different Tx beams and 56 different Rx beams. The signal power for all different beam pair combinations were measured, making it possible to identify the directions of beam reflections. The distance is obtained via channel estimations for each beam pair combination. To add some more complexity and interactivity to the sensing measurements, several measurements were performed while a person was walking by. The results from the measurements can be seen in Figure 3-36, Figure 3-37, and Figure 3-38. The figure in the bottom left shows the received power as a function of the beam directions. On the y-axis is the Tx beam direction, and on the x-axis is the Rx beam direction. The strongest combination is when both modules have beam index 0, corresponding to the line-of-sight path. Another strong combination can be seen around Tx index 45 and Rx index 32. This corresponds to the reflection in the glass wall. As seen in the figures, these peaks are constant for all three measurements. What can also be seen is a much fainter peak at Tx index 32 and Rx index 18, which in the following measurements move to (22,27) and (12,42), respectively. This peak originates from the reflections of the person walking by.

The second plot, which can be seen in the three figures, is a range plot; it indicates the distance to the reflected surface. This setup has been calibrated to be 0 m for the line-of-sight path, meaning that all the other peaks show the distance difference relative to the line-of-sight path. In all the three figures below, the peak corresponding to the line-of-sight path at 0 m is clearly visible, and the peak around 5 m corresponds to the reflection at the glass wall. Between these peaks, there is an additional smaller peak corresponding to the person passing by. As can be seen in the figures, this peak does not change much between the different measurements. The reason for this is that the person is moving in an arch between the transmitter and receiver; this has the consequence that the length of the signal path is the same for all the different measurements, and hence the peak in the range plot will not change.

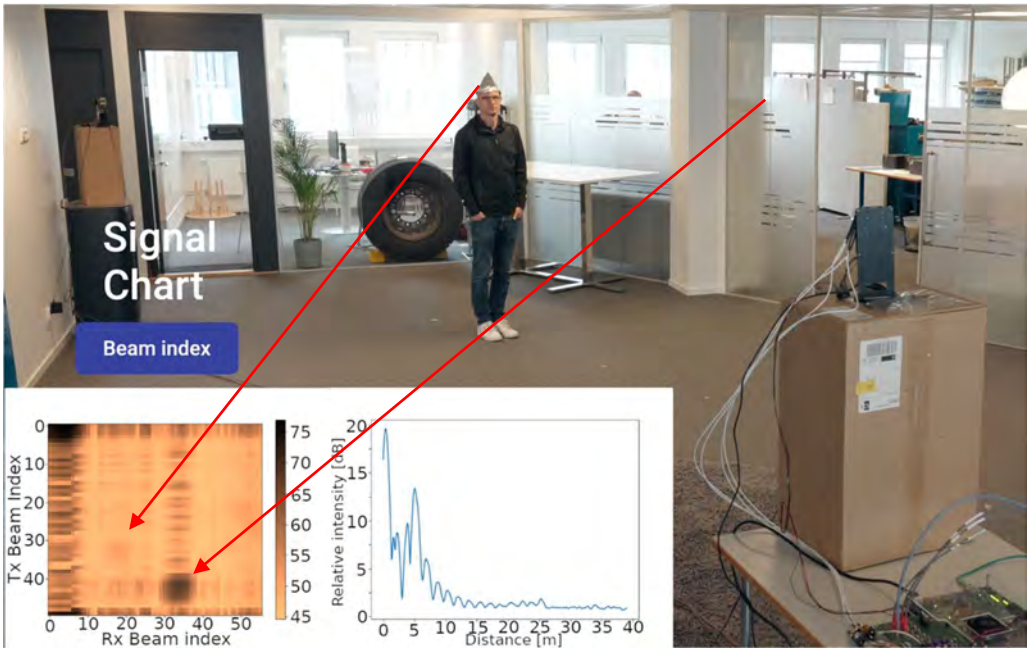

Figure 3-36. Demonstration of sensing. The left figure shows the received power as a function of beam directions. Beam index 0 corresponds to the direction where the Tx and Rx modules point towards each other. The larger the beam index, the further away towards the glass wall the beams are pointing. The right figure shows the range plot where the peak at 0 m corresponds to the line-of-sight path, and the reflection in the glass wall causes the peak at 5 m. The small peak between these peaks comes from reflections of the person in the picture.

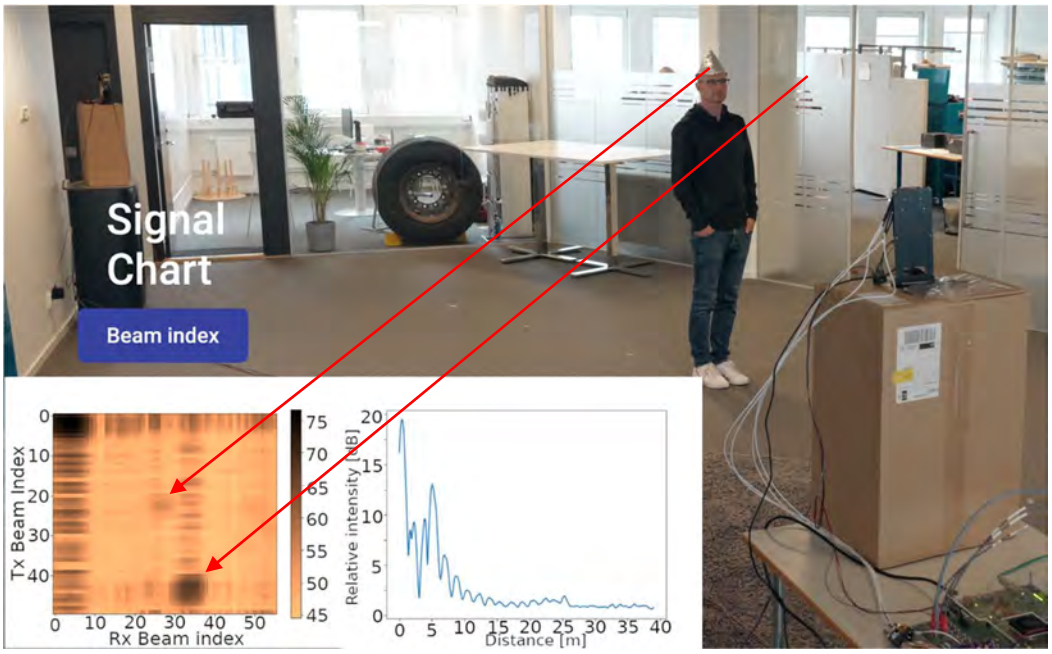

Figure 3-37. As the person moves, the faint peak in the left plot is also moving, while the stronger peaks are constant as they originate from reflections at static objects.

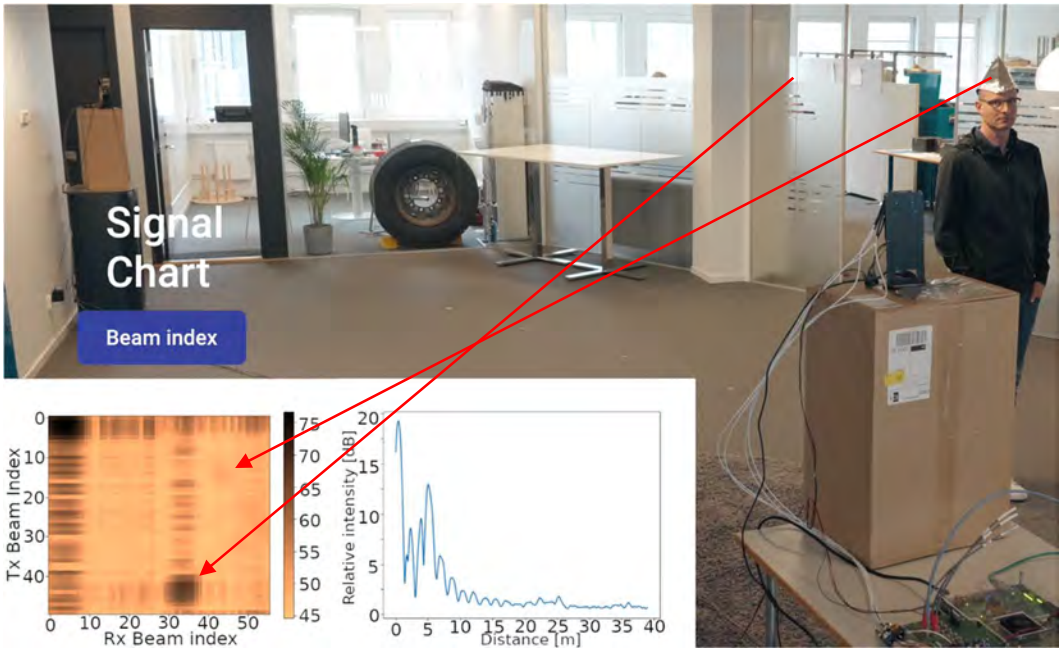

Figure 3-38. Once again, the person has moved, and the change can be seen in the left plot. It can also be noted that the range plot does not change much between the pictures because the distance in the signal path does not change much even though the person is moving.

The results from these measurements can also be found in the form of a video on the Hexa-X YouTube channel at https://www.youtube.com/watch?v=8uNwjm5FvL4.

4 Enhanced location and sensing services

With the further enhancement of the UE localisation capabilities and the introduction of the new sensing features, such as radar-like localisation (without UEs), localisation and sensing services will gain in importance and play a key role alongside the core business of offering communication.
Location and enhanced sensing services will be the base for new and emerging context-aware services, e.g., geofencing and other applications based on such services. Section 4.1 will highlight some specific use cases where this interplay of different services is motivated.
A core benefit for next-generation mobile communication is the location and sensing information availability to enhance communications and vice versa. Hence section 4.2 shows examples and the first results of how this optimisation process could look like.
Section 4.3 deduces requirements for the whole ecosystem and the interplay between sensing, localisation, communication, and further relevant services such as geofencing, digital twins, etc. These requirements are based on the selected ecosystem use cases of section 4.1 and the ongoing technical work done within Hexa-X regarding connecting communication and localisation/sensing services to enhance the overall performance. The goal is to enable the interaction between services to create an ecosystem for new and emerging services and applications.

4.1 Enabling and enriching applications

This section focuses on aspects how localisation and sensing can enhance certain use cases. Firstly, security use cases (section 4.1.1) are mentioned, elaborating on how location information can enhance security use cases, secondly, non-radar type sensing (section 4.1.2), for example, weather monitoring, and finally factory optimisation (section 4.1.3).

4.1.1 Location information to enhance security use cases

Many use cases exist that deal with security applications and are based on the availability of correct, uncompromised location information. The following list highlights some examples:

- **Secure track and trace:**
  In logistics, track and trace determine an item's current and past locations (and other information). For example, suppose valuable goods, e.g., cash, is transported. In that case, the position of the used vehicles or transport containers can be tracked to verify whether the vehicle or transport container takes the expected route. Likewise, a robbery can be detected, e.g., if the vehicle is hijacked or the transport container is stolen.

Figure 4-1. Track and trace visualisation

- **Location-based access control:**
  Also, access to IT systems or manufacturing equipment can be secured with the location. Location-based access control (LBAC) will ensure that only people or devices located at a certain location, for example, within a special room can access special systems or features of a system. For example, for operating safety-critical machines using a wireless panel as a user interface device, it has to be ensured that the user operating the panel is nearby the controlled machine.
- **Geo-fencing for mobile machines:**
  Mobile automated teller machines (ATMs) set up, for example, in rural areas where less bank branches exist or for special occasions, such as festivals, can be equipped with a localisation sensor. The ATMs shall only work as long as they are located on the specified site. The ATM should be disabled if the location changes and notification messages are sent. The goal is to minimise misuse. Such a feature is also called "geo-fencing," ensuring that a device operates only within a defined area.
  Similarly, construction machines for rent shall only function while on the construction site. The business case is built on the knowledge of where the machines are located at every time. Therefore, machines shall only function during booked rental periods even though they might reside longer on the construction site and will be picked up at a later point in time. A further use case for geofencing is firearms that can be used only within a defined region.
- **Security gates:**
  This scenario is rather straightforward. Security gates, for example, at the entrance to factory premises or other restricted areas, e.g., in airports, offices, or data centres, require that each person be identified, and access rights verified before granting access. Normally, this is realised by speed gates or portal turnstiles to ensure that only one person can enter at a time and some identification mechanism such as badges or tickets. If the identification and access right check were successful, the gate will let this one person pass. If identification and access right verification can be realised based on the current location in front of the gate, humans would not need to interact with gates as the access right management system could automatically notify which person is approaching.

The above-mentioned security use cases benefit if the localisation information is secured in two ways: First, the location information shall be determined in a secure uncompromised manner, and second, it must be provided in a secure way to the entity relying on the position information, while protecting it against unauthorised use. Some use cases may require that the location information can also be proved to third parties at

later times. Multiple sensors with heterogeneous hardware and software may also strengthen the trustworthiness, and sensor fusion could enhance these use cases. But not just use cases focusing on security application require protection against cyber attacks. The next generation mobile networks must ensure security over all levels.

4.1.2 Non-radar type sensing

The typical sensing using radars includes detecting the target and estimating its parameters such as velocity, range, etc. In this section, we discuss sensing from a perspective which is different from estimating the range and Doppler of the target. One such non-radar type of sensing is sensing the landscapes around the UE.

4.1.2.1 Landscape sensing

The landscape around the UE indicates the macro environment around the UE, such as forests, streets, buildings, waterbody, etc. Sensing the landscape around the UE can have several benefits; it will aid the BS in tailoring the signal to the UE. For example, if the UE is in the forested region, then BS can adapt the signal towards the UE to counter extreme propagation conditions due to foliage, vegetation, etc. Furthermore, knowing the landscape around the UE can help the BS predict the likelihood of handover and aid in mobility management. It can also enhance the digital twin representation of the UE for improved 6G network management [YHS+21].
6G wireless systems need to support stringent connectivity, throughput, latency, and other requirements to satisfy various use cases [SBG+19]. To support these 6G wireless systems will have wide bandwidths and are deployed densely. These dense deployments can be leveraged to perform cooperative distributed sensing using multiple network nodes to perform macro sensing of landscapes around the UE.
If the UEs have radars built in them, they can easily sense the environment around them; for example, in [WZ09], authors use the synthetic aperture radar (SAR) to detect the parking lot environment. However, most of the network's UEs do not have radars. Another approach could be to use a GPS sensor or PRS signal to localise the UE and use the geographic information system (GIS) server with high-resolution maps to draw inference on landscapes. These discussed methods require UE to have external aid in the form of radars, sensors, signalling, etc., which limits its applicability to a wider set of UEs in the network. Therefore, sensing the UE landscape without any external aid is preferred. Below we discuss an AI method which employs computationally efficient feature engineering and leverages the dense deployment.

System and method
To illustrate the proposed method, we consider a simple two-node network, as shown in Figure 4-2. Here, we show two UEs, one in an urban canyon and another in a forested area. The UL multi-path profile carries information regarding the UEs environment. Harvesting the multi-path profile from multiple BS provides higher diversity due to the different geometric perspectives of the same observation. However, with this approach, there will be significant communication between BSs as the non-serving BSs have to report the multipath profiles to the serving BS to infer the macro environment of the UE. Also, the AI method must work on large dimension data, which can be computationally intensive, especially for embedded BS hardware. To ameliorate these issues, we represent the multi-path profile of the link using a single large-scale statistic such as path-gain, a representation of which can be obtained in the form of reference signal received power (RSRP) of reference signals [YHS+21].

To illustrate the AI method, we consider a deployment with K BSs. The training set is constructed by randomly dropping the UEs across different landscapes and collecting the path gains. This training set is used to supervise the AI agent [YHS+21].

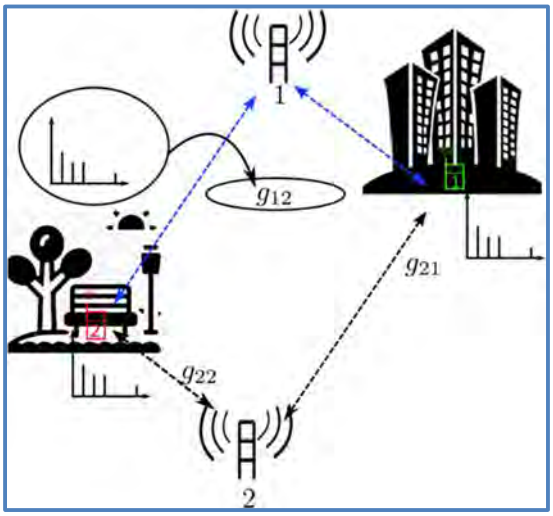

Figure 4-2. Illustration of the UEs in forest and urban landscape; Two BSs are serving them. The landscape around the UE can be detected by harvesting the path gains from multiple BSs.

Only N dominant path gains are considered in the classification of the landscapes. Several AI methods are feasible, we chose the random forest algorithm since it is robust against outliers and performs well for non-linear classification. The random-forest algorithm is described in [BDR+21]

Results

We use London city with its rich urban environment for evaluating the performance. We consider $K = 54$ BS deployment operating at 5 GHz. The typical landscape categories considered are forests, streets, buildings, barren-land, etc. We use simulation data from a ray-tracing propagation model on a 1 km^2 section of London city. An AI agent using the random-forest algorithm is trained from the simulator data to access the performance.

Binary Hypothesis: In this problem, we try to answer the hypothesis questions such as "Whether UE is on the street?". Answers to these can aid the network in taking appropriate actions to optimise performance. We binarise the labels depending on whether UE is in the particular type of landscape, as described in equation (5) of [YHS+21].

The results for the two types of landscapes, street and forest, are accessed through the precision score. The precision score is defined as the fraction of the true positives to all positives (true or false). The precision score is an important metric since detecting the UE in a landscape will trigger the network to take certain actions that can be catastrophic in case of the false alarm. The performance for the street and forest landscapes is shown in Figure 4-3. Notice that performance improves with the increasing N (more BSs collaborating) and achieves greater than 90 percent with $N > 10$. Performance of the detector against perturbation noise indicates the robustness of the AI agent against measurement uncertainties. From the results, one can conclude that with sufficient densification and collaboration between BSs, it is possible to perform macro-level sensing of the UE environment.

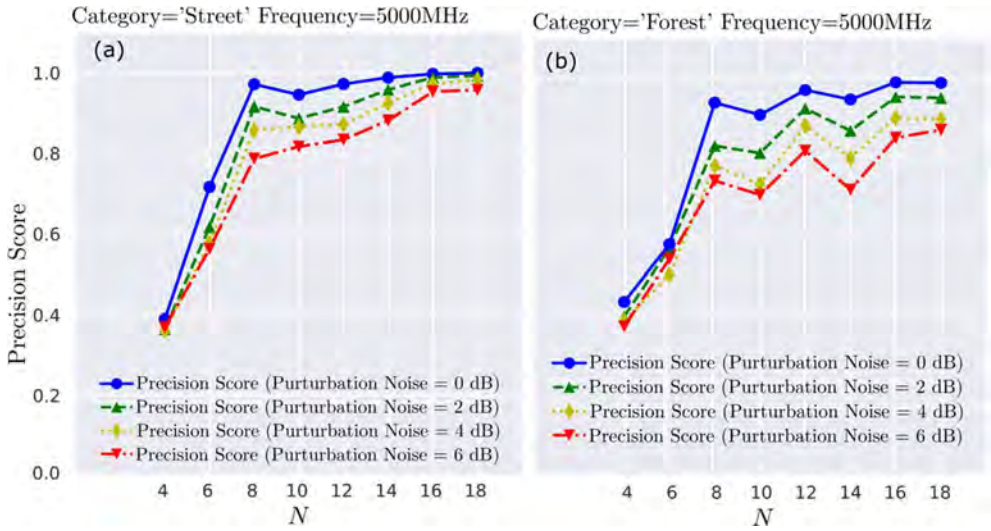

Figure 4-3. Performance of random-forest based AI method for "Forest" and "Street" landscape detection for a section of London city.

Multiple Hypothesis: Here, we discuss the method where we are interested in identifying the correct landscape among many potential landscapes. We use the same feature set consisting of path-gains observations from multiple BSs. We consider the landscape categories such as street (category-class 11), building (category-class 15), and barren-land (category-class 4) for the classification problem. We used landscape category-class 0 to indicate that UE is in neither of the landscape categories 11, 15, and 4. The proportions of the landscape categories in the training data play a crucial role in the agent's performance. Figure 4-4a shows the ratio of different landscape categories from the London map considered. For multi-label classification the typically prediction results are expressed through confusion matrix with diagonal elements indicating the detection accuracy and off-diagonal entries indicating the misclassification towards a particular label. The confusion matrix of the random forest algorithm with $N = 64$ for the multi-class classification is shown in Figure 4-5a. The performance of the algorithm can be improved by re-sampling the training set so that the class ratios are as shown in Figure 4-4b. The agent trained with this data set yields improved performance, as shown in the confusion matrix in Figure 4-5b. Even though the overall performance improved, the performance of the dominant classes, such as "barren-land" has slightly deteriorated. Based on the applications, the class ratio needs to be controlled to achieve the right detector performance trade-off.

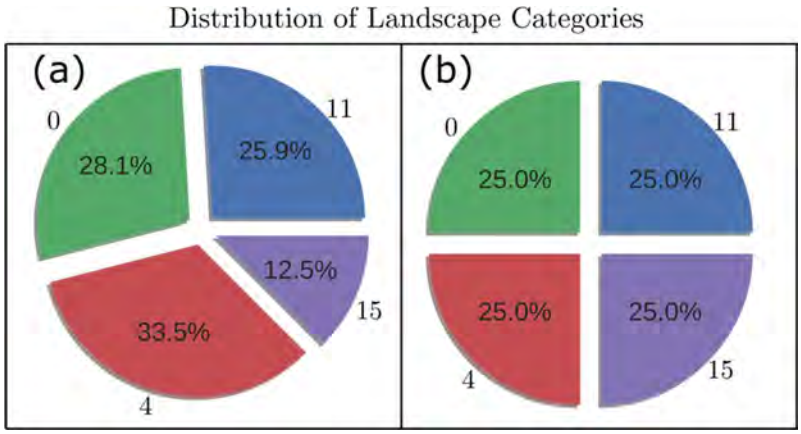

Figure 4-4. The ratio of landscape categories 11, 15, 4, and 0 for the section of London city considered for simulation. a) Class-ratio as per the map; b) Class-ratio after re-sampling the features for balancing the classes.

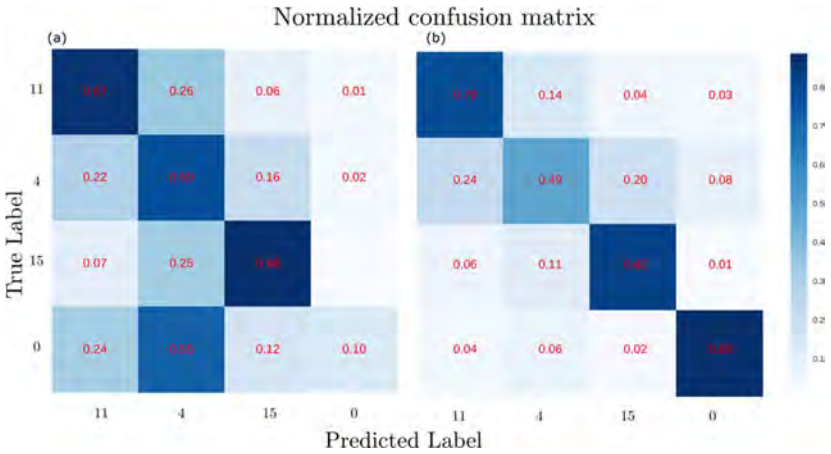

Figure 4-5. The confusion matrices. a) Before class-ratio re-balancing; b) After class-ratio re-balancing.

4.1.2.2 Contextual sensing

Typical contextual sensing algorithms deal with identifying the target context, which can aid in the higher-level tasks. For example, sensing the context that the user is in a movie theatre can aid in silencing the notification alerts. Similarly, sensing the context that a user is crossing the road can help BS to alert an approaching connected automobile [CBS+12][SH16].

Contextual sensing can be performed in an active or passive way. In the active sensing of context, typically target uses its communication capability to share its sensor values with the anchor-node or edge server where the complex algorithm senses the context. In contrast, in passive context sensing, the target does not have communication capabilities; typically, the context is detected through the perturbations in the environment. Below we describe active sensing of human activity using inertial sensor values captured from the accelerometer and gyroscope.

4.1.2.2.1 Human Activity Detection

The goal of human activity detection (HAD) is to identify common activities such as sitting, standing, walking, etc. HAD can aid in applications such as industrial control to prevent accidents; these algorithms can aid in elderly care such as assisted living. The algorithms can also aid in medicine by detecting coma patients when they wake up, so that necessary first aid can be provided. HAD methods can assist in identifying

neurological disorders; for example, when patients have brain strokes such as haemorrhagic or ischemic strokes, they vibrate and fall in a certain pattern which can be identified by these algorithms to reduce the door-to-needle time.
For this work, we used the publicly available dataset from the University of Genova [AGO+13]. The dataset consists of 30 subjects performing various daily activities. These activities include static activities such as sitting, standing, and laying, and dynamic activities such as walking, climbing upstairs, and descending downstairs, as shown in Table 4-1.

Table 4-1. Activity descriptions.

Activity-ID	Activity-Name	Type
1	Walking	Dynamic
2	Walking Upstairs	Dynamic
3	Walking Downstairs	Dynamic
4	Sitting	Static
5	Standing	Static
6	Laying	Static

The measurements are captured using a tri-axial accelerometer and gyroscope in X, Y, and Z directions at the rate of 50 Hz. The data is collected in windows of 2.56 seconds (128 samples). The data from 21 subjects is used for training the algorithms, and the data from the remaining 9 subjects is used for testing purposes.

AI methods for HAD
In order to detect human activities, two types of algorithms are developed. The first type of algorithm uses a deep understanding of the domain to perform appropriate feature engineering to convert the raw samples into relevant features, which are subsequently used for classification. Another class of methods is feature agnostic and works directly on the raw samples to arrive at the inference on human activity. With feature engineering-based methods as the upper bound, we want to understand whether feature agnostic methods come close to feature engineering-based methods.
Feature-based methods: Here, we used 561 features extracted from the time-domain samples. First, the time domain raw samples are converted into many other time and frequency domain samples. These include constructing the jerk signal by taking the derivative of the acceleration and angular velocity. Then, fast Fourier transform is applied on the time-domain waveforms to form frequency domain samples. Finally, various features are extracted by considering the statistical parameters such as mean, variance, kurtosis, entropy, etc., of these time and frequency domain samples. The results after applying the support vector machine (SVM)-based supervised classifier [BGV92] using the 561 features are shown in Figure 4-6. Notice that all the activities can be detected at high accuracy of greater than 90 percent. However, the confusion matrix shown in Figure 4-7 indicates that there is confusion in resolving the activity, such as sitting and standing for some of the activity.

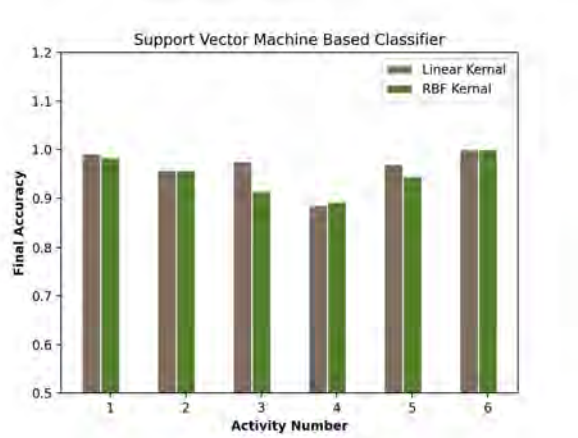

Figure 4-6. Accuracy of the detection of various human activities. Refer to Table 4-1 for activity descriptions.

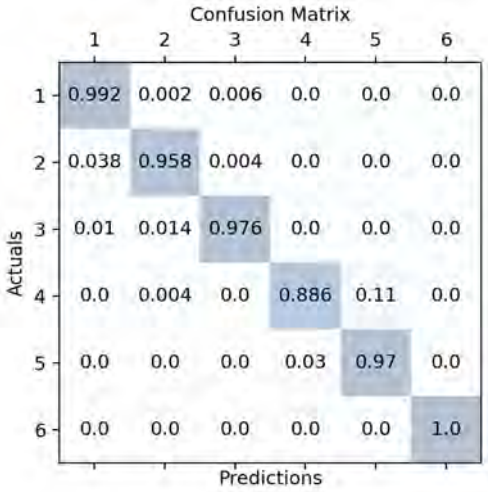

Figure 4-7. Confusion matrix for the classification of various activities.

Feature agnostic methods: Here, we employ an AI pipeline similar to image processing and recognition algorithms. We use a stack of 1D convolutional neural network pooling followed by a fully connected network. The performance of the algorithm is shown in Figure 4-8.

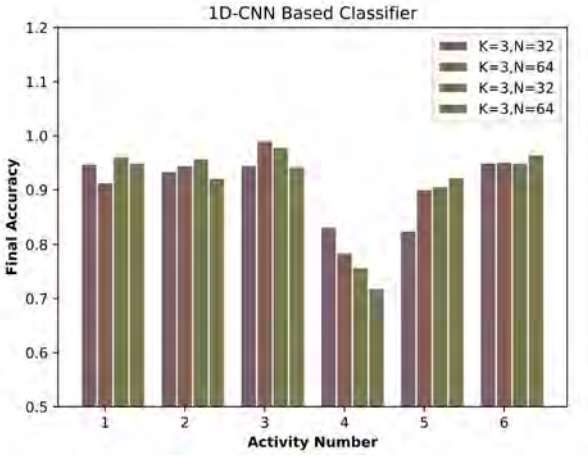

Figure 4-8. The performance of the proposed feature agnostic method. K indicates the kernel size used in the 1D convolutional neural network, and N indicates the number of filters used.

Results indicate that feature engineering-based AI methods such as SVM yield very high accuracy in detecting human activity. Furthermore, though there is a slight loss of performance when feature agnostic methods are used, they come close to feature engineering methods. This indicates that when deep domain expertise or modelling of the observation is complex, one can use feature agnostic methods and still achieve comparable performance to the feature aided methods.

4.1.2.3 Sensing information to enable novel weather monitoring applications

Although sensing is often assumed as the function of range and velocity estimation, there are several applications where channel knowledge can be used for a general understanding of the environment beyond the location and velocity of certain objects in the surrounding. One such application is weather monitoring which includes particle or pollution detection and rain and snow detection.

In the case of rainfall measurement, the principal idea is that electromagnetic waves in the 10-100 GHz microwave bands are slightly weakened by rain. By measuring the attenuation and comparing the historical data, the density of rainfall can be measured for a single link between a transmitter and receiver. Figure 4-9 illustrates how the method works in rainfall measurement by means of measurements on the received signal in a microwave link (between base stations).

Attenuation on the link caused by the rain is processed in the network, and by combining it with information from links in the entire grid, a high-resolution picture of the rain can be plotted and mapped. It has been shown in a field test [EMR16] that rain measurements can be done at far better resolution with higher accuracy than other methods and be deployed globally to support millions of people living in areas where current technologies have not been deployed due to high costs.

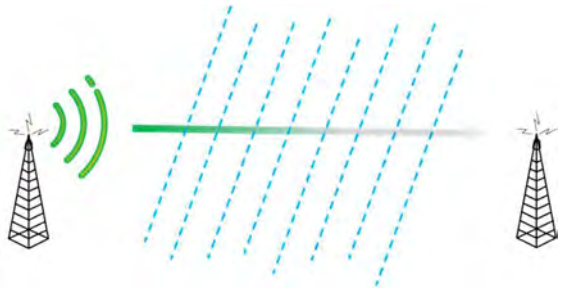

Figure 4-9. Rain measurement by the sensing.

Table 4-2. shows a comparison of different rainfall measurement methods. Compared to traditional methods of rainfall measurements used in meteorologies, such as rain gauges that have a high time resolution of several minutes and a coverage area of a few dm^2, microwave sensing of rainfall provides time resolutions in the order of 10s of seconds and a coverage area as large as 100 of square meters. Also, compared to weather radar, a microwave radar has better time resolution and a smaller coverage area. But as we mentioned before, the collective measurements from all links in an area provide the weather map, which can be several hundred kilometres radius. Therefore, the spatial resolution of microwave weather is much larger than rain gauge's and about the same as weather radar. However, this is not necessarily a limitation since high resolution in space has an insignificant effect in any use cases. Also, the ground-level measurement of microwave link accuracy is rather good since the link is only 10 meters from the ground. A weather radar measures hundreds of meters above the ground level, while a rain gauge is at the ground level.

Table 4-2. Comparison of different rainfall measurement methods.

	Rain gauge	Weather radar	Microwave link
Time resolution	15 min	5-15 min	10 s
Spatial resolution	~2 dm^2	~1 km^2	~ 100 m
Coverage area	~2 dm^2	~200 km radius	~ 100 m
Accuracy on the ground level	Very good	Not good	good

It is foreseen that higher carrier frequencies are more commonly used in 6G for data transmission as well as positioning and sensing, which makes its access layer as well as the microwave backhaul link better suitable for high accuracy weather sensing as a service on the top of communication at almost no additional cost.

4.1.3 Location, sensing, and map information to optimise factory environments

The vision of the I4.0 (Industry 4.0 / 4th industrial revolution) scenarios is all about the digitalisation of enterprises and described in more detail in [HEX22-D72]. By generating, combining, and analysing data, the processes and decisions within factories and enterprises can be optimised, automated, and accelerated. The digital transformation of enterprises means combining the digital world with the physical world and is based on a comprehensive digital twin. For the industrial internet of things, where collaboration and interaction between things are essential, both communication and localisation (plus sensing) are essential, as flexibility of assets within factories relies largely on reliable wireless communication and the knowledge of the current location of both mobile and stationary assets and their surrounding/environment/maps. But the enterprise digital twin will need more: A flexible and interactive ecosystem of services and applications. Geo-fencing, for example, is the combination of process know-how, asset know-how, environment know-how, and position information of the asset.

As a simple example in automated guided vehicles (AGV): *if AGV_579 (asset id) enters (position of asset, a combination of asset ID and UE ID) maintenance area (environment, map information), then slow down for human-robot collaboration (process know-how and safety lidar sensor to detect human).* It becomes more and more complex if additional rules and KPIs are added. Although the scenario is just as before, when entering the maintenance area, the communication between AGV and its backend services needs to be optimised (the more bandwidth, the more reliability) to update the firmware of the AGV and run the safety-critical tests. And the worker uses augmented reality glasses to receive repair notifications.

And if another KPI is to optimise routes and trajectories of all AGVs on site, an additional optimisation step would be that AGVs should only enter the maintenance area if their route bypasses the maintenance area and maintenance is required. Trajectory planning, current localisation, communication planning, AGV maintenance requirements, and process know-how must go hand in hand to enable that scenario, as shown in Figure 4-10.

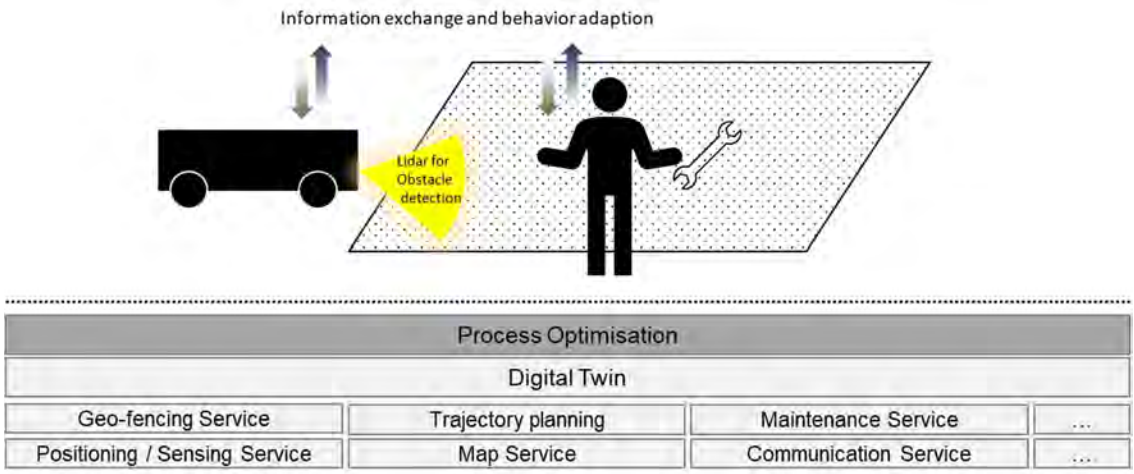

Figure 4-10. Sketch of AGV maintenance area and some required services

Certain KPIs can only be optimised if seamless information exchange is possible. Next-generation mobile networks must enable different access levels to information such as sensing and localisation data with a well-defined exposure framework. The interplay with non-6G services must be envisioned, and sensor fusion with non-6G technologies (such as Lidar, Cameras, BLE, UWB) for sensing and localisation purposes must be realised.

4.2 Enhancing communication services with location and sensing information

The interplay between communication and sensing with radio waves has the potential to enable novel use case families and provide side information to improve communication performance. Furthermore, local networks enabling proximity-based interactions between cooperative devices can take advantage of location information to establish radio links and share radio resources. In this section, the potential of sensing with radio waves is discussed, regarding localisation, mapping, and tracking, aiming at enabling new use cases and applications and improving communication aspects of the 6G systems.

4.2.1 Context-aided communications for dynamic blockage avoidance

Background

In 5G and beyond, users expect similar communication performance inside moving vehicles as the one at home/office, e.g., fixed wireless access (FWA). In addition, emerging applications such as video chat and online stream onboard require a high data rate. From another perspective, connected vehicles such as platooning and autonomous vehicles can realise advanced traffic features, which require reliable communication links to satisfy the need for a stable control loop. Moving relays (MRs) and connected vehicles are two main use-cases for Internet-of-vehicle (IoV) communications, and they require up to 99.99% reliability and up to 1000 Mbps data rate depending on specific scenarios [GMB+21].

The stringent quality of service (QoS) requirements call for developing advanced communication technologies, among which network densification and utilising mmW frequency bands are the dominant ones. Deploying multiple BSs could densify the network with more resource blocks, while using mmW technologies provides wide frequency bands and multi-antenna potentials, e.g., MIMO. In addition, massive BS

deployment utilising mmW could boost the system performance in terms of efficiency and reliability.
On the other hand, due to the physical features of mmW that the signals are highly sensitive to blockages, the qualification of mmW communications could be affected by e poor propagation characteristics and high path loss. Also, IoV communications face the challenge of channel aging such that the channel state information becomes outdated quickly at high speeds because of the control loop delay from sensing the channel to transmit the data.
To avoid the problem of dynamic blockage as well as channel aging, one can utilise context information-assisted communications. With advanced sensors and localisation techniques, the BS could potentially predict the position of UE and blockers, and this information could be useful for dynamic blockage avoidance. Moreover, channel variance issues could be mitigated by using the recently proposed concept of predictor antenna (PA) [GMP+21]. PA system refers to a setup with two groups of antennas deploying on the top of a vehicle, where the front antennas (called PAs) sense and report back the CSI to the BS. Then, the receive antenna(s) (RA(s)) followed behind the PAs could use the CSI from PAs when they reach the same positions as the PAs. In this way, the quality of CSI is improved, leading to better system performance.

State-of-the-art and motivations
In stationary or low mobility systems, the network deployment, especially for non-fixed access points such as MR, can be learned and optimised to avoid (semi-)static blockages such as buildings and trees. Also, different resource allocation and cooperative communication schemes can be applied to improve the QoS. For example, one can deploy back-up NLoS links when a LoS link is blocked as an alternative option.
However, the blockage problem becomes more challenging in high-speed scenarios such as on highways. The back-up NLoS links are rare in highways, and probabilistic blockage prediction or (machine learning-based) deployment learning methods [KSP21] may not cope well with the dynamics of the network at high speeds/frequencies due to the fact of low height small cells.
On top of the blockage issue, the system performance is considerably affected by the channel aging phenomena where high speeds cause the channel state information at the transmitter (CSIT) to become inaccurate quickly. One can use Kalman prediction and PA [GMP+21] to improve the small-scale channel prediction quality in vehicle communications. However, 1) Kalman filter-based prediction has a limited prediction horizon, and the PA system may encounter a spatial mismatch between the point of measurement of the PA and the point of reception of the RA when the control loop is not properly designed and 2) both methods are not able to avoid dynamic blockage, which leads to considerable SINR drop.

Proposed setup
In our study [GMA+22], focusing on highway scenario, we incorporate the PA concept into a large-scale cooperative PA (LSCPA) setup with cooperative communications among BSs, and utilise the information provided by different vehicles to avoid not only temporal blockages but also the CSIT outdating.

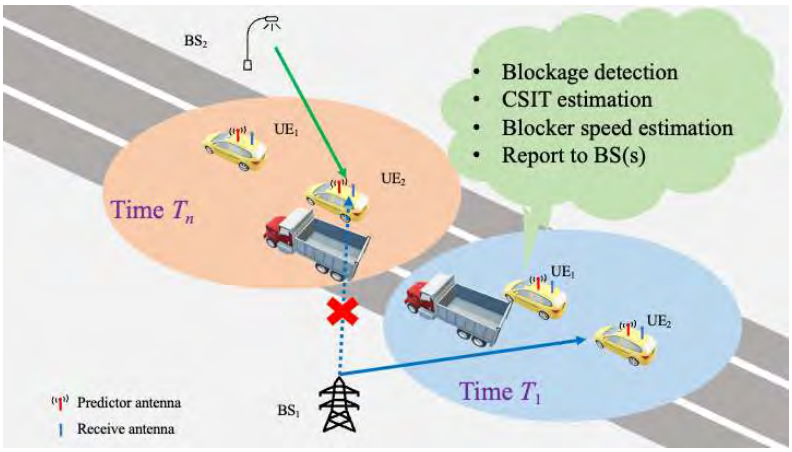

Figure 4-11. Proposed LSCPA setup to avoid not only temporal blockages but also the CSIT outdating.

As can be seen from Figure 4-11, UE1 and UE2 are served by BS1 at the time slot *T1*. If the front vehicle, i.e., UE1 detects a truck passing by as a potential blocker, it estimates the truck's speed and UE2. Then, UE1 informs one (or multiple) BS(s) about both the instantaneous CSIT of the location as well as the speed of the blocker and UE2. Knowing the speeds, the BS(s) can predict the slots, e.g., Slot *Tn* in Figure 4-11, when the second vehicle will be blocked by the truck and, in those slots, using cooperative BSs, BS2 may be used to serve UE2 blockage-free.
Without blockage, the instantaneous CSIT provided by the PA of the behind and the front vehicle can both assist the data transmission to the second vehicle. The self-PA CSIT has higher accuracy but allows only short spatial displacement during the control loop delay, while using CSIT from the front vehicles can support higher speeds and/or additional delay control loop delays, provided the spatial mismatch can be kept low. For accurate CSIT acquisition, the spatial mismatch would need to be within a fraction of a wavelength, whereas for blocking mitigation, it would be sufficient to be within a fraction of the beamwidth.

Results

We have investigated the effectiveness of the proposed scheme in terms of spectral efficiency for different system configurations [GMA+22]. Specifically, we compare our proposed scheme (Methods 1-3) with benchmark techniques (Methods 4-7) in terms of end-to-end (E2E) throughput as a function of transmit SNR. The details of the methods considered are presented in Table 4-3.

Table 4-3. Summary of the considered methods.

	Cooperative vehicles to avoid dynamic blockage	MIMO/MISO	CSIT availability using PA
Method 1	Yes	MIMO	Perfect CSIT
Method 2	Yes	MISO	Perfect CSIT
Method 3	Yes	MISO	Mismatched CSIT
Method 4	No	MISO	Perfect CSIT
Method 5	Yes	MIMO	No CSIT
Method 6	Yes	MISO	No CSIT
Method 7	No	MISO	No CSIT

Table 4-4. Simulation parameters.

Parameter	Value
Number of BS's antenna	32
Carrier frequency	28 GHz
Bandwidth	100 MHz
Speed	50 km/h
BS processing delay	5 ms
Codeword length	8000 symbols
Antenna separation	6.6 times the wavelength
Blockage probability	33%

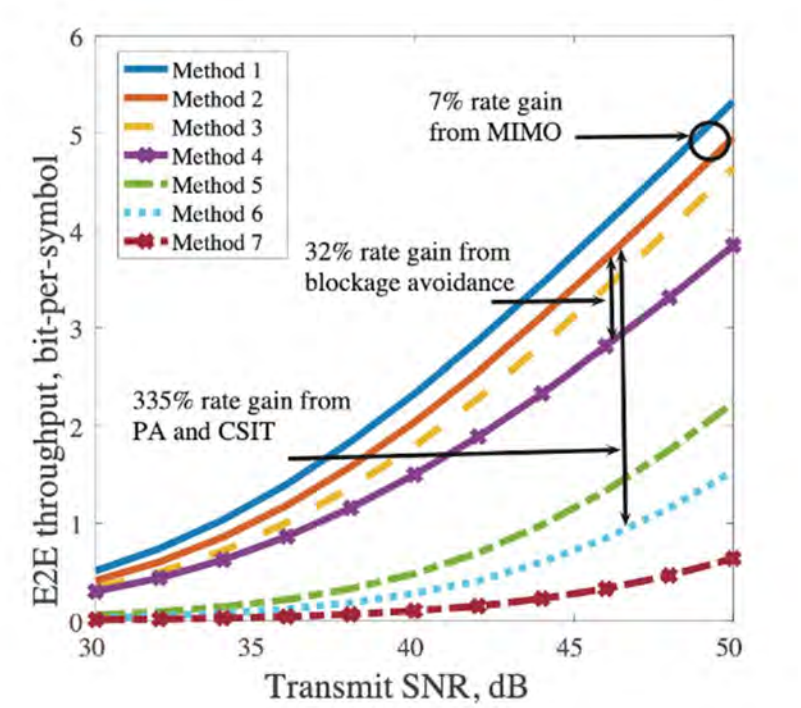

Figure 4-12. E2E throughput of the behind vehicle (UE2) as a function of transmit SNR.

With the parameters given in Table 4-4, the simulation results are shown in Figure 4-12. Results indicate that the E2E throughput for the given time slot of IoV networks can be improved by 32% using context information in the form of coarse localisation and trajectory information, whereas with highly accurate localisation and trajectory information, reliable CSIT can be obtained with the PA concept, resulting in 335% gain.

4.2.2 Energy efficiency in location-aided communications

Problem statement and motivation

This sub-section investigates the concept of channel knowledge map (CKM) as an enabler for environment-aware wireless communications. CKM is a site-specific database that involves the transmitters' and receivers' locations and channel-related information useful to enhance environmental awareness and facilitate real-time CSI acquisition. Hence,

CKM plays a vital role in 6G networks aiming for super high capacity, extremely low latency, and ultra-massive connectivity by providing potential solutions for the challenges brought by the drastically increased channel dimensions and training overhead [WZJ+21]. Figure 4-13 shows the impact of environmental awareness on wireless communication systems. Figure 4-13a shows two UEs with equal distances from the BS, but a building is located between UE2 and the BS. With the classic distance-dependent path loss model, one may wrongly conclude that UE1 and UE2 have identical channels to the BS. However, the knowledge of geometry, i.e., the location of BS and UEs as well as the position and size of the building, reveals that one channel is much worse than the other. Such information is either static or readily available with built-in sensors, such as GPS receivers. Therefore, with environmental awareness, accurate channel prediction is provided with no need for any sophisticated channel acquisition technique, such as pilot-based training. As another example, two training-free beamforming schemes are shown in Figure 4-13b: location-based beamforming, which sends out the signal in the direction from the BS to the UE, i.e., along the LoS if it were not blocked, and environment-aware beamforming, which beams the signals toward the potential reflectors/scatterers to send it to the UE indirectly. It is clear that by exploiting the environment knowledge, a more significant beamforming gain is achieved. In Figure 4-13c, we are interested to know whether a line-of-sight (LoS) link exists when the UE moves toward the BS. The LoS probability with the classical probabilistic model is based on the random event, which models as a function of the relative positions given by the distance and angle of the UE and BS, as illustrated by the red dashed line in Figure 4-13c. However, considering the environment, it can be observed that the existence/absence of a LoS link is deterministic, as shown by the solid blue line in Figure 4-13c. Such a discrepancy is mainly because the probabilistic LoS model is meaningful only by considering many realisations of similar communication environments. The three examples above show the importance of environmental awareness in contemporary wireless networks.

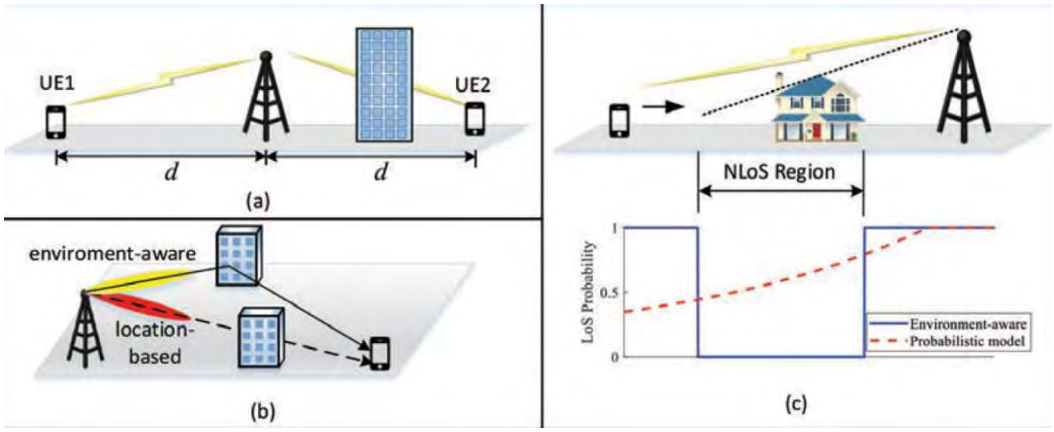

Figure 4-13. Three examples for illustrating the importance of environment-awareness: a) environment-aware channel gain prediction; b) environment-aware versus location-based training-free beamforming; c) environment-aware versus probabilistic LoS prediction [ZX21].

With no need for traditional channel training, the key parameters of the wireless channels can be attained with CKM. The transmitter and receiver locations, radio wave properties (such as wavelength), and the actual radio propagation environment determine a wireless channel gain. Also, by advancing localisation and environmental awareness, the issue of prohibitive training overhead in large dimension MIMO systems can be resolved [ZX21]. By utilising CKM, which is a site-specific database, tagged with the locations of the transmitters and receivers and containing channel-related information to enable

environment awareness, as illustrated in Figure 4-14, a more accurate channel knowledge is provided [DWZ+21].

For a RIS-aided communication system, with the fixed locations of the BS and the RIS, the channel mainly varies with the UE location and the actual propagation environment. However, compared to the UE locations, the wireless propagation environment (such as the locations, heights, and dielectric properties of surrounding objects) changes on a much larger time scale, as illustrated in Figure 4-14. It is notable that the impact of those environmental factors that may vary with comparable time scale as UE locations (such as pedestrians) on the wireless channel is much less than UE locations in practice. Therefore, the CKM needs to be updated only when there is a significant environmental change (that can be monitored by dedicated environment-sensing nodes as shown in Figure 4-14) that happens at a much larger time scale than the channel coherence time. As a result, having known the sufficiently accurate UE locations (provided via GPS and other advanced localisation technologies), the wireless channel gain can be approximately obtained with the CKM without any channel training needed.

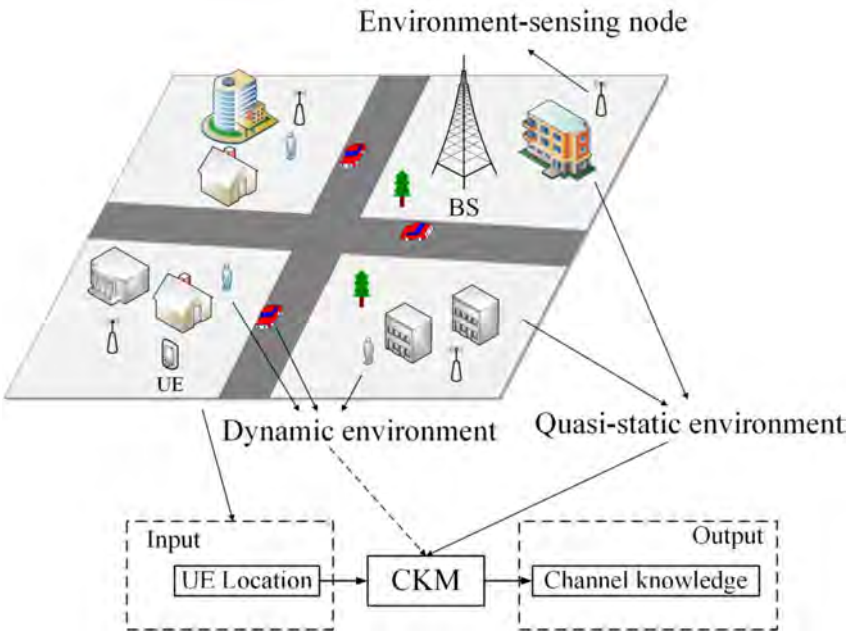

Figure 4-14. An illustration of CKM for enabling environment-awareness [WZJ+21].

Methodology

Based on the concept of CKM and knowing the UEs' locations, the active beamformers at the BS and passive beamformers at the RIS are optimised to achieve maximum energy efficiency. An actual physical environment is considered with fixed BS and RIS locations. The UEs are randomly distributed in a $50m \times 50m$ square area. The BS and RIS are placed such that a LoS path exists between them, while there is a blockage in BS-UEs direct channels. Other blockers are randomly located in the considered square area, which may block the LoS link for the RIS-UEs channels. The BS has an 8×8 uniform planar array (UPA) with adjacent elements separated by half wavelength. The RIS is composed of 10×10 reflecting passive elements. At the carrier frequency of 73 GHz, the noise power spectral density and the system bandwidth are set as $-174\ dBm/Hz$ and $300\ MHz$, respectively. The transmit power P at the BS varies from $10\ dBm$ to $40\ dBm$.

Results

Figure 4-15 and Figure 4-16 show the average network spectral efficiency (SE) and energy efficiency (EE) for CKM based on accurate UEs' locations, CKM based on estimating the UEs' locations with error, and channel training-based, respectively. By comparing the curves, it is observed that although the error in estimating the locations degrades the rate performance logarithmically, it still outperforms the channel training-based scheme that affects the communication rate linearly.

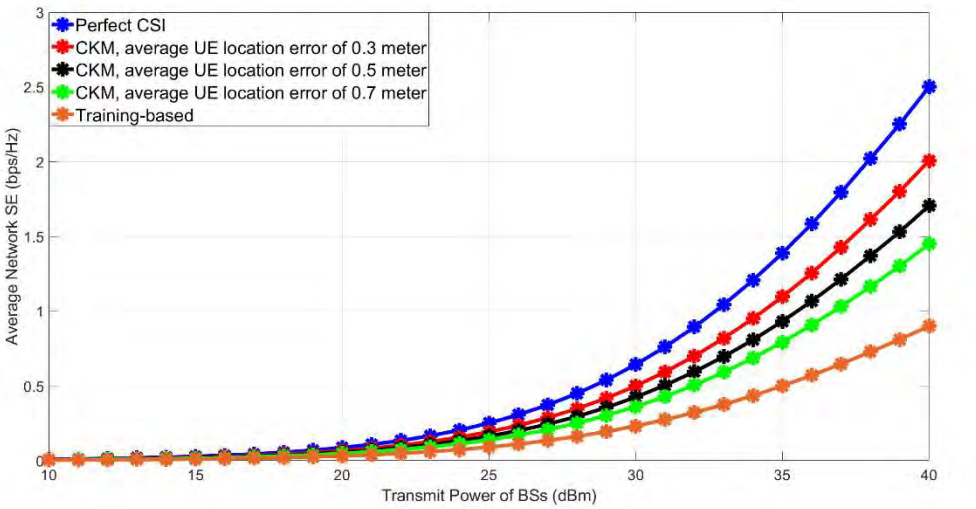

Figure 4-15. Average network SE for CKM with UE location error, perfect CSI, and training-based beamforming.

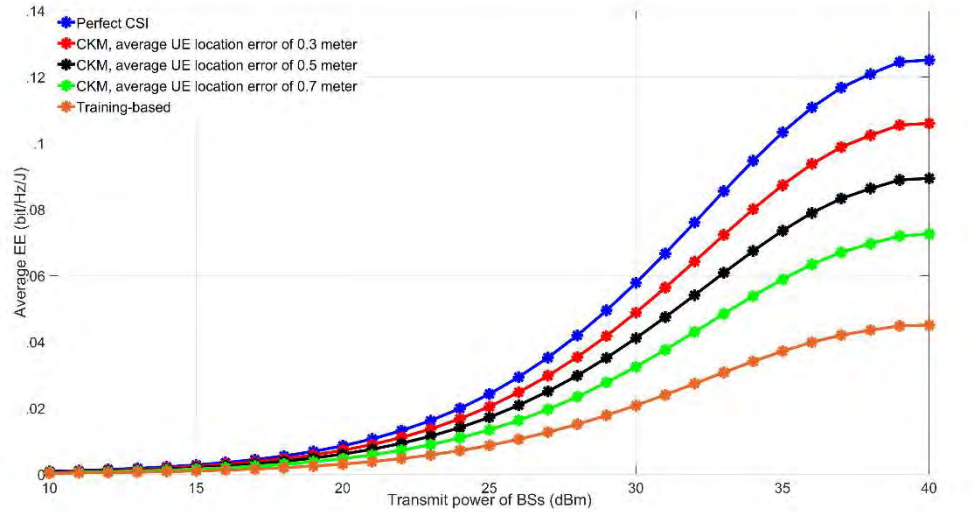

Figure 4-16. Average EE for CKM with UE location error, perfect CSI, and training-based beamforming.

Conclusion and outlook

In this sub-section, we investigated environment-aware beamforming for RIS-aided communication enabled by the CKM, which requires no online training. The simulation results have shown that applying CKM in active/passive beamforming yields significant rate improvement over the training-based beamforming and is also quite robust to UE location errors in practice.

4.3 Implications of localisation and sensing for the next-generation mobile networks

Seamless integration of localisation and sensing features into the next-generation mobile communication networks implies an integrated system architecture design. Requirements and impairments need to be evaluated, researched, and overcome. To release the full potential of localisation and sensing, an ecosystem is needed where all components and functions interact in a frictionless manner.

Section 4.3.1 and section 4.3.2 address the technical and functional challenges of localisation and sensing. Because when it comes to enabling integrated sensing and communication, one of the first design principles is that this should be achieved by reusing the spectrum that is used for communication and at the same time imposing as little changes to hardware and waveforms as possible.

Waveform design may be done in an integrated fashion for communication and sensing, or separately. The receiver processing used for a pulse-Doppler radar is independent of the waveform type and is equally applicable to any typical communication waveform such as OFDM, etc. As one example, the waveform can be one or several OFDM or DFTS-OFDM symbols (or even sub-symbols), as it is the common waveform used in most of the existing wireless access links.

In integrated sensing and communication, the transmission and reception points may be UEs or base stations, meaning that the communication can be in downlink, uplink, UE to UE, or base station to base station. In the context of existing cellular communications such as 5G, this could mean that the sensing signal can be a DL reference signal, a UL reference signal, or a sidelink reference signal. The sensing signal can be any of the existing signals, such as downlink positioning reference signal (DL PRS), channel state information reference signal (CSI-RS), demodulation reference signal (DM-RS), and UL sounding reference signal (SRS), etc., or a new sensing/positioning specific signal.

Section 4.3.3 highlights technical and non-technical requirements for an ecosystem with focus on context-based and location-based applications. Not only do the communication service and the localisation/sensing services need to interact smoothly, but all other (context/location based) services based on top of the sensing feature should support an open integrative ecosystem approach.

4.3.1 Time-frequency signal resource allocation for sensing

For better integration with communication in terms of resource utilisation, it is desirable to use OFDM or a similar waveform that can be scheduled by the same type of algorithm and jointly with the ongoing communication. Figure 4-17 shows a sensing signal based on OFDM symbols. The sensing signal in the figure has a bandwidth of BW, and the OFDM symbol duration is T_{sym}. To satisfy a minimum velocity range, the signal is repeated with a periodicity of T_r, and to meet a minimum velocity resolution, the OFDM symbols are transmitted over a duration of T_f.

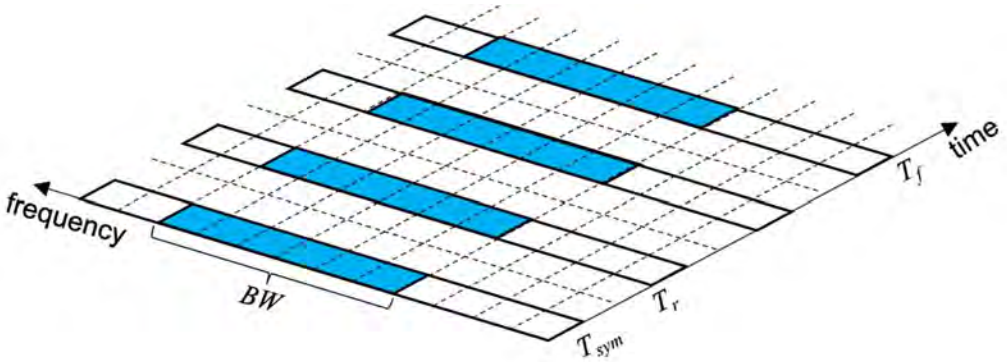

Figure 4-17. A train of OFDM symbols as a sensing signal.

To put the resource utilisation in context, we consider the traffic monitoring use case where the required accuracies are range resolution R_r = 0.5 m, unambiguous range R_u = 100 m, velocity resolution v_r = 0.5 m/s, and unambiguous velocity v_u in the range of [-20 to 20] m/s. Table 4-5 shows the required bandwidth, sensing signal repetition factor, and sensing frame length for different carrier frequencies and corresponding subcarrier spacing. Also, the table shows the percentage of resources that need to be used to meet those requirements.

Table 4-5. An example illustration of parameterisation of sensing signal.

f_c [GHz]	SCS [kHz]	BW [MHz]	T_r [µs]	T_f [ms]	Overhead
3.5	30	300	1071	85.7	3.5%
6	30	300	625	50.0	7.1%
10	60	300	375	30 .0	7.1%
28	120	300	134	10.7	2.7%
60	480	300	62	5.0	0.7%
96	1920	300	39	3.1	0.2%

When beamforming is used (e.g., at higher frequencies), the overhead percentage becomes larger because sensing must be performed in several directions. So, depending on the beamforming solution and the angular range that is covered in sensing, overhead increases further.

4.3.2 Sensing in a communication network

In the following, we show simulation results for detecting objects with the above parameters by transmitting Zadoff-Chu sequences in OFDM symbols and measurements based on the received reflections. After the matched filter, the received signal is transformed from the time-frequency domain to the Doppler-delay domain. Figure 4-18 shows the detection of two objects in the range 20 m and 40 m, moving with the radial speed of 10 m/s and 20 m/s, respectively, using the above setup for the sensing signal. The results are based on link-level simulations with sensing signals as described above at *SNR = -30 dB*. As it is observed, even at an SNR value that is about *30-40 dB* below those of communication signal levels, the objects can be detected with acceptable accuracy.

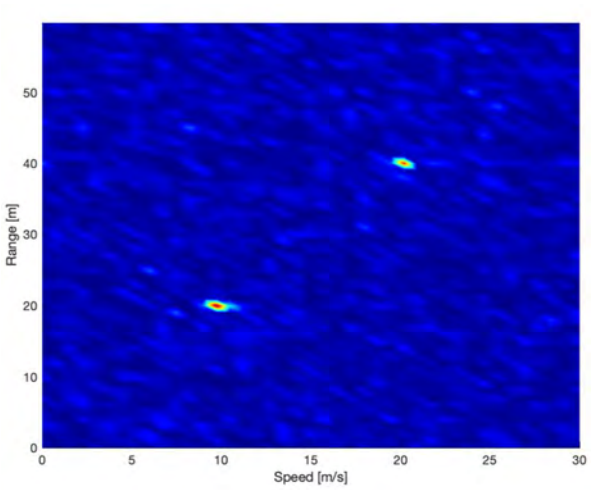

Figure 4-18. Detection of two objects with the range of 20 m and 40 m and speeds of 10 m/s and 20 m/s.

To get a better understanding of the performance of the sensing that was described above, we can look at the probability of miss-detection when a certain target probability of false alarm is considered. Figure 4-19 shows simulation results for the probability of miss-detection as a function of SNR for different target false alarm rates, when the above setup is used to sense an object at the range of 50 m, moving at the radial speed of 10 m/s. In the context of sensing, a false alarm is defined as detecting a peak in the delay-Doppler domain, that is above the detection threshold, when there has been no object to be detected. Detection of an object is defined as receiving a peak in the delay-Doppler domain, within the expected range and Doppler accuracy, that is above a threshold. The probability of miss-detection follows from that which is the probability of not detecting an object within the expected Doppler and delay bound when there is in fact an object present.

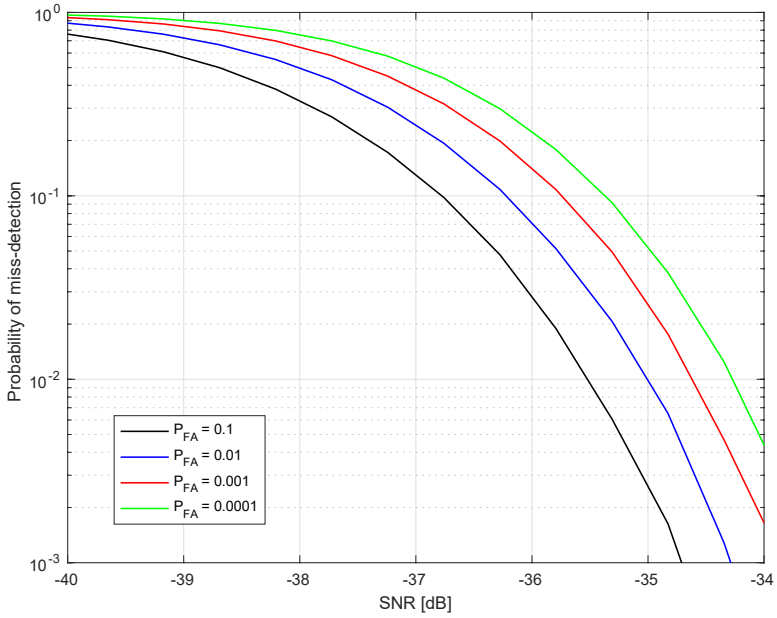

Figure 4-19. Probability of miss-detection as a function of SNR for different false alarm rates.

4.3.2.1 Network and hardware requirements for integrated sensing and communication

4.3.2.1.1 Hardware requirements

In a mono-static sensing scenario, a communication node should be capable of transmitting and receiving the sensing signal almost instantly, i.e., it needs to support full-duplex. The challenge of transceiver design with full-duplex capability is well-known, as it requires a high level of self-interference cancellation for acceptable sensing accuracy. On the other hand, in bi-static and multi-static cases, there is no need for full-duplex support; however, they require a high degree of synchronisation between nodes and accurate information on their position.

4.3.2.1.2 Spectrum considerations

Due to the large available bandwidth, the mmW and sub-THz frequency ranges enable very accurate sensing. However, systems operating in the mmW range and, to a larger extent, in the sub-THz range will have limited coverage. In contrast, the lower-frequency spectrum provides much wider coverage. Although higher frequencies provide better sensing accuracy, we should keep in mind that data communication at higher frequencies comes at the cost of higher propagation loss and more complex hardware. Even though we usually use beamforming for high frequencies to compensate for the propagation loss, beamforming means higher overhead due to sensing over multiple beams. Another important consideration in choosing a spectrum for sensing is the field of view, which is the angular range that can be sensed at different frequencies. At higher frequencies, array antennas have larger gains and smaller apertures. This means that operating at higher frequencies results in a smaller receiver cross-section, i.e., a narrower field of view. Depending on the sensing application, this could be a desired property or a disadvantage of operating at higher frequencies.

4.3.3 Implications and requirements for next-generation mobile networks to enable new context-aware services

Future services and applications based on or integrating next-generation mobile networks will have many requests on each layer of the Hexa-X E2E 6G architecture view. Figure 4-20 depicts the current status of the future architecture with three main layers [HEX22-D13]:

- The infrastructure layer includes mandatory and optional physical resources to host the network service and application layer functionalities. Resources are Radio Access (RAN), Core (CN), and transport Networks, including radio equipment, switches, routers, communication links, data centres, cloud infrastructure, etc.
- The cloud-based network service layer with a vast amount of functions and microservices may expand from the central cloud to the extreme edge cloud (which can consist of heterogeneous devices such as wearables, smartphones, laptops, industrial devices, etc.). It is foreseen that all network functions, operations, and applications shall be realised as microservices.
- The application layer is granted access to all kinds of services and information through the exposure framework and integration fabric. This is the interface for seamless interoperation and networking across different domains and applications.

Efficient, flexible, and straightforward management and orchestration for and between all layers are essential. In addition, end-to-end security must be guaranteed.

It is important to research if special requirements exist from a localisation and sensing perspective that go beyond the current 5G vision.

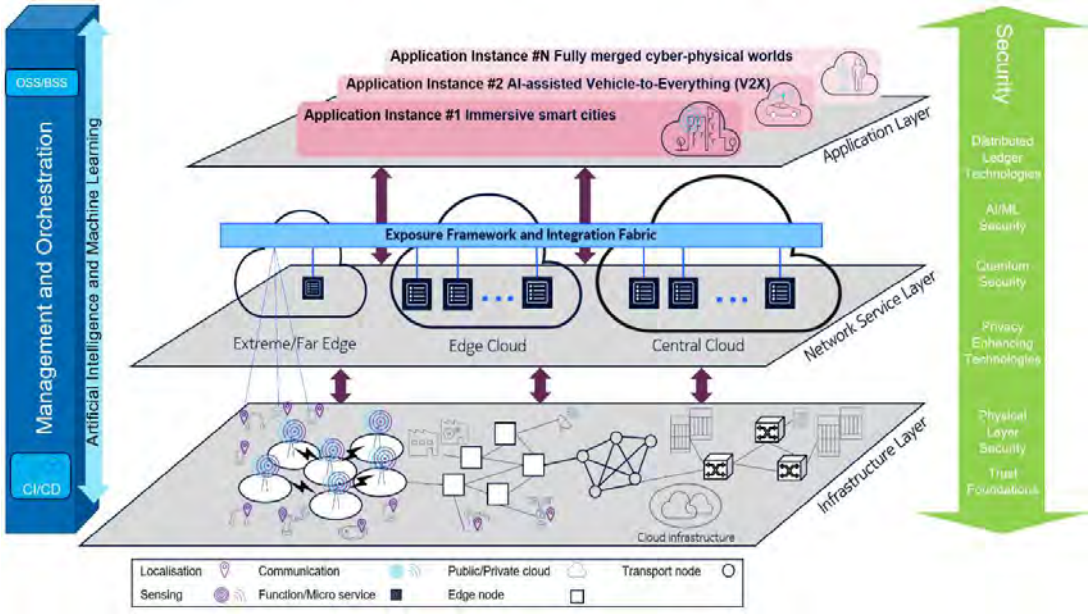

Figure 4-20. 6G E2E architecture overview.

Figure 4-21. Examples of localisation and sensing scenarios (A: UE localisation, B: Asset localisation, and C: Detection of assets and humans without UEs via sensing).Figure 4-21 shows three scenarios: Highly accurate localisation of UEs (A) as well as assets (B) but also radar-like sensing scenarios where next-generation mobile communication devices can detect and track objects or humans that do not carry any device (C), and even gesture detection of humans without UEs will be possible.

As elaborated already in the previous sections, two sets of concentric circles in Figure 4-21 illustrate the combination of communication and sensing (overlap between blue and purple areas): *integrated radar, communication, computation, localisation, and sensing (IRC2LS)*. Pure communication or pure sensing scenarios should also be made possible in the future.

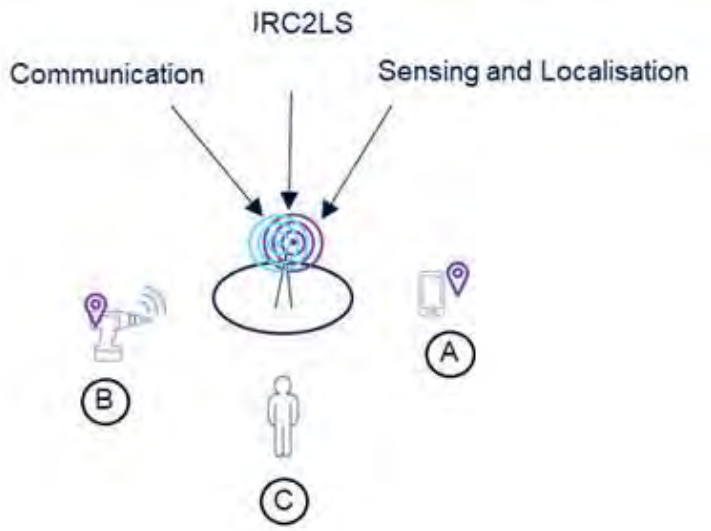

Figure 4-21. Examples of localisation and sensing scenarios (A: UE localisation, B: Asset localisation, and C: Detection of assets and humans without UEs via sensing).

To enable a flourishing ecosystem that can serve different scenarios and use cases will require flexibility, scalability, and ultra-low latency. It will be challenging to address all the requirements at the same time.

- **Configuration, flexible switching, and prioritisation:** Some applications will require only a communication service, some only environmental sensing, and some only localisation features, whereas other applications will need these functions in different combinations at the same time. Hence, in future mobile communication networks, the service of orchestrating these sub-functions must be extended to handle all sub-features in a very flexible way. Note that all three cases (communication, sensing, and localisation) are envisioned to share the same hardware. Therefore, trade-offs will need to be considered, and the prioritisation of the sub-features according to applications' requirements must be organised seamlessly.
  In some scenarios, it might not be clear what service will be needed in the initial phase of installing hardware and deploying the system. Furthermore, if requirements change, it must be possible to easily extend and integrate new hard- and software. The configuration service should be able to react accordingly to such scenarios.
- **Exposure framework and data interpretation:** It is important that localisation and sensing services have well-defined interfaces for easy information access. Therefore, interfaces for localisation services will need to be extended, e.g., from 3D to 6D (3D position + 3D orientation); new services, protocols, and interfaces must be developed for sensing features. And for non-UE-based sensing, no ID is available but classes of objects and patterns that have been detected (a human person or certain activity movement patterns, etc.). Moreover, information access should be possible at different processing stages (e.g., raw sensing data as well as readily calculated position information).
- **Security (information access and information generation):** Security aspects as cross-topic are multifaceted and layer-dependent. Depending on service consumers' permissions, access to raw and preprocessed location and sensing information shall be possible to limit to authorised personnel. Position and sensing data are often very sensitive as they can easily be linked to personal information or business/trade secrets that must be protected from misuse. In industrial scenarios, this might even mean that the factory operator must stay under the control of sensing data related to the factory's operation and production processes and that data is not supposed to leave the factory data storages and networks. Therefore, not only access to sensing data must be regulated, but a policy for acceptable use of sensing information must be clearly defined. It must be ensured that obtained sensing information is used only for the defined purpose.
  Localisation and sensing information will be generated by the mobile communication network. Securing this information will be a very important architectural design requirement as the mobile network is not only passing information from application to application through the network but generating sensing information itself. Furthermore, this generated localisation and sensing information must be correct and trustworthy. Attacks that may falsify the localisation and sensing information concern the entire processing chain, from the sensing process and signal processing up to providing and using localisation and sensing data. Such attacks against raw signals have been published, e.g., for GPS [PH16]. But also, the integrity of the signal processing system can be manipulated,

e.g., if manipulated or vulnerable software would be used or manipulated sensing, and localisation information could be provided to users.

- **User Privacy:** Position and sensing data may endanger the privacy of users. It has to be considered that the legal requirements for privacy protection depending on the legislation, e.g., the General Data Protection Regulation (GDPR) regulation in the EU and the California Consumer Privacy Act (CCPA). Therefore, the different regulatory rules concerning privacy protection have to be fulfilled.
- **Flexible quality of service:** Low latency, which is understood as a short duration between the initialisation of sensing/localisation procedure and acquiring a localisation/sensing estimate, is also a challenge for the E2E architecture. But in general, service consumers must be able to describe applications' functional and non-functional localisation and sensing requirements like latency or reliability towards next-generation mobile communication services and must be able to rely on these agreed quality parameters. These parameters are not necessarily static and might change over time which requires flexibility both in the agreement /contract between consumer and producer as well as technically by allowing to flexible adjust to latency requirements.
- **Sensor and Information fusion:** In outdoor and indoor scenarios, other localisation and sensing technologies exist. To enable the full potential with maximum flexibility and best quality results, it is necessary to allow for the integration of multiple technologies, radio and non-radio based. Fusing information across multiple technologies can enable or enhance information completeness and hence, service quality. Especially when integrating with other IoT sensors. But much more research needs to be done to allow for trust in regard to the Internet-of-Things and information fusion [AG19].

An initial graphical summary of the above requirements is depicted in Figure 4-22Figure 4-22. The figure doesn't specify which stakeholder implements what service. The calculation of the position of a UE will remain a core service that needs enhancement in regard to non-functional requirements (latency, accessibility, accuracy, etc.) and the extension from 3D to 6D localisation (including orientation). It is obvious that more core services need to be implemented to handle the future sensing feature and that not just raw data like x,y,z coordinates will be delivered but also more contextualised data (in the sense of semantically enriched and classified data). The exposure framework including interfaces of all new emerging services will need to be able to handle different data granularity requests (from raw data to fully contextualised, enriched, and classified information) and potentially needs to be tightly coupled with the communication service to truly enable efficient integrated communication and sensing.

RIS (reflecting intelligent surfaces) as an example of new hardware components being introduced to the next generation mobile networks may play a role in some scenarios and applications. Interfaces should allow for easy integration of such emerging technologies independent of hardware ownership.

The number of stakeholders in the ecosystem of next-generation mobile communication systems will increase with localisation becoming more accurate, scalable, and reliable, especially with sensing becoming available for the first time. Furthermore, context-based applications and services will emerge if these features (highly accurate indoor/outdoor localisation and sensing) become equally relevant to the core communication service.

- Context information is essential both as a producer (radio maps, maps generated by SLAM mechanisms) and consumer (information from 3D models or HMI systems, etc.). Accessing third-party information as well as offering information generated by next-generation mobile networks must be well designed and

orchestrated. For real-time digital twins, as one example, localisation and sensing information will play a crucial role, especially when digitalising mobile and/or moving objects within an environment. The information flow between the digital twin and the sensing and localisation service shall be well designed and organised, by addressing above mentioned challenges such as security, latency, and flexibility.

- Context/ and Location-based services exist already in many fashions, often based on non-5G technologies such as lidar, cameras, or RFID. For example, tracking of mobile vehicles and collision avoidance to optimise traffic flows and reduce waiting times or Geo-fencing based notifications if UEs enter a certain area to optimise processes within factories. With higher accurate localisation (also indoors), next-generation mobile networks could address many of those use cases and offer such services as core service well. Though the figure does not imply that these emerging services must be standardised as core services. In combination with sensing the environment and optimised (joined) communication capabilities, the next-generation mobile networks have the potential to create a wide ecosystem with perfectly integrated services.

Hexa-X will further detail the view from the localisation and sensing perspective on the next-generation mobile network ecosystem.

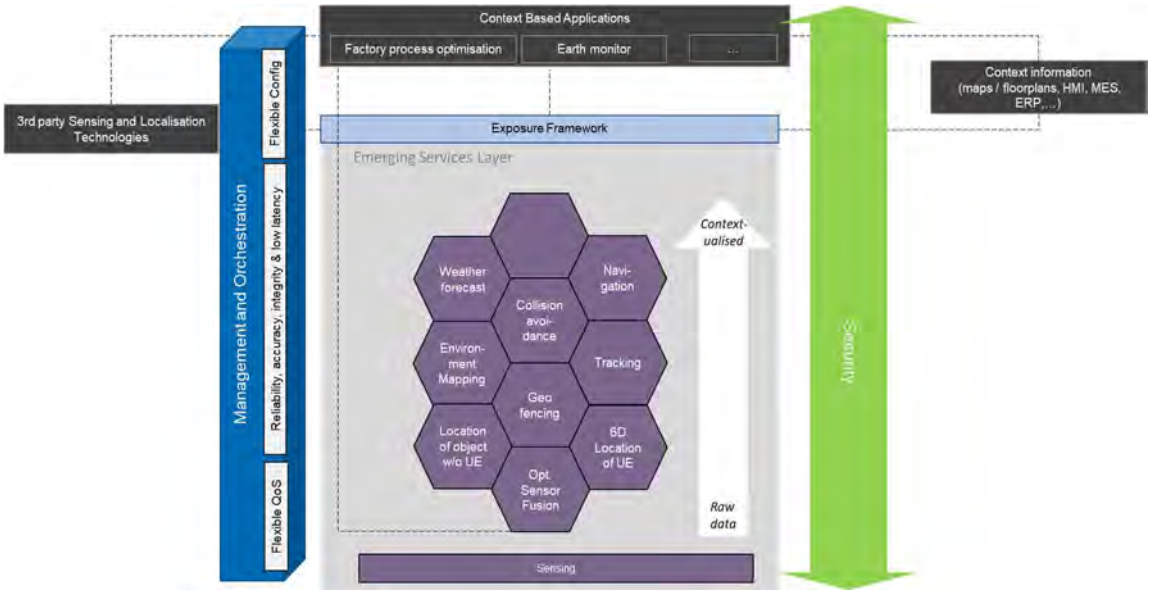

Figure 4-22. First view on localisation and sensing ecosystem

5 Conclusions

In 6G systems, localisation will no longer be a by-product of the communication development but integrated from the outset and thus must become one of the design targets. Integrating localisation and sensing with high accuracy and low latency are required to support many use cases identified in Hexa-X. However, NR positioning and sensing used in 5G cannot meet these requirements. 6G, as the next generation of mobile communication network, potentially exploiting a wide bandwidth and large antenna arrays (among other enablers), must be able to support and meet the sensing requirements of the identified use cases.

The sensing and localisation capabilities in 6G enable the new use cases depending on what performance levels can be achieved in practice. Therefore, the performance of existing signals, methods, and protocols needs to be understood in the 6G context, and novel approaches will need to be developed. Preliminary analyses indicate that 6G performance benefits stem mainly from improved resolution, not from improved integrated SNR, compared to NR positioning. In this document, we provided a categorisation of our initial solutions in methods, signals, and protocols for localisation and mapping with respect to the targeted KPIs and KVIs. The initial solutions include signal design based on spatial signal optimisation, detection and channel parameter estimation, localisation/sensing under the impact of HWIs, integrated communications and sensing, and the approaches for interference mitigation. To experimentally verify simulation results, make proof of concepts and demonstrate different use cases, a platform for integrated communication, localisation and sensing has been developed.

6G location and sensor information enable many new applications. To support these applications and use cases, sensing and localisation capabilities must be designed as an integral part of the next generation of mobile communications and be offered to all potential consumers. On the one hand, the environment can be observed, and conclusions are drawn based on 6G mobile communications itself; but on the other hand, there will be other 6G-external sensors and (positioning) systems that could be merged via sensor fusion with the information from the 6G network. This opens many opportunities to improve existing services, but also to create completely new service offerings. Extending the borders of the 6G communication system to allow external sensor information to be integrated into such a next-generation communication system requires architectural adaptions. WP3 will only deal with a subset of the new opportunities around sensing and localisation, clearly focusing on 6G-based options, but always embed them in the larger context. From the concepts, models, simulations, and algorithms created, future network requirements and potential requirements for the end-to-end architecture will be identified. WP3's goal is to show possible architecture blueprints that represent the interaction within 6G (sensing and localisation) information on the one hand, by examining new 6G internal services. One example could be the exploitation of location information to assist resource allocation for communication, which could then be optimised depending on the location of UEs. WP3 will investigate and evaluate this interplay. WP3 will also show the connection with external information, such as external sensors embedded in UEs as well as localisation systems not based on 6G.

6 References

[38.211] 3GPP TS 38.211 "Physical channels and modulation (Release 17)," version 17.1.0, 2022.

[AEL+14] A. Alkhateeb, O. El Ayach, G. Leus, and R. W. Heath, "Channel estimation and hybrid precoding for millimeter wave cellular systems," IEEE journal of selected topics in signal processing, vol. 8, no. 5, pp. 831-846, July 2014.

[AG19] F. Azzedin and M. Ghaleb, "Internet-of-Things and information fusion: Trust perspective survey," *Sensors*, vol. 19, no. 8, pp. 1929, Apr. 2019.

[AGO+13] D. Anguita, A. Ghio, L. Oneto, X. Parra, and J. L. Reyes-Ortiz, "A Public Domain Dataset for Human Activity Recognition Using Smartphones," 21st European Symposium on Artificial Neural Networks, Computational Intelligence and Machine Learning, ESANN 2013. Bruges, Belgium 24-26 April 2013.

[BDR+21] M. Berriri, S. Djema, G. Rey, and C. Dartigues-Pallez, "Multi-Class Assessment Based on Random Forests," Education Sciences , vol. 11, no. 3, pp. 1-12, 2021.

[BGV92] B. E. Boser, I. M. Guyon, and V. N. Vapnik, "A training algorithm for optimal margin classifiers," COLT '92: Proceedings of the fifth annual workshop on Computational learning theory, July 1992, pp. 144-152, DOI: 10.1145/130385.130401.

[CAK+22] H. Chen, S. R. Aghdam, M. F. Keskin, Y. Wu, S. Lindberg, A. Wolfgang, U. Gustavsson, T. Eriksson, and H. Wymeersch, "MCRB-based Performance Analysis of 6G Localisation under Hardware Impairments," 2022 IEEE International Conference on Communications Workshops (ICC Workshops), 2022, pp. 115-120.

[CBS+12] B. Chihani, E. Bertin, I. Suprapto, J. Zimmermann, N. Crespi, "Enhancing Existing Communication Services with Context Awareness," Journal of Computer Networks and Communications, vol. 2012, pp.1-10, 2012.

[CD20] Y. Chi and M. F. Da Costa, "Harnessing sparsity over the continuum: Atomic norm minimization for super resolution," IEEE Signal Processing Magazine, vol. 37, no. 2, pp. 39–57, 2020.

[CDR01] E. Conte, A. De Maio, and G. Ricci, "GLRT-based adaptive detection algorithms for range-spread targets," IEEE transactions on signal processing, vol. 49, no. 7, pp. 1336-1348, July 2001.

[CSB+22] H. Chen, H. Sarieddeen, T. Ballal, H. Wymeersch, M. S. Alouini, and T. Y. Al-Naffouri, "A Tutorial on Terahertz-Band Localisation for 6G Communication Systems," accepted by IEEE Communications Surveys & Tutorials, 2022.

[DWZ+21] D. Ding, D. Wu, Y. Zeng, S. Jin, and R. Zhang, "Environment-Aware Beam Selection for IRS-Aided Communication with Channel Knowledge Map," 2021 IEEE Globecom Workshops, 2021, pp. 1-6, doi: 10.1109/GCWkshps52748.2021.9681979.

[EMR16] "Microweather: Unlocking potential," Ericsson Mobility Report, June 2016.

[FGG+17] S. Fortunati, F. Gini, M. S. Greco, and C.D. Richmond, "Performance bounds for parameter estimation under misspecified models: Fundamental findings and applications," IEEE Signal Processing Magazine, vol. 34, no. 6, pp.142-57, November 2017.

[GCH20] S. Guruacharya, B. K. Chalise, and B. Himed, “MAP ratio test detector for radar system,” IEEE Transactions on Signal Processing, vol. 69, pp. 573-588, December 2020.

[GMA+22] H. Guo, B. Makki, M. Alouini, and T. Svensson, “High-rate uninterrupted internet-of-vehicle communications in highways: Dynamic blockage avoidance and CSIT acquisition,” in IEEE Communications Magazine, vol. 60, no. 7, pp. 44-50, July 2022.

[GMB+21] M. H. C. Garcia, A. Molina-Galan, M. Boban, J. Gozalvez, B. Coll-Perales, T. Şahin, and A. Kousaridas, “A tutorial on 5G NR V2X communications,” IEEE Communications Surveys & Tutorials, vol. 23, no. 3, pp. 1972–2026, Feb. 2021.

[GMP+21] H. Guo, B. Makki, D. Phan-Huy, E. Dahlman, M.Alouini, and T.Svensson, “Predictor antenna: A technique to boost the performance of moving relays,” IEEE Communications Magazine, vol. 59, no. 7, pp. 80–86, Jul. 2021.

[GWK+20] Y. Ge, F. Wen, H. Kim, M. Zhu, F. Jiang, S. Kim, L. Svensson, H. Wymeersch. “5G SLAM using the clustering and assignment approach with diffuse multipath,” Sensors, vol. 20, no. 16, p. 4656, 2020.

[HEX21-D21] Hexa-X, “Deliverable D2.1: Towards Tbps Communications in 6G: Use Cases and Gap Analysis,” Jun. 2021.

[HEX21-D31] Hexa-X, “Deliverable D3.1: Localisation and sensing use cases and gap analysis,” Dec. 2021.

[HEX22-D13] Hexa-X, “Deliverable D1.3: Targets and requirements for 6G - initial E2E architecture,” Feb. 2022.

[HEX22-D72] Hexa-X, “Deliverable D7.2: Special-purpose functionalities: intermediate solutions,” April 2022.

[HGR+16] R. W. Heath Jr., N. Gonzalez-Prelcic, S. Rangan, W. Roh, and A. M. Sayeed, “An Overview of Signal Processing Techniques for Millimeter Wave MIMO Systems,” IEEE Journal of Selected Topics in Signal Processing, vol. 10, no. 3, pp. 436-453, 2016.

[HWJ21] J. He, H. Wymeersch, and M. Juntti, “Channel Estimation for RIS-Aided mmWave MIMO Systems via Atomic Norm Minimization,” IEEE Transactions on Wireless Communications, vol. 20, no. 9, pp. 5786-5797, 2021.

[JC20] T. L. Jensen and E. D. Carvalho, “An optimal channel estimation scheme for intelligent reflecting surfaces based on a minimum variance unbiased estimator,” in proc. IEEE ICASSP, pp. 5000–5004, 2020.

[KJM+22] M. F. Keskin, F. Jiang, F. Munier, G. Seco-Granados, and H. Wymeersch, “Optimal Spatial Signal Design for mmWave Positioning under Imperfect Synchronisation,” IEEE Transactions on Vehicular Technology, vol. 71, no.5. pp. 5558-5563, May 2022, doi: 10.1109/TVT.2022.3149974.

[KSP21] S. Khosravi, H. Shokri-Ghadikolaei and M. Petrova, "Learning-Based Handover in Mobile Millimeter-Wave Networks," IEEE Transactions on Cognitive Communications and Networking, vol. 7, no. 2, pp. 663-674, June 2021.

[KWK21] M. F. Keskin, H. Wymeersch, and V. Koivunen, “MIMO-OFDM Joint Radar-Communications: Is ICI Friend or Foe?,” IEEE Journal of Selected Topics in Signal Processing, vol. 15, no. 6, pp. 1393-1408, Nov. 2021.

[KWS+21] A. Kakkavas, H. Wymeersch, G. Seco-Granados, M. H. Castañeda García, R. A. Stirling-Gallacher, and J. A. Nossek, “Power Allocation and Parameter Estimation for Multipath-based 5G Positioning,” IEEE

Transactions on Wireless Communications, vol. 20, no. 11, pp. 7302-7316, Nov. 2021.

[LGL16] J. Lee, G.-T. Gil, and Y. H. Lee, "Channel estimation via orthogonal matching pursuit for hybrid MIMO systems in millimeter wave communications," IEEE Transactions on Communications, vol. 64, no. 6, pp. 2370–2386, 2016.

[MMB+19] R. Mendrzik, F. Meyer, G. Bauch, and M. Z. Win, "Enabling situational awareness in millimeter wave massive MIMO systems," IEEE Journal of Selected Topics in Signal Processing, vol. 13, no. 5, pp. 1196–1211, 2019.

[Nic06] U. Nickel, "Overview of generalized monopulse estimation," IEEE Aerospace and Electronic Systems Magazine, vol. 21, no. 6, pp. 27–56, Jun. 2006.

[NSJ+22] M. A. Nazari, G. Seco-Granados, P. Johannisson, and H. Wymeersch, "MmWave 6D Radio Localization with a Snapshot Observation from a Single BS," arXiv preprint, arXiv:2204.05189. April 2022.

[OH17] T. O'shea and J. Hoydis, "An introduction to deep learning for the physical layer," IEEE Transactions on Cognitive Communications and Networking, vol. 3, no. 4, pp. 563-575, October 2017.

[PH16] M. L. Psiaki and T. E. Humphreys, "GNSS Spoofing and Detection," in Proceedings of the IEEE, vol. 104, no. 6, pp. 1258-1270, June 2016.

[RH15] C. D. Richmond and L. L. Horowitz, "Parameter bounds on estimation accuracy under model misspecification," IEEE Transactions on Signal Processing, vol. 6, no. 63, pp. 2263-2278, March 2015.

[SBG+19] E. C. Strinati, S. Barbarossa; J. L. Gonzalez-Jimenez, D. Ktenas, N. Cassiau, L. Maret, and C. Dehos, "6G: The Next Frontier: From Holographic Messaging to Artificial Intelligence Using Subterahertz and Visible Light Communication," IEEE Vehicular Technology Magazine, vol. 14, no. 3, pp. 42-50, Sept. 2019, doi: 10.1109/MVT.2019.2921162.

[Sch86] R. Schmidt, "Multiple emitter location and signal parameter estimation," IEEE Trans. Antennas Propag., vol. 34, no. 3, pp. 276–280, Mar. 1986.

[SH16] F. Schneemann and P. Heinemann, "Context-based detection of pedestrian crossing intention for autonomous driving in urban environments," 2016 IEEE/RSJ International Conference on Intelligent Robots and Systems (IROS), pp. 2243-2248, 2016, doi: 10.1109/IROS.2016.775935

[SHB+22] R. Schroeder, J. He, G. Brante, and M. Juntti, "Two-stage channel estimation for hybrid RIS assisted MIMO systems," IEEE Transactions on Communications, vol. 70, no. 7, pp. 4793-4806, July 2022, doi: 10.1109/TCOMM.2022.3176654.

[SZL+22] A. L. Swindlehurst, G. Zhou, R. Liu, C. Pan, and M. Li, "Channel estimation with reconfigurable intelligent surfaces–a general framework," Proceedings of the IEEE, pp. 1– 27, 2022.

[TAA21] A. Taha, M. Alrabeiah, and A. Alkhateeb, "Enabling Large Intelligent Surfaces with Compressive Sensing and Deep Learning," IEEE Access, vol. 9, pp. 44304-44321, 2021.

[TMR+14] R. D. Taranto, S. Muppirisetty, R. Raulefs, D. Slock, T. Svensson, and H. Wymeersch, "Location-aware communications for 5G networks: How location information can improve scalability, latency, and robustness of 5G," IEEE Signal Processing Magazine vol. 31, no. 6 pp. 102-112, 2014.

[TSF+17] J. Tranter, N. D. Sidiropoulos, X. Fu, and A. Swami, "Fast unit-modulus least squares with applications in beamforming," IEEE Transactions on Signal Processing, vol. 65, no. 11, pp. 2875-2887, February 2017.

[WSM+21] H. Wymeersch, D. Shrestha, C. Morais de Lima, V. Yajnanarayana, B. Richerzhagen, M. Furkan Keskin, K. Schindhelm, A. Ramirez, A. Wolfgang, M. F. de Guzman, K. Haneda, T. Svensson, R. Baldemair, and S. Parkvall, "Integration of Communication and Sensing in 6G: a Joint Industrial and Academic Perspective," IEEE PIMRC workshops, 2021.

[WZ09] H. Wu and T. Zwick, "Automotive SAR for Parking Lot Detection," German Microwave Conference, 2009.

[WZJ+21] D. Wu, Y. Zeng, S. Jin, and R. Zhang, "Environment-Aware and Training-Free Beam Alignment for mmWave Massive MIMO via Channel Knowledge Map," IEEE International Conference on Communications Workshops (ICC) Workshops, 2021.

[YHS+21] V. Yajnanarayana, D. Huang, D. Shrestha, Y. Geng, A. Behravan, and E. Dahlman, "AI Based Landscape Sensing Using Radio Signals," 2021 IEEE 32nd Annual International Symposium on Personal, Indoor and Mobile Radio Communications (PIMRC), pp. 1-5, 2021, doi: 10.1109/PIMRC50174.2021.9569617.

[ZB11] R. Zekavat and R. M. Buehrer (eds.), "Handbook of position location: Theory, practice and advances," Vol. 27. John Wiley & Sons, 2011.

[ZX21] Y. Zeng and X. Xu, "Toward environment-aware 6G communications via channel knowledge map," IEEE Wireless Communications, vol. 28, no. 3, pp. 84-91, 2021.